Precision nucleon and nuclear structure from light (muonic) atoms

Randolf Pohl

Johannes Gutenberg
Universität Mainz

MITP
Workshop on alpha
30.10.25

Hydrogen-like atoms

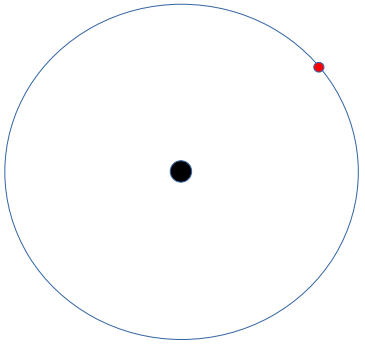

"There's a reason physicists are so successful with what they do, and that is they study the hydrogen atom and the helium ion and then they stop."

- Richard Feynman

Proton Radius and Hydrogen

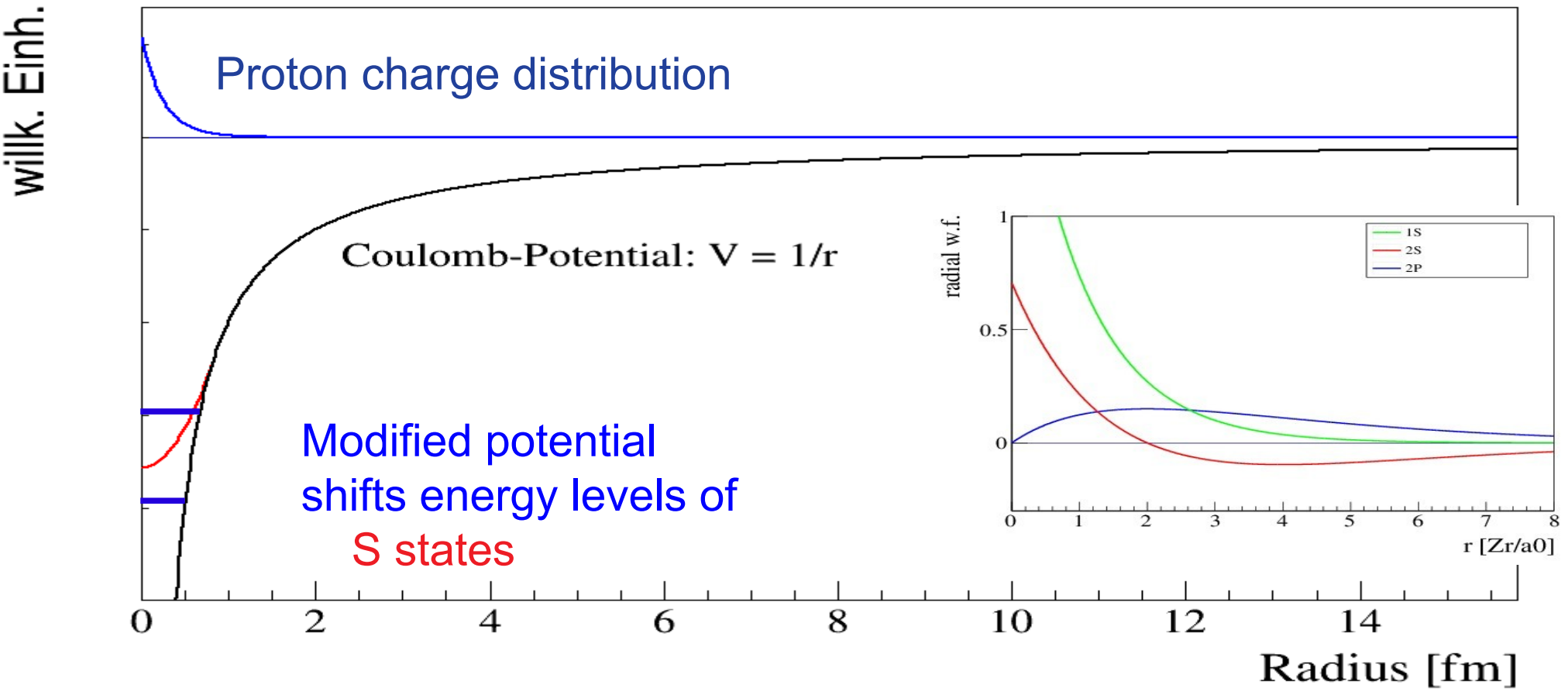

Muonic Atoms

A **bare** nucleus, orbited by **one negative muon.**

Hydrogen theory!

Muonic atoms in a nutshell

Regular hydrogen:

Bohr radius ~ 50’000 x nuclear radius

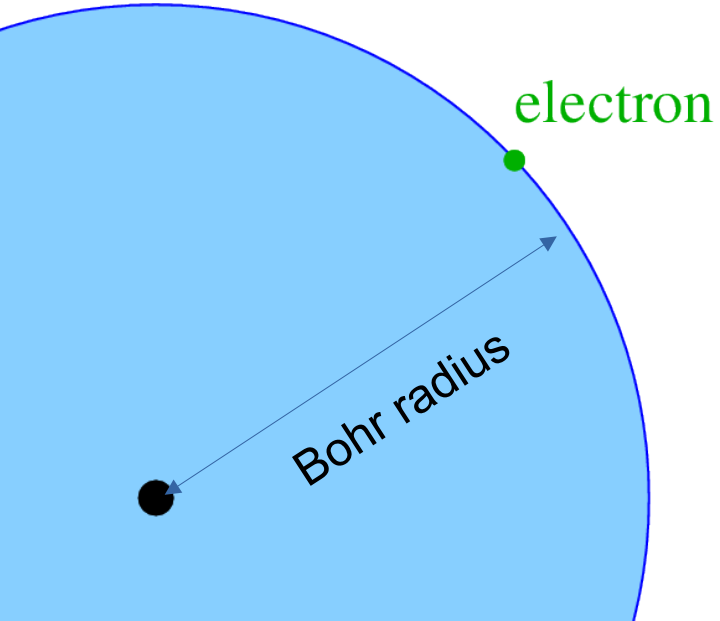

Muonic hydrogen:

Muon **mass** = **200** * electron mass

Bohr **radius** = **1/200** of H

200^3 = a **ten million times** more sensitive to nuclear size & structure

==> Our (laser) spectroscopy at **10^{-5}** level

can compete with **10^{-12}** from normal atoms

Vastly not to scale!!

Lamb shift in Muonic Hydrogen

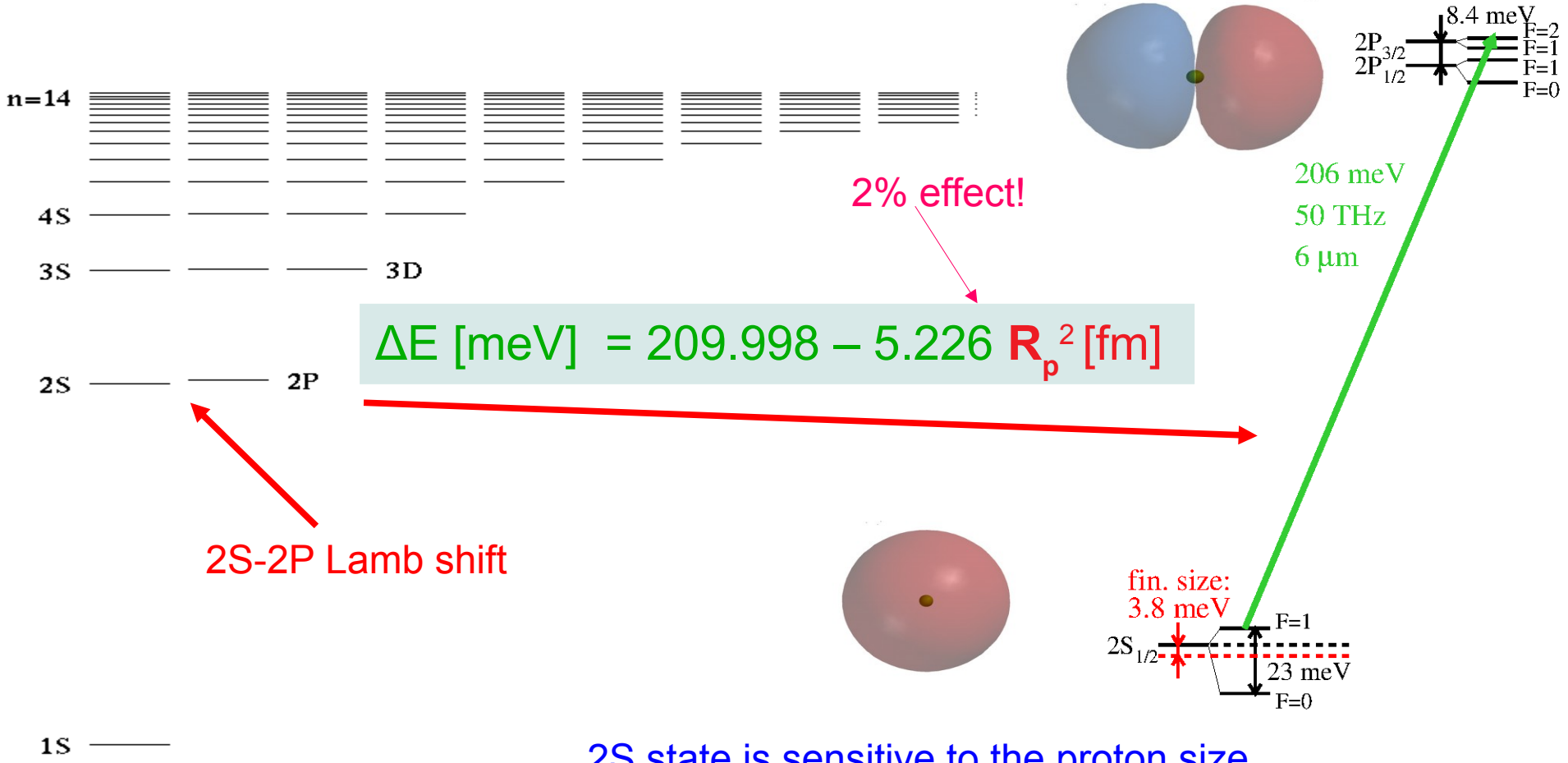

The accelerator at PSI

PAUL SCHERRER INSTITUT

PSI

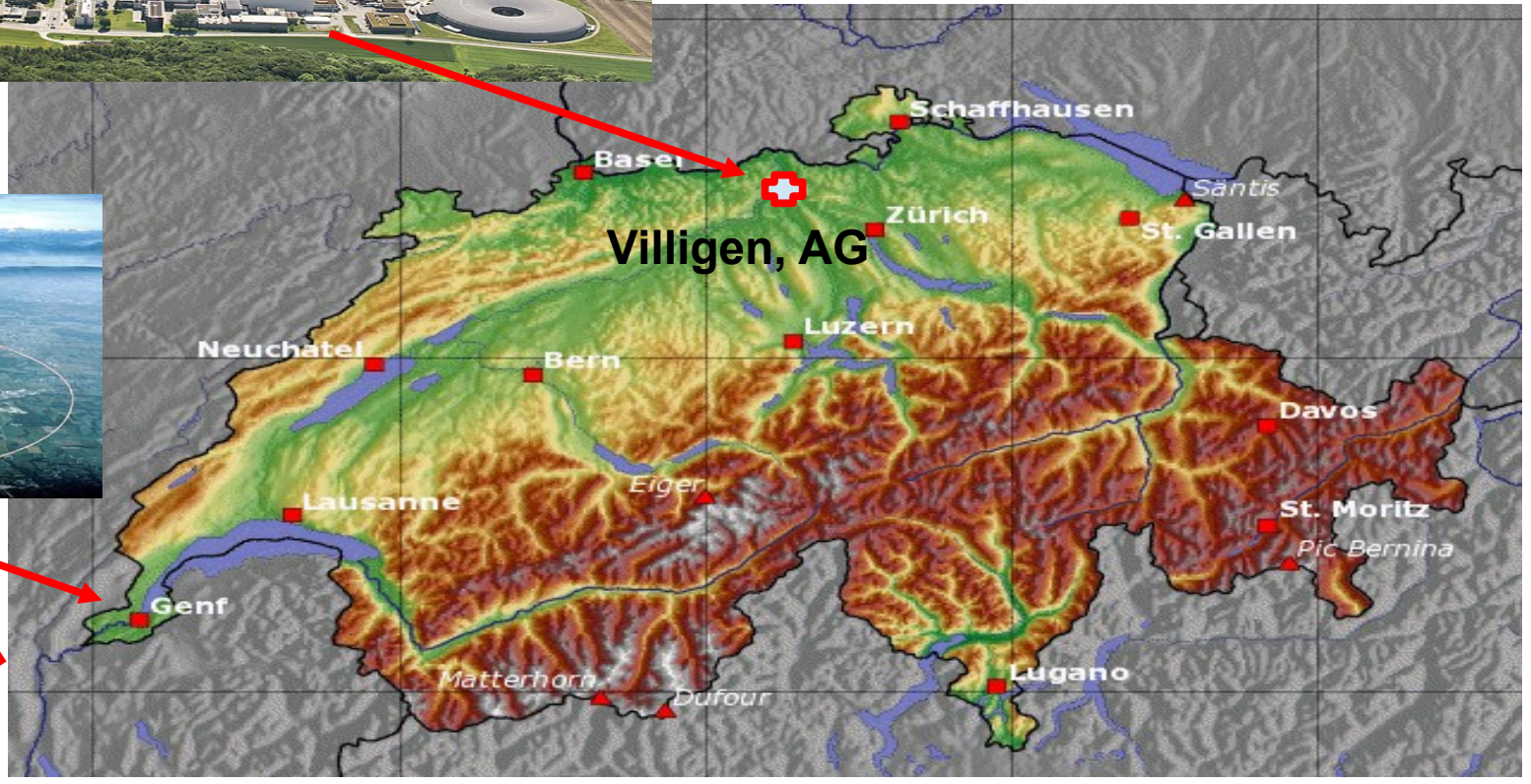

Time Spectra

13 hours of data

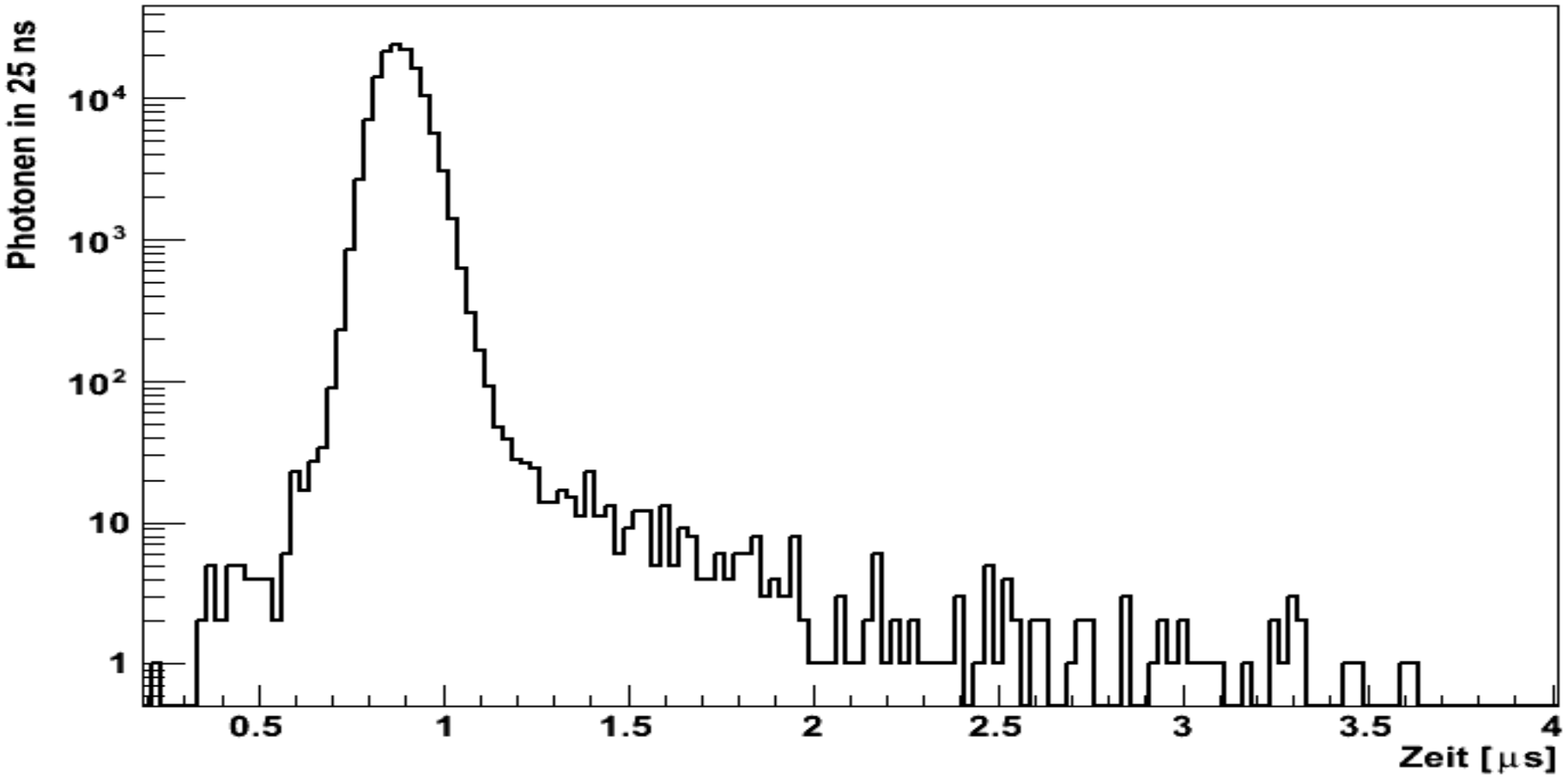

Time Spectra

13 hours of data

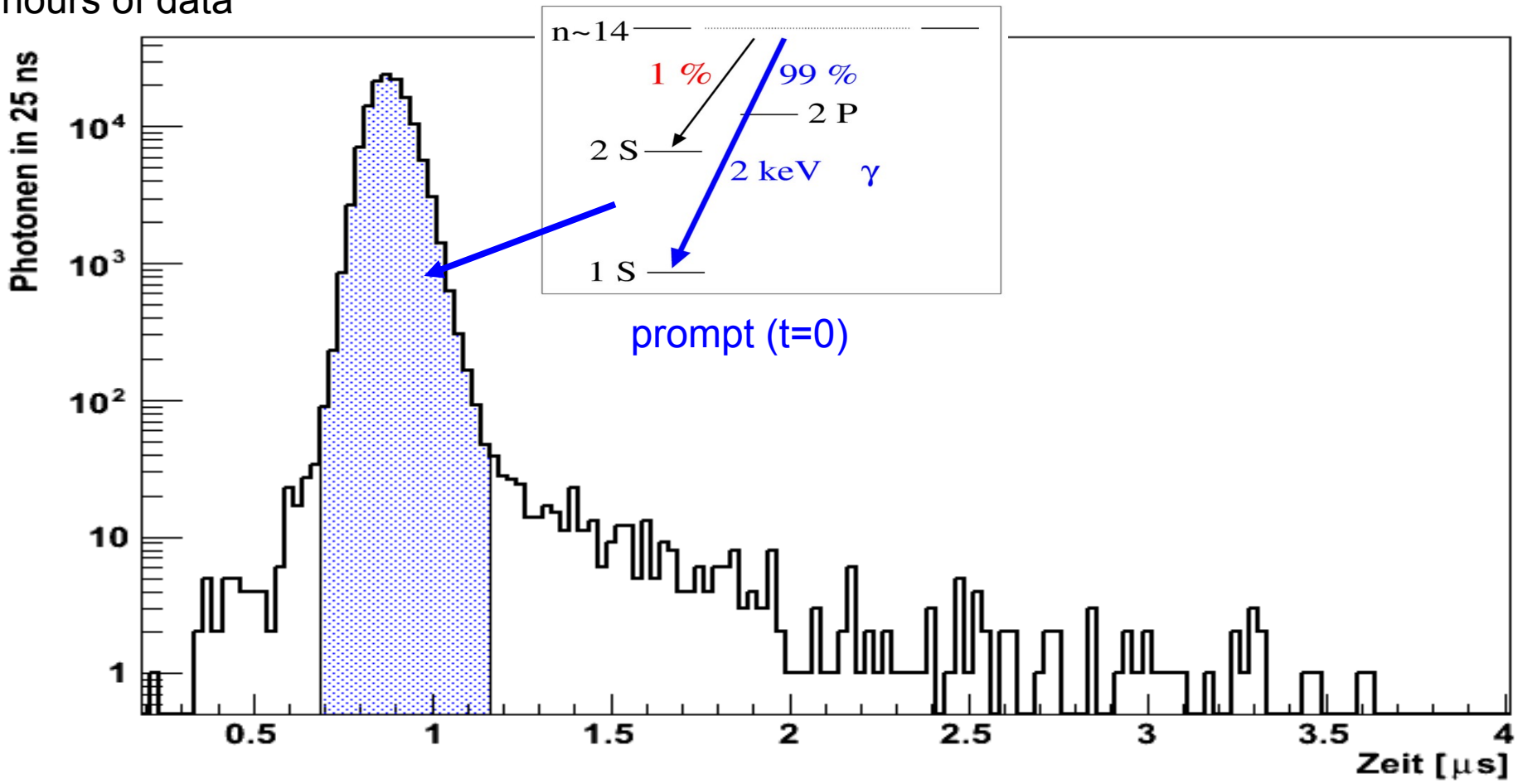

Time Spectra

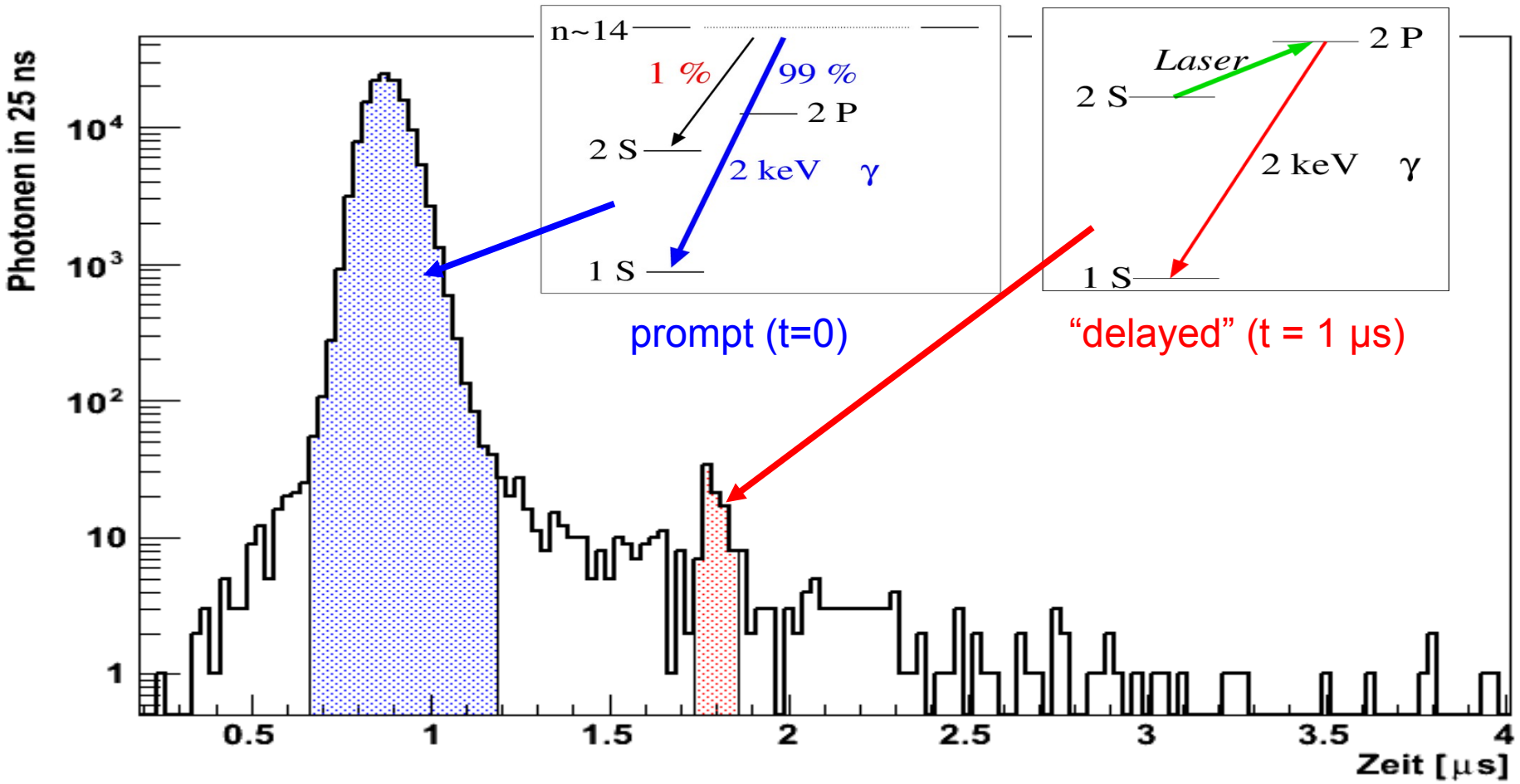

Time Spectra

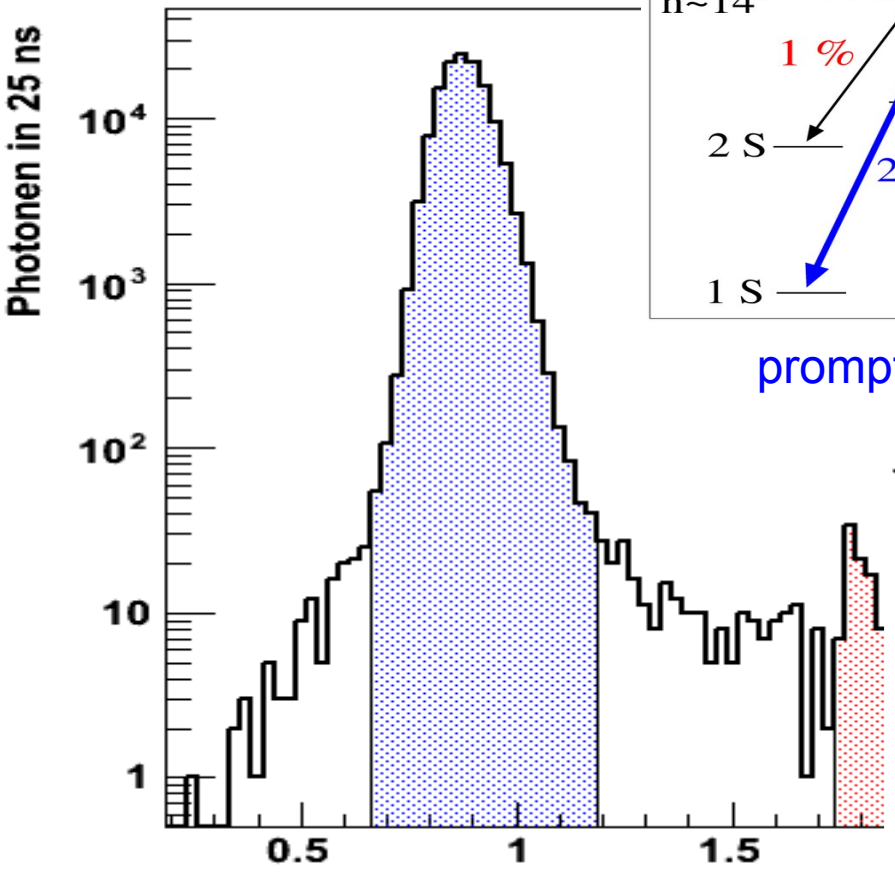

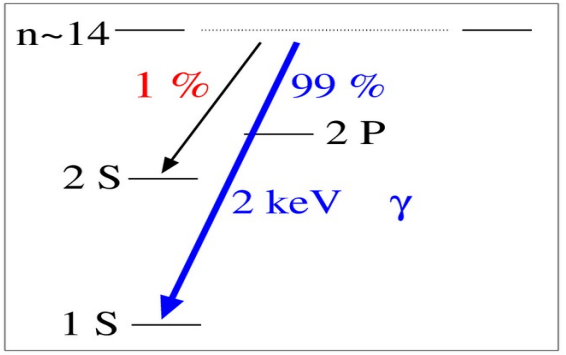

prompt (t=0)

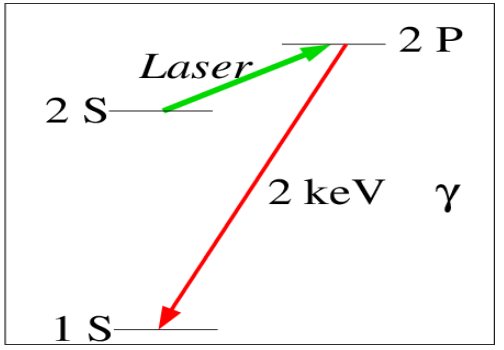

“delayed” (t = 1 µs)

resonance curve

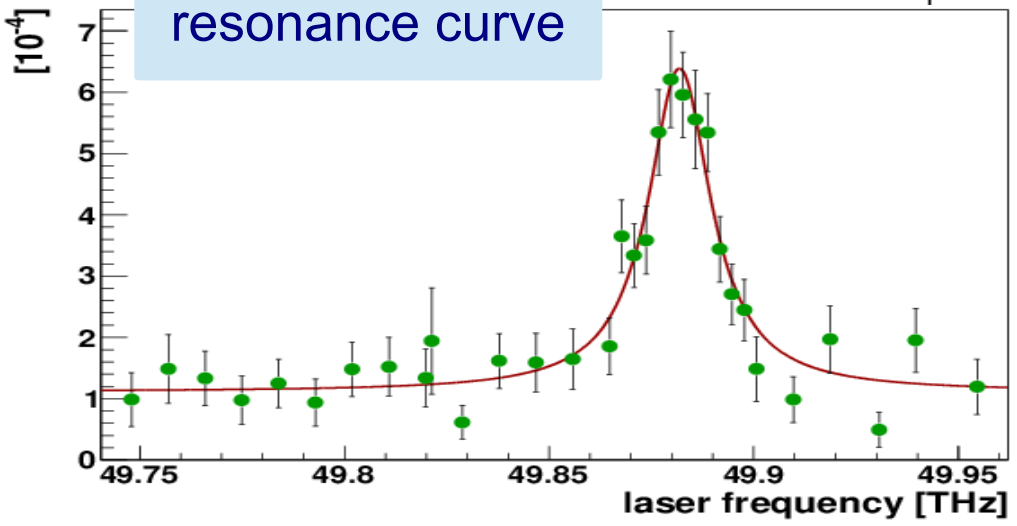

Resonance

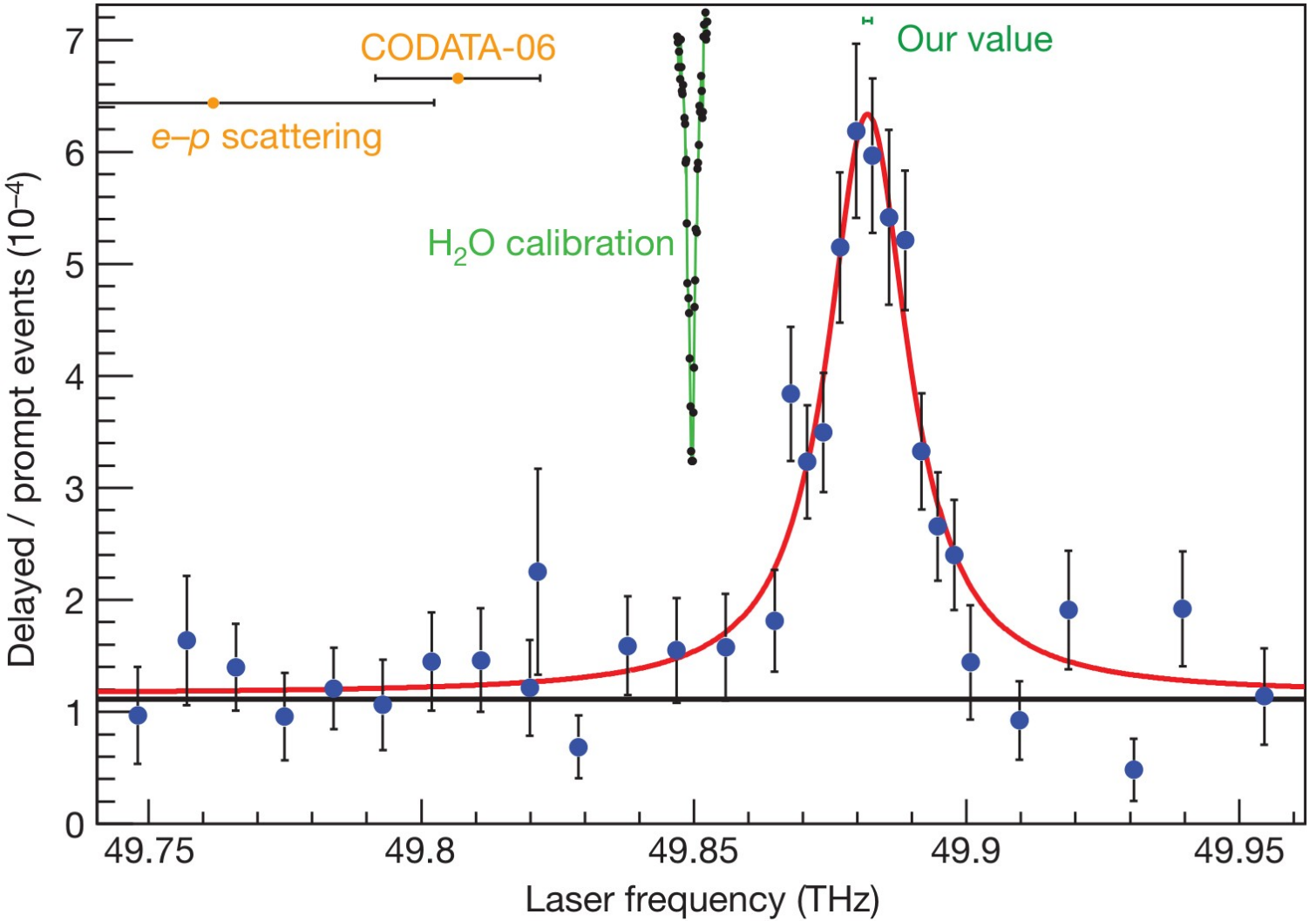
CODATA-06
e–p scattering
H2O calibration
Our value
Delayed / prompt events (10–4)
Laser frequency (THz)
0
1
2
3
4
5
6
7
49.75
49.8
49.85
49.9
49.95

Theory in muonic H (D, $^{3,4}He^{+}$ similar)

ΔE_{Lamb} = 206.0344 (3) meV_{QED} + 0.0289 (25) meV_{TPE} – 5.2259 (1) meV/fm^2 * $\mathbf{R_p^2}$

Uehling

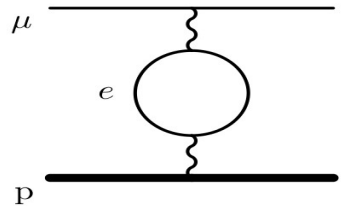

Källen-Sabry

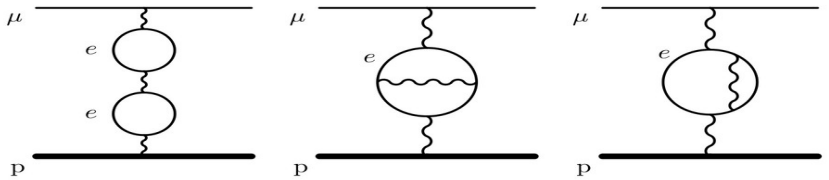

Muon SE+VP

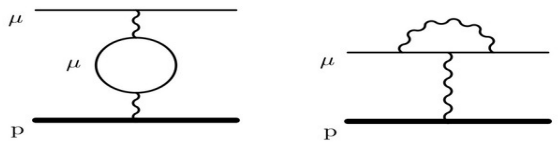

and 20+ more….

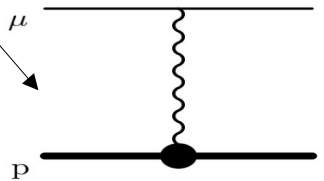

Proton form factor

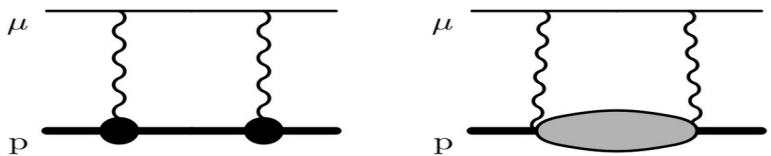

elastic and inelastic two-photon exchange
(Friar moment and polarizability)

Theory

TABLE I. Contributions to the $2P_{1/2} - 2S_{1/2}$ energy difference E_L in meV, with the charge radii r_C given in fm. All corrections larger than 3% of the overall uncertainty are included. Theoretical predictions for E_L are $E_L(\text{theo}) = E_{\text{QED}} + \mathcal{C}r_C^2 + E_{\text{NS}}$. The last two rows show the values of r_C determined from a comparison of $E_L(\text{theo})$ to $E_L(\text{exp})$.

Section	Order	Correction	μH	μD	μ^3He$^+$	μ^4He$^+$
III.A	$\alpha(Z\alpha)^2$	eVP$^{(1)}$	205.007 38	227.634 70	1641.886 2	1665.773 1
III.A	$\alpha^2(Z\alpha)^2$	eVP$^{(2)}$	1.658 85	1.838 04	13.084 3	13.276 9
III.A	$\alpha^3(Z\alpha)^2$	eVP$^{(3)}$	0.007 52	0.008 42(7)	0.073 0(30)	0.074 0(30)
III.B	$(Z, Z^2, Z^3)\alpha^5$	Light-by-light eVP	−0.000 89(2)	−0.000 96(2)	−0.013 4(6)	−0.013 6(6)
III.C	$(Z\alpha)^4$	Recoil	0.057 47	0.067 22	0.126 5	0.295 2
III.D	$\alpha(Z\alpha)^4$	Relativistic with eVP$^{(1)}$	0.018 76	0.021 78	0.509 3	0.521 1
III.E	$\alpha^2(Z\alpha)^4$	Relativistic with eVP$^{(2)}$	0.000 17	0.000 20	0.005 6	0.005 7
III.F	$\alpha(Z\alpha)^4$	μSE$^{(1)}$ + μVP$^{(1)}$, LO	−0.663 45	−0.769 43	−10.652 5	−10.926 0
III.G	$\alpha(Z\alpha)^5$	μSE$^{(1)}$ + μVP$^{(1)}$, NLO	−0.004 43	−0.005 18	−0.174 9	−0.179 7
III.H	$\alpha^2(Z\alpha)^4$	μVP$^{(1)}$ with eVP$^{(1)}$	0.000 13	0.000 15	0.003 8	0.003 9
III.I	$\alpha^2(Z\alpha)^4$	μSE$^{(1)}$ with eVP$^{(1)}$	−0.002 54	−0.003 06	−0.062 7	−0.064 6
III.J	$(Z\alpha)^5$	Recoil	−0.044 97	−0.026 60	−0.558 1	−0.433 0
III.K	$\alpha(Z\alpha)^5$	Recoil with eVP$^{(1)}$	0.000 14(14)	0.000 09(9)	0.004 9(49)	0.003 9(39)
III.L	$Z^2\alpha(Z\alpha)^4$	nSE$^{(1)}$	−0.009 92	−0.003 10	−0.084 0	−0.050 5
III.M	$\alpha^2(Z\alpha)^4$	$\mu F_1^{(2)}$, $\mu F_2^{(2)}$, μVP$^{(2)}$	−0.001 58	−0.001 84	−0.031 1	−0.031 9
III.N	$(Z\alpha)^6$	Pure recoil	0.000 09	0.000 04	0.001 9	0.001 4
III.O	$\alpha(Z\alpha)^5$	Radiative recoil	0.000 22	0.000 13	0.002 9	0.002 3
III.P	$\alpha(Z\alpha)^4$	hVP	0.011 36(27)	0.013 28(32)	0.224 1(53)	0.230 3(54)
III.Q	$\alpha^2(Z\alpha)^4$	hVP with eVP$^{(1)}$	0.000 09	0.000 10	0.002 6(1)	0.002 7(1)
IV.A	$(Z\alpha)^4$	r_C^2	$-5.197\,5r_p^2$	$-6.073\,2r_d^2$	$-102.523r_h^2$	$-105.322r_\alpha^2$
IV.B	$\alpha(Z\alpha)^4$	eVP$^{(1)}$ with r_C^2	$-0.028\,2r_p^2$	$-0.034\,0r_d^2$	$-0.851r_h^2$	$-0.878r_\alpha^2$
IV.C	$\alpha^2(Z\alpha)^4$	eVP$^{(2)}$ with r_C^2	$-0.000\,2r_p^2$	$-0.000\,2r_d^2$	$-0.009(1)r_h^2$	$-0.009(1)r_\alpha^2$
V.A	$(Z\alpha)^5$	TPE	0.029 2(25)	1.979(20)	16.38(31)	9.76(40)
V.B	$\alpha^2(Z\alpha)^4$	Coulomb distortion	0.0	−0.261	−1.010	−0.536
V.C	$(Z\alpha)^6$	3PE	−0.001 3(3)	0.002 2(9)	−0.214(214)	−0.165(165)
V.D	$\alpha(Z\alpha)^5$	eVP$^{(1)}$ with TPE	0.000 6(1)	0.027 5(4)	0.266(24)	0.158(12)
V.E	$\alpha(Z\alpha)^5$	μSE$^{(1)}$ + μVP$^{(1)}$ with TPE	0.000 4	0.002 6(3)	0.077(8)	0.059(6)
III	E_{QED}	Point nucleus	206.034 4(3)	228.774 0(3)	1644.348(8)	1668.491(7)
IV	$\mathcal{C}r_C^2$	Finite size	$-5.225\,9r_p^2$	$-6.107\,4r_d^2$	$-103.383r_h^2$	$-106.209r_\alpha^2$
V	E_{NS}	Nuclear structure	0.028 9(25)	1.750 3(200)	15.499(378)	9.276(433)
	E_L (exp)	Experiment[a]	202.370 6(23)	202.878 5(34)	1258.598(48)	1378.521(48)
	r_C	This review	0.840 60(39)	2.127 58(78)	1.970 07(94)	1.678 6(12)
	r_C	Previous work[a]	0.840 87(39)	2.125 62(78)	1.970 07(94)	1.678 24(83)

Pachucki, Lensky, Hagelstein, LiMuli, Bacca, RP, RMP 96 (2024)

Theory

TABLE I. Contributions to the $2P_{1/2} - 2S_{1/2}$ energy difference E_L in meV, with the charge radii r_C given in fm. All corrections larger than 3% of the overall uncertainty are included. Theoretical predictions for E_L are $E_L(\text{theo}) = E_{\text{QED}} + Cr_C^2 + E_{\text{NS}}$. The last two rows show the values of r_C determined from a comparison of $E_L(\text{theo})$ to $E_L(\text{exp})$.

Section	Order	Correction	μH	μD	μ^3He$^+$	μ^4He$^+$
III.A	$\alpha(Z\alpha)^2$	eVP$^{(1)}$	205.007 38	227.634 70	1641.886 2	1665.773 1
III.A	$\alpha^2(Z\alpha)^2$	eVP$^{(2)}$	1.658 85	1.838 04	13.084 3	13.276 9
III.A	$\alpha^3(Z\alpha)^2$	eVP$^{(3)}$	0.007 52	0.008 42(7)	0.073 0(30)	0.074 0(30)
III.B	$(Z, Z^2, Z^3)\alpha^5$	Light-by-light eVP	−0.000 89(2)	−0.000 96(2)	−0.013 4(6)	−0.013 6(6)
III.C	$(Z\alpha)^4$	Recoil	0.057 47	0.067 22	0.126 5	0.295 2
III.D	$\alpha(Z\alpha)^4$	Relativistic with eVP$^{(1)}$	0.018 76	0.021 78	0.509 3	0.521 1
III.E	$\alpha^2(Z\alpha)^4$	Relativistic with eVP$^{(2)}$	0.000 17	0.000 20	0.005 6	0.005 7
III.F	$\alpha(Z\alpha)^4$	μSE$^{(1)}$ + μVP$^{(1)}$, LO	−0.663 45	−0.769 43	−10.652 5	−10.926 0
III.G	$\alpha(Z\alpha)^5$	μSE$^{(1)}$ + μVP$^{(1)}$, NLO	−0.004 43	−0.005 18	−0.174 9	−0.179 7
III.H	$\alpha^2(Z\alpha)^4$	μVP$^{(1)}$ with eVP$^{(1)}$	0.000 13	0.000 15	0.003 8	0.003 9
III.I	$\alpha^2(Z\alpha)^4$	μSE$^{(1)}$ with eVP$^{(1)}$	−0.002 54	−0.003 06	−0.062 7	−0.064 6
III.J	$(Z\alpha)^5$	Recoil	−0.044 97	−0.026 60	−0.558 1	−0.433 0
III.K	$\alpha(Z\alpha)^5$	Recoil with eVP$^{(1)}$	0.000 14(14)	0.000 09(9)	0.004 9(49)	0.003 9(39)
III						
III						
III						
III						
IV						
IV						
IV						
V.A						
V.B						
V.C	$(Z\alpha)^6$	3PE	−0.001 3(3)	0.002 2(9)	−0.214(214)	−0.165(165)
V.D	$\alpha(Z\alpha)^5$	eVP$^{(1)}$ with TPE	0.000 6(1)	0.027 5(4)	0.266(24)	0.158(12)
V.E	$\alpha(Z\alpha)^5$	μSE$^{(1)}$ + μVP$^{(1)}$ with TPE	0.000 4	0.002 6(3)	0.077(8)	0.059(6)
III	E_{QED}	Point nucleus	206.034 4(3)	228.774 0(3)	1644.348(8)	1668.491(7)
IV	Cr_C^2	Finite size	$-5.225\,9r_p^2$	$-6.107\,4r_d^2$	$-103.383r_h^2$	$-106.209r_\alpha^2$
V	E_{NS}	Nuclear structure	0.028 9(25)	1.750 3(200)	15.499(378)	9.276(433)
	E_L (exp)	Experiment[a]	202.370 6(23)	202.878 5(34)	1258.598(48)	1378.521(48)
	r_C	This review	0.840 60(39)	2.127 58(78)	1.970 07(94)	1.678 6(12)
	r_C	Previous work[a]	0.840 87(39)	2.125 62(78)	1.970 07(94)	1.678 24(83)

Pachucki, Lensky, Hagelstein, LiMuli, Bacca, RP, RMP 96 (2024)

The “Proton Radius Puzzle“

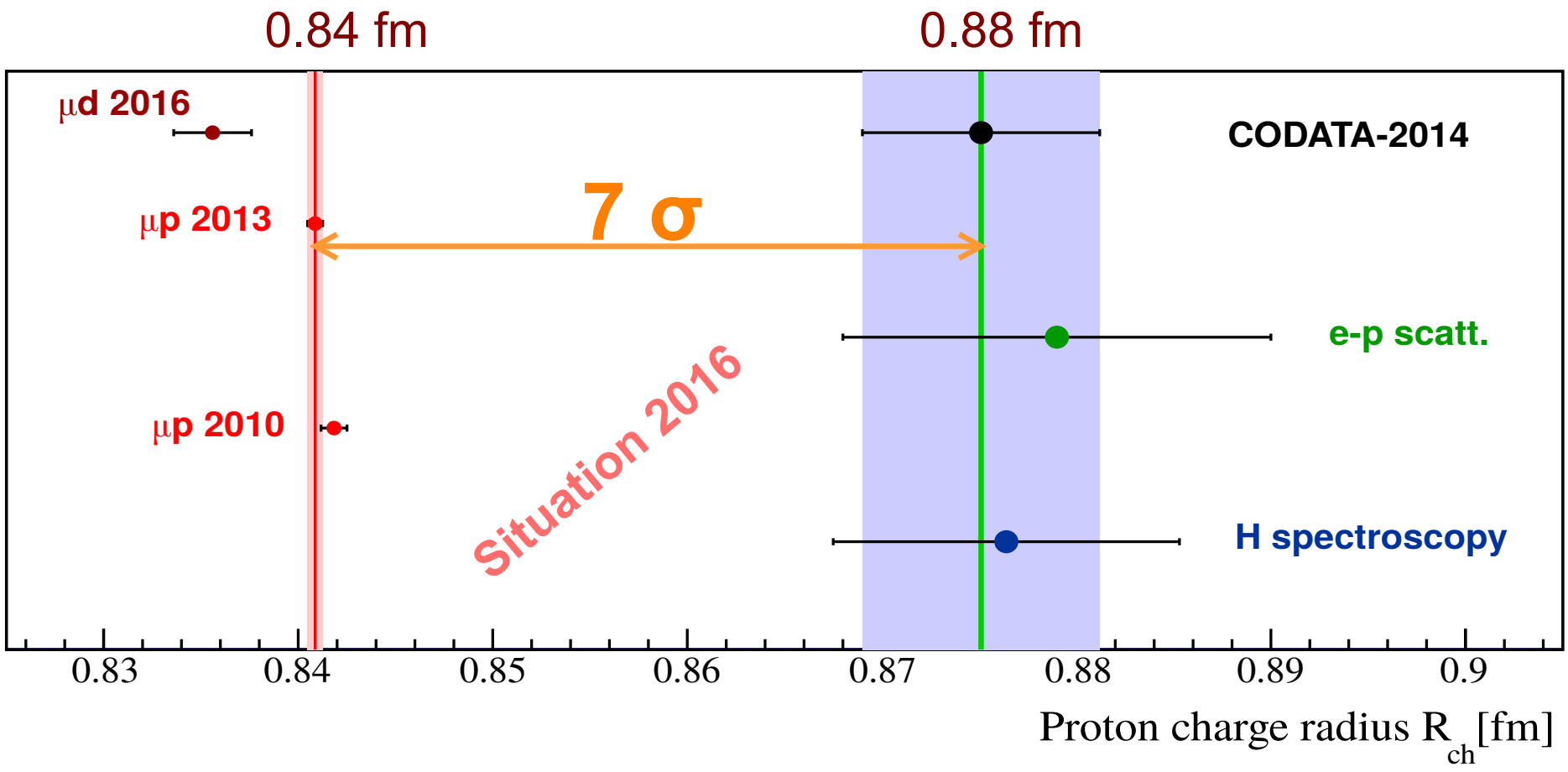

μd 2016: RP et al (CREMA Coll.) Science 353, 669 (2016)
μp 2013: A. Antognini, RP et al (CREMA Coll.) Science 339, 417 (2013)

Proton radius from **ordinary** hydrogen

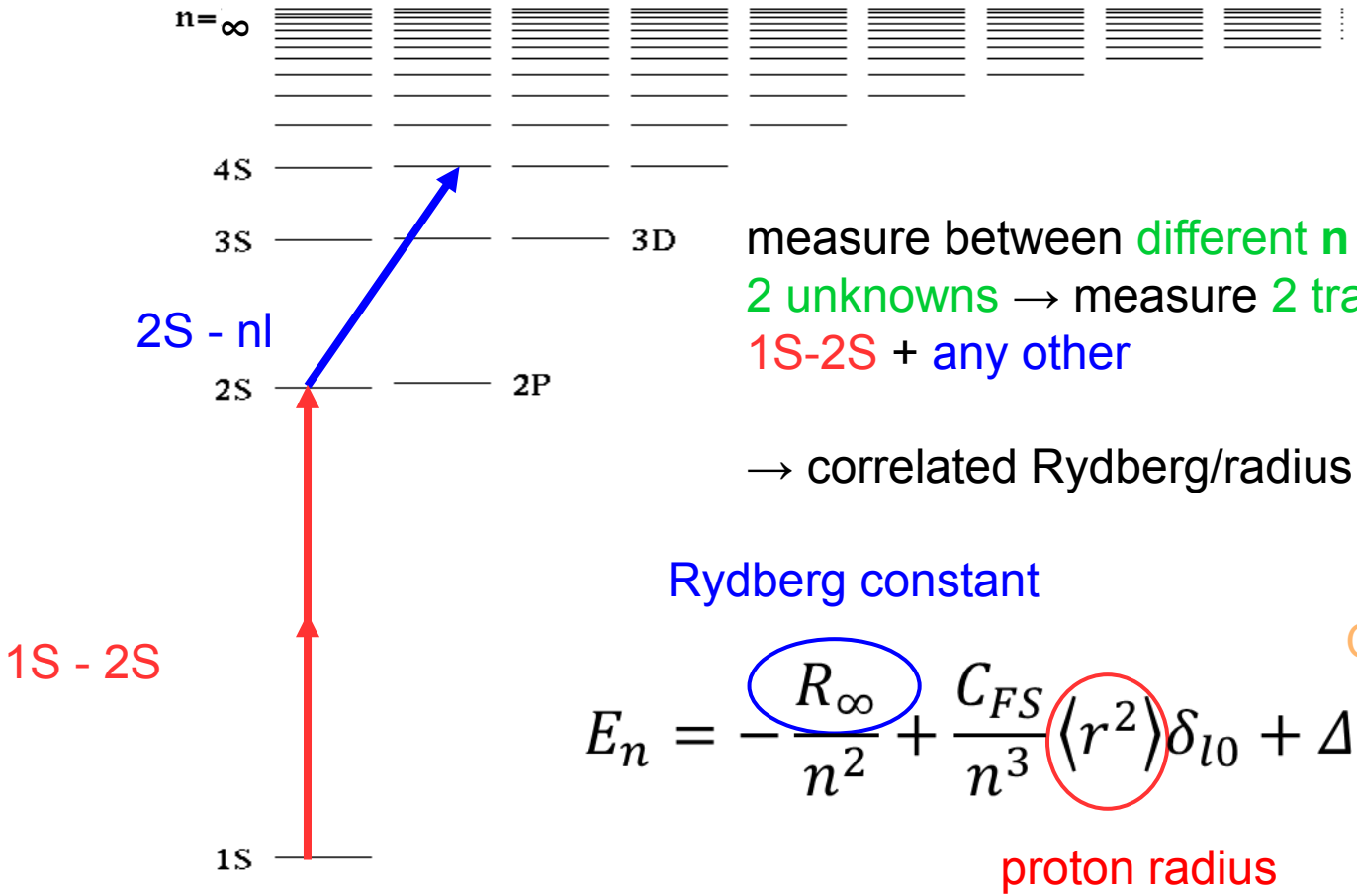

measure between different **n**

2 unknowns → measure 2 transitions:

1S-2S + any other

→ correlated Rydberg/radius pairs

Rydberg constant

QED etc.

$$E_n = -\frac{R_\infty}{n^2} + \frac{C_{FS}}{n^3}\langle r^2 \rangle \delta_{l0} + \Delta(n,l,j)$$

proton radius

(Normal) Hydrogen 2S-nP in Garching

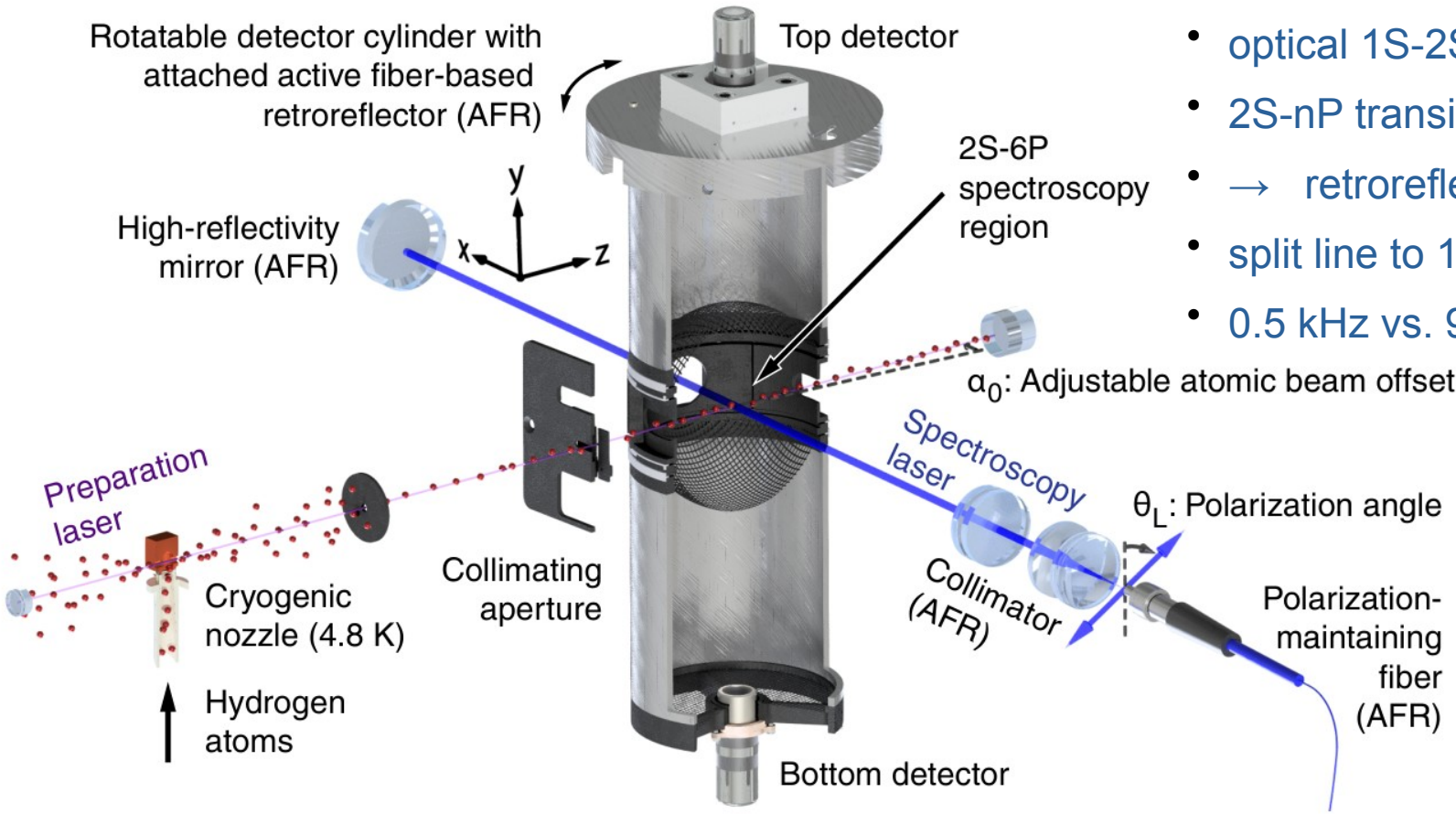

- cryogenic H beam (6 K)
- optical 1S-2S excitation (2S, F=0)
- 2S-nP transition is 1-photon
- → retroreflector (“AFR”)
- split line to 10^{-4}
- 0.5 kHz vs. 9 kHz PRP

Beyer, Maisenbacher, RP et al, Science 358, 79 (2017)

Hydrogen 2S-nP in Garching

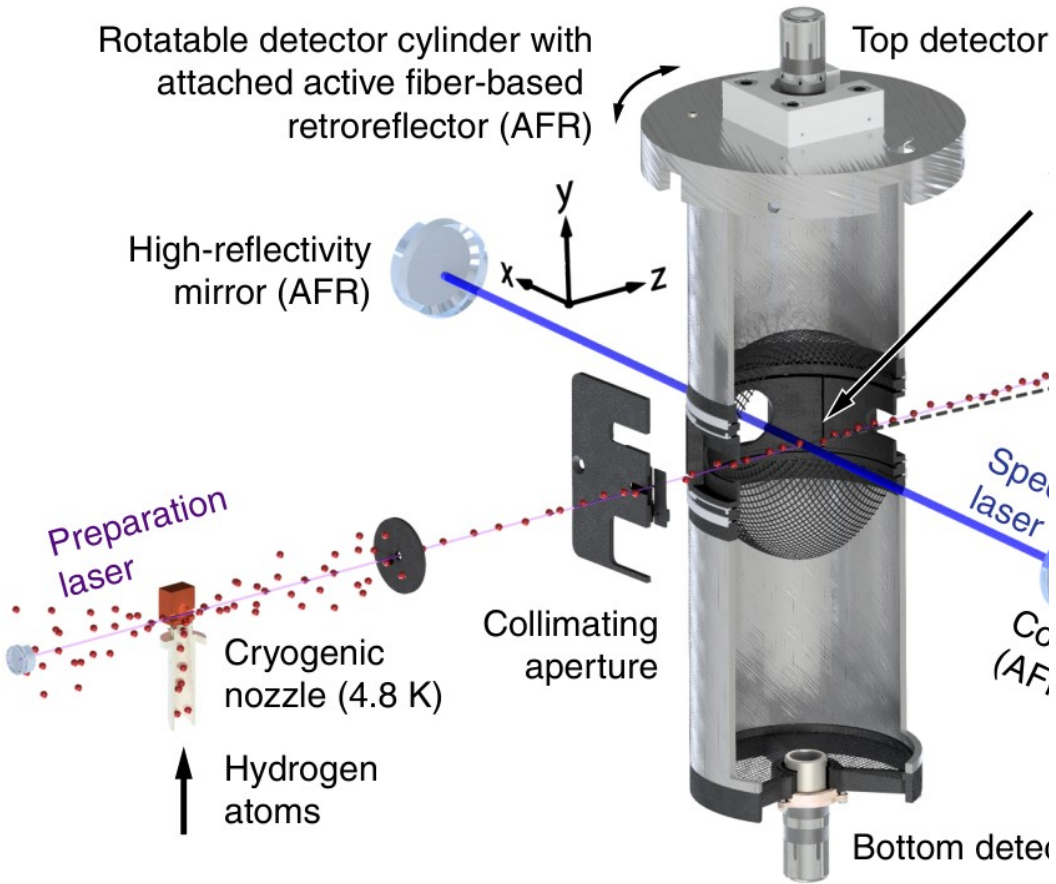

1st order Doppler cancellation (2S-4P)

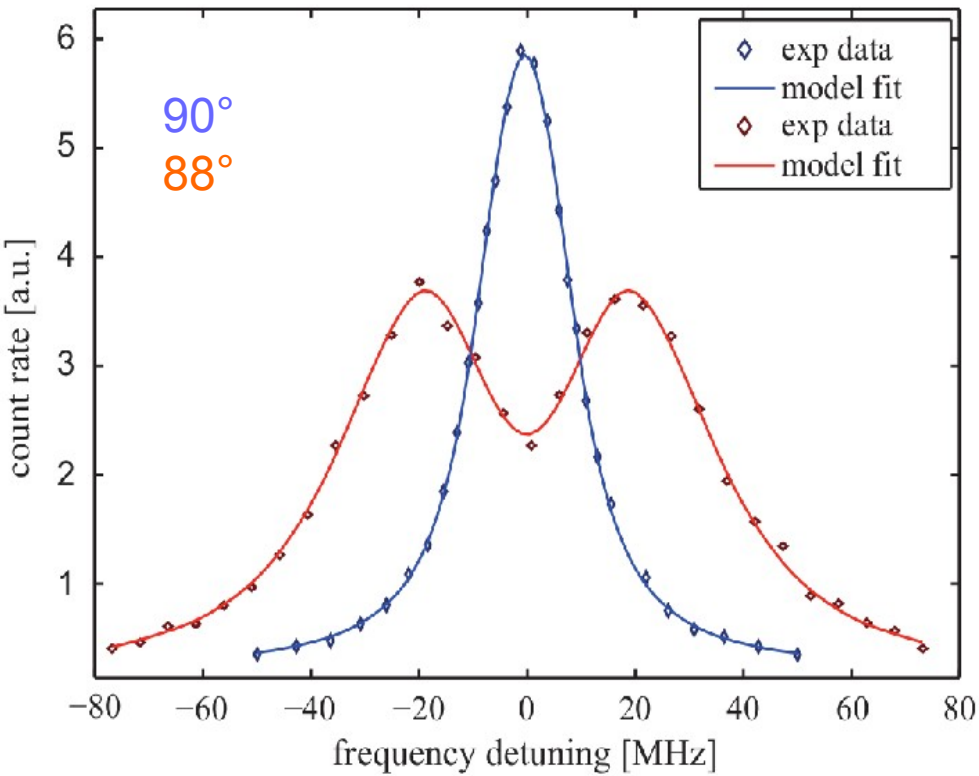

Beyer, Maisenbacher, RP et al, Science 358, 79 (2017)

The proton radius situation “yesterday”

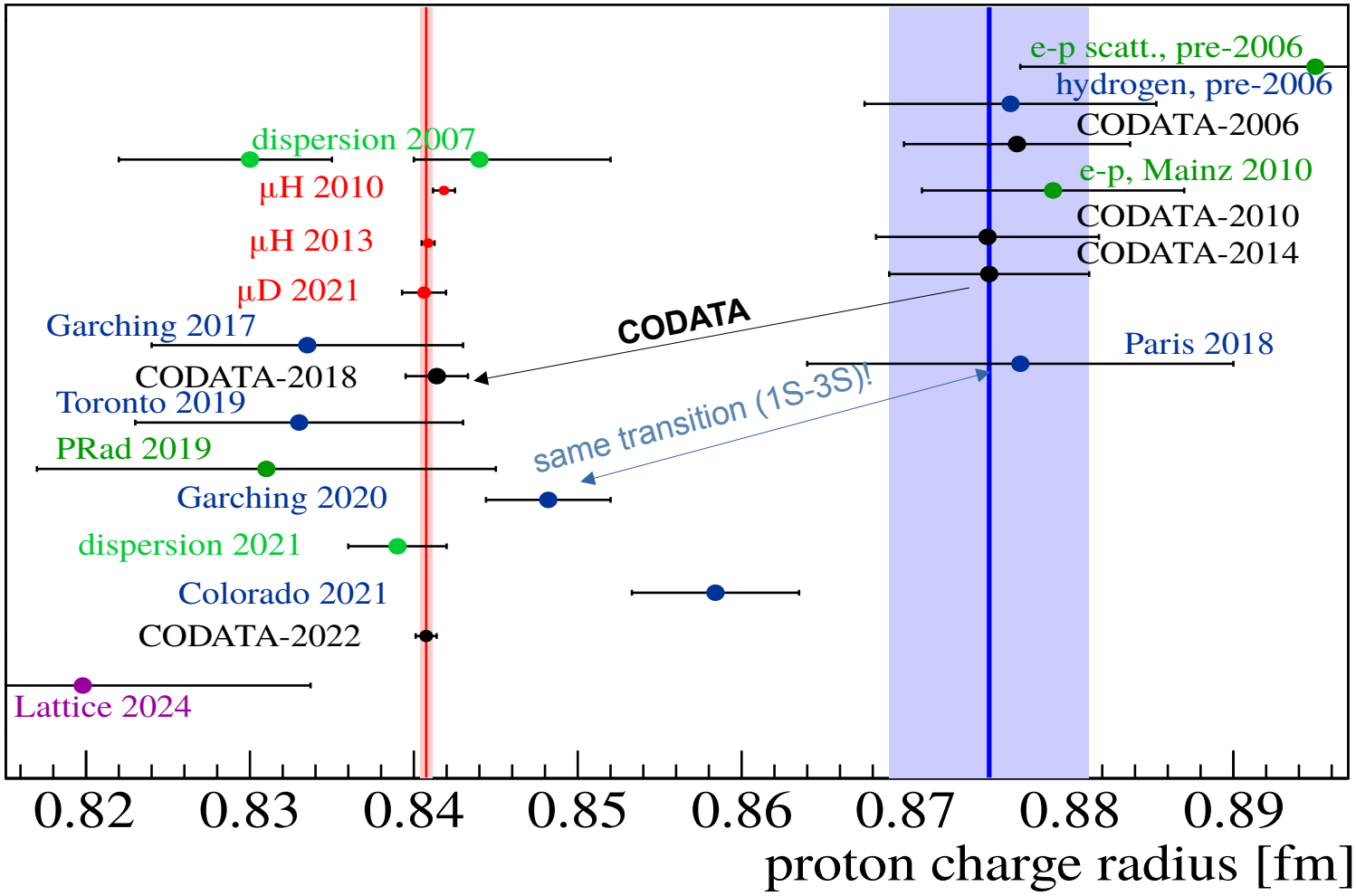

Not really “solved”

NEW Hydrogen 2S-6P in Garching

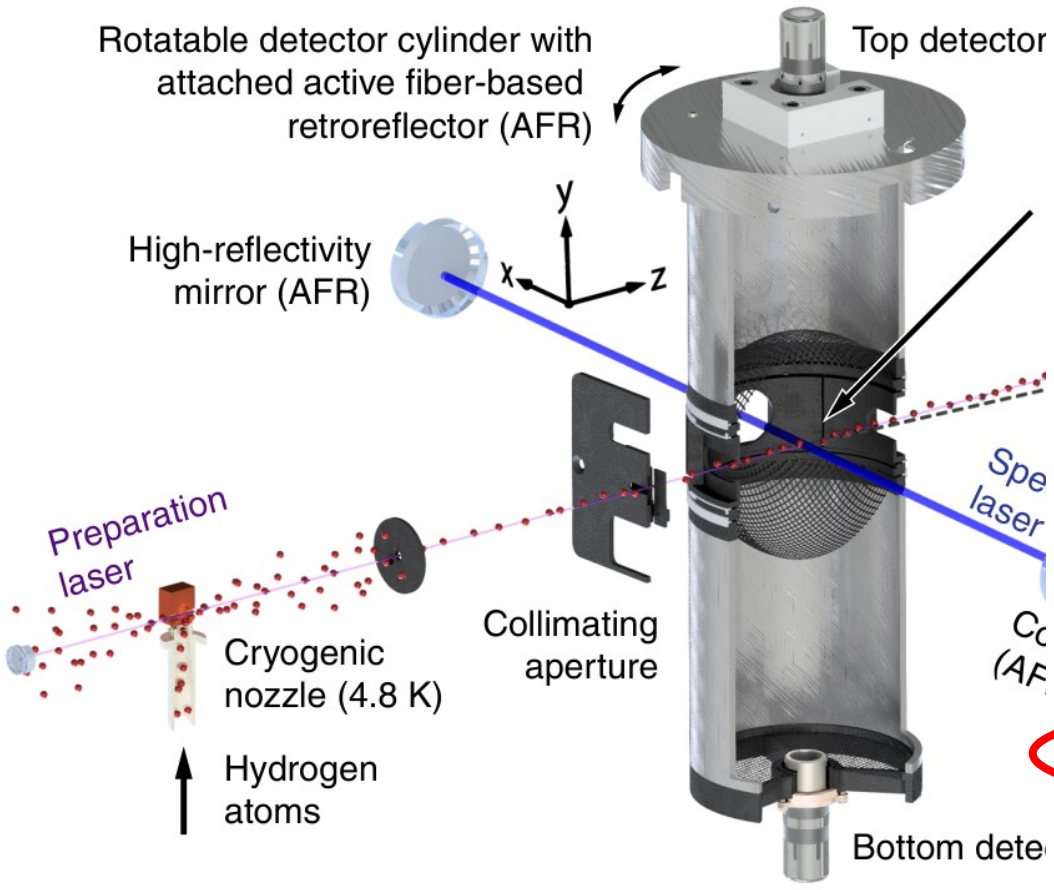

Systematics (2S-6P)

Contribution	$\Delta\nu$ (kHz)	σ (kHz)
First-order Doppler shift	0.34	0.43
Extrapolation (statistical)	0.34	0.43
Simulation of atom speeds	—	0.01
Simulation corrections	1.05	0.17
Light force shift	1.15	0.17
Quantum interference shift	0.05	0.02
Second-order Doppler shift	−0.14	0.01
dc-Stark shift	0.05	0.07
BBR-induced shift	0.28	0.01
Zeeman shift	0.00	0.08
Pressure shift	0.00	0.02
Sampling bias	0.00	0.06
Signal background	0.00	0.03
Laser spectrum	0.00	0.07
Frequency standard	0.02	0.01
Subtotal (experiment-specific contributions)	1.74	0.48
Recoil shift	−1 176.03	0.00
HFS correction $\Delta\nu_{\mathrm{HFS}}(\nu_{\mathrm{2S\text{-}6P}})$	−132 985.25	0.01
Total (all contributions)	−134 159.54	0.48

Maisenbacher, RP et al., submitted (2025)

QED Test

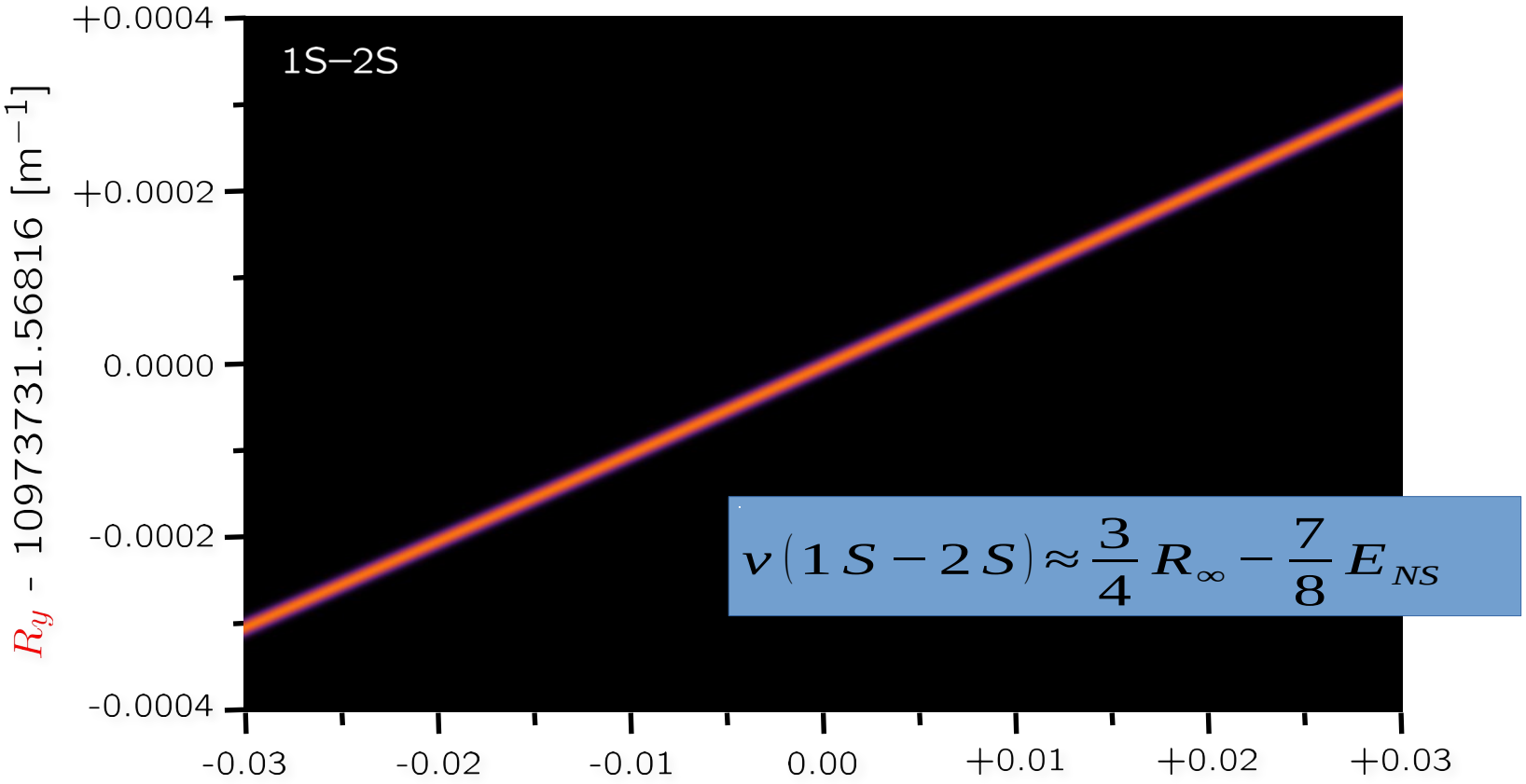

$$E_n = -\frac{R_\infty}{n^2} + \frac{C_{FS}}{n^3}\langle r^2 \rangle \delta_{l0} + \Delta(n,l,j)$$

QED Test

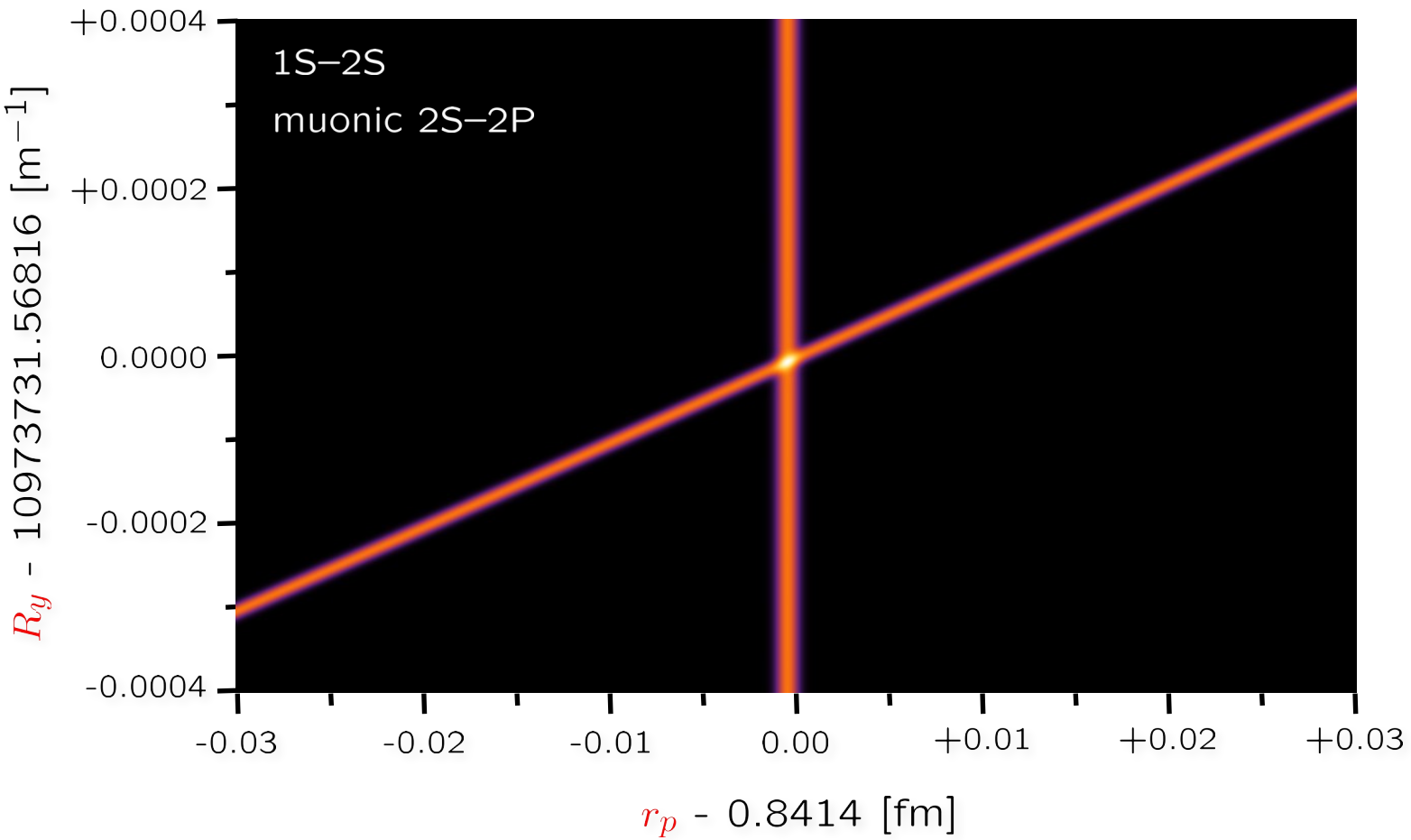
1S–2S
muonic 2S–2P
+0.0004
+0.0002
0.0000
-0.0002
-0.0004
R_y - 10973731.56816 [m^{-1}]
-0.03
-0.02
-0.01
0.00
+0.01
+0.02
+0.03
r_p - 0.8414 [fm]

QED Test

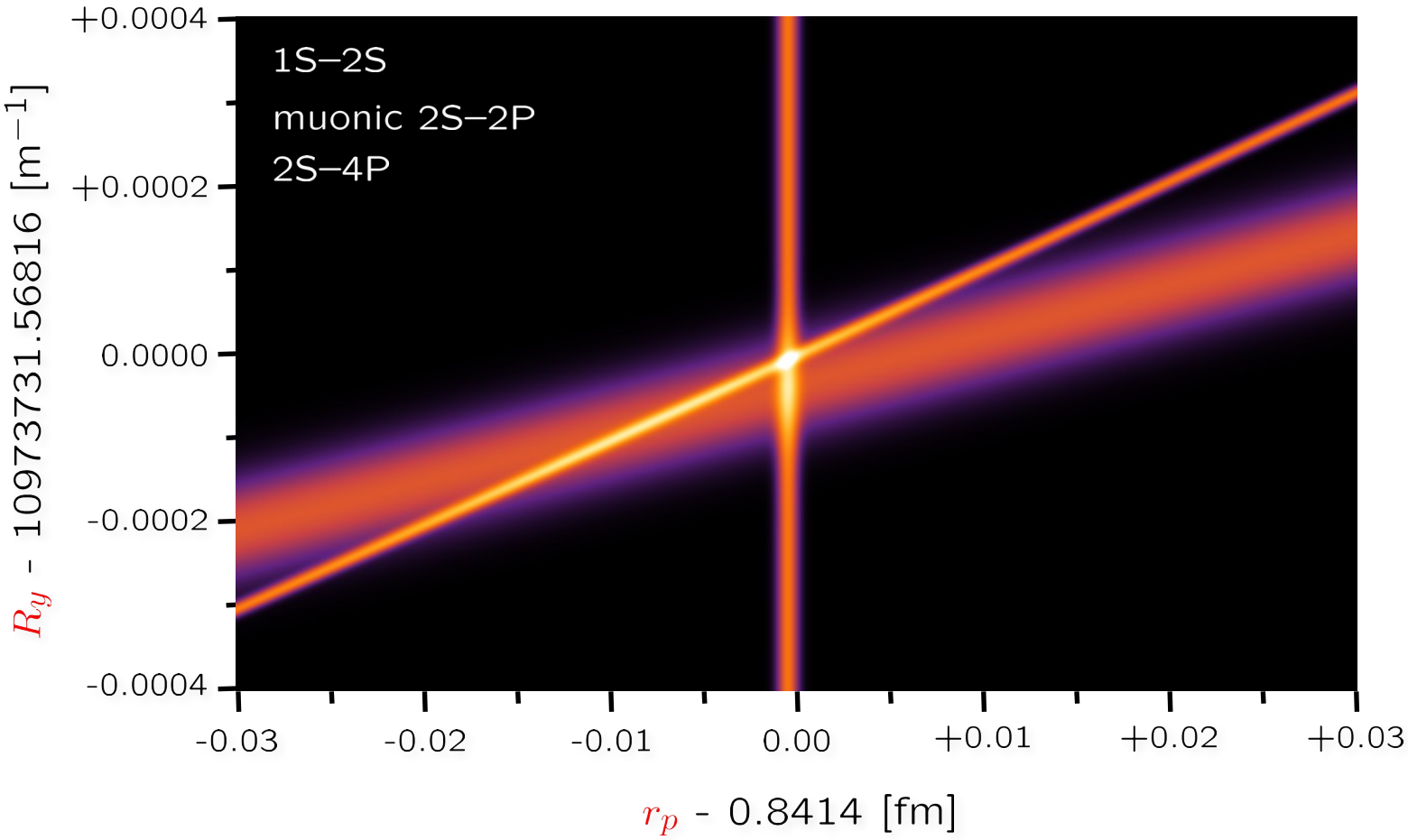
1S–2S
muonic 2S–2P
2S–4P
+0.0004
+0.0002
0.0000
-0.0002
-0.0004
R_y - 10973731.56816 [m^{-1}]
-0.03
-0.02
-0.01
0.00
+0.01
+0.02
+0.03
r_p - 0.8414 [fm]

QED Test

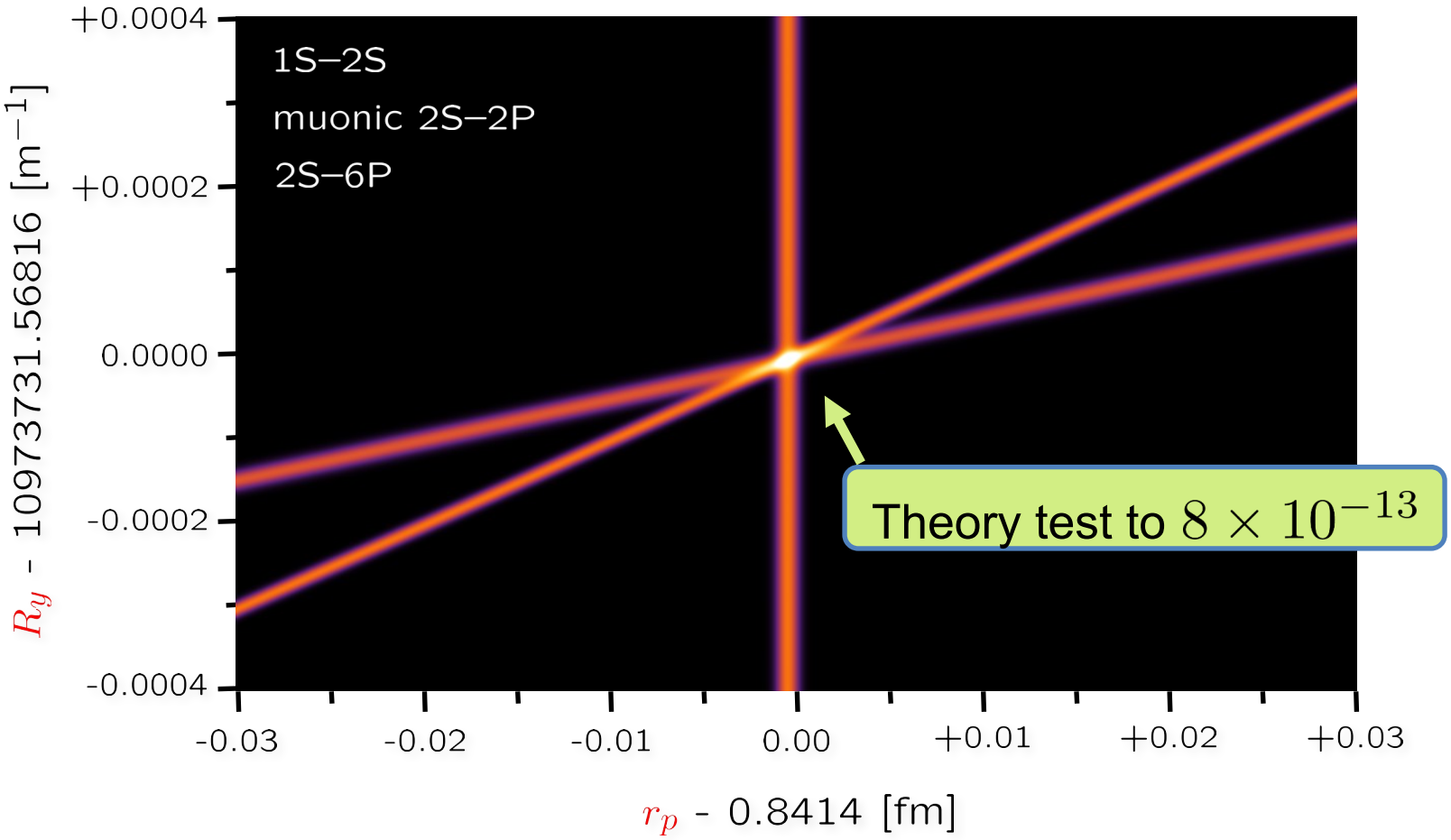
1S–2S
muonic 2S–2P
2S–6P
Theory test to 8×10^{-13}
R_y - 10973731.56816 [m^{-1}]
+0.0004
+0.0002
0.0000
-0.0002
-0.0004
-0.03
-0.02
-0.01
0.00
+0.01
+0.02
+0.03
r_p - 0.8414 [fm]

The proton radius situation today

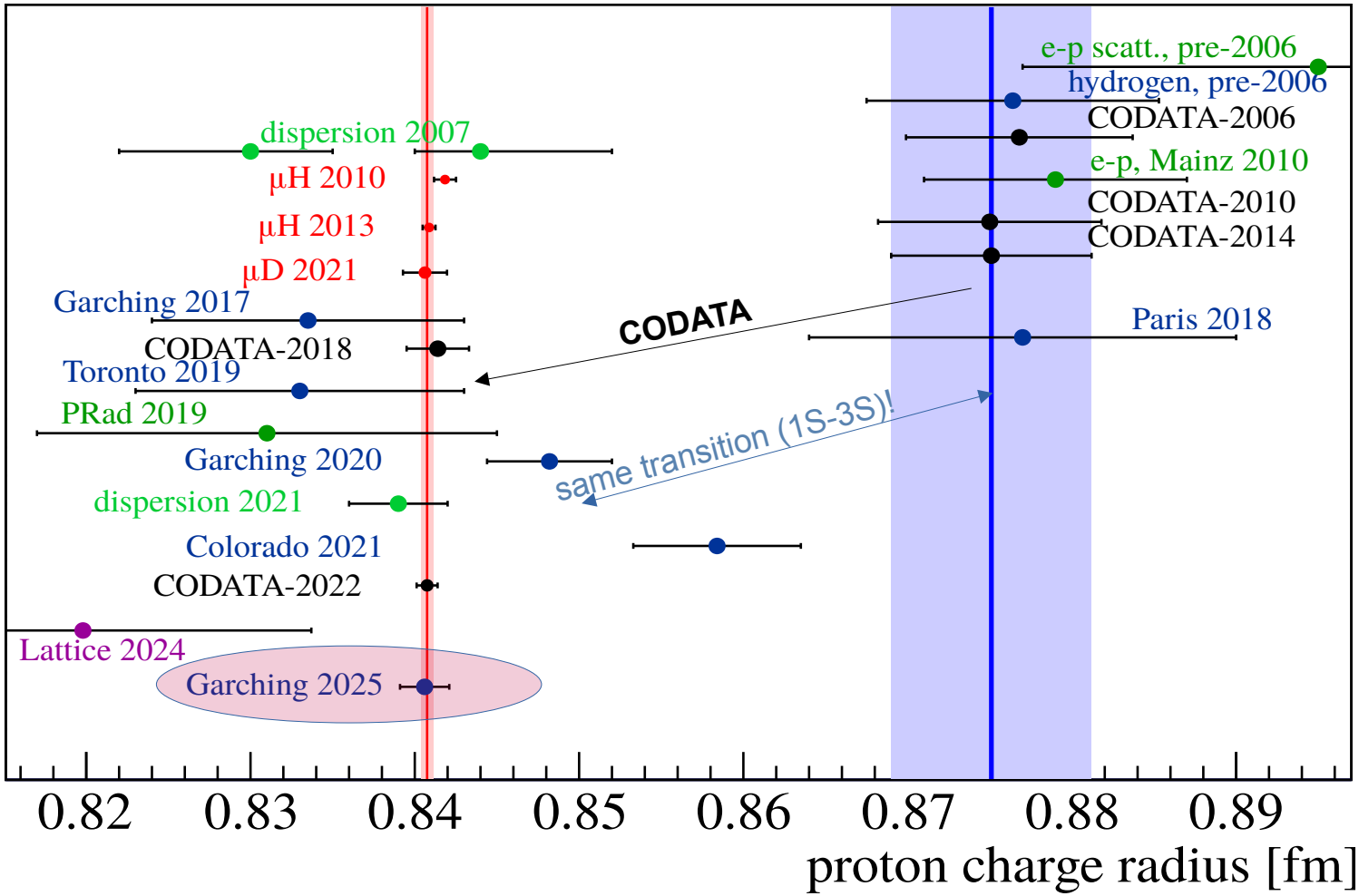

Not really “solved”

H (2S-6P) Nature (accepted)

Muonic Deuterium

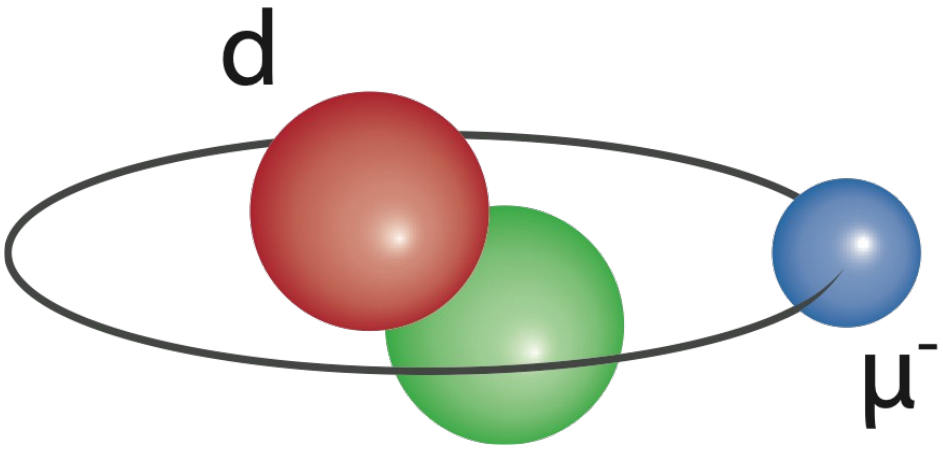

Pohl et al. (CREMA), Science (2016)

2.5 transitions in muonic D

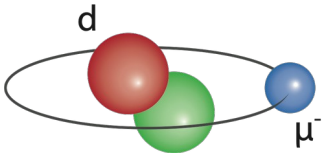

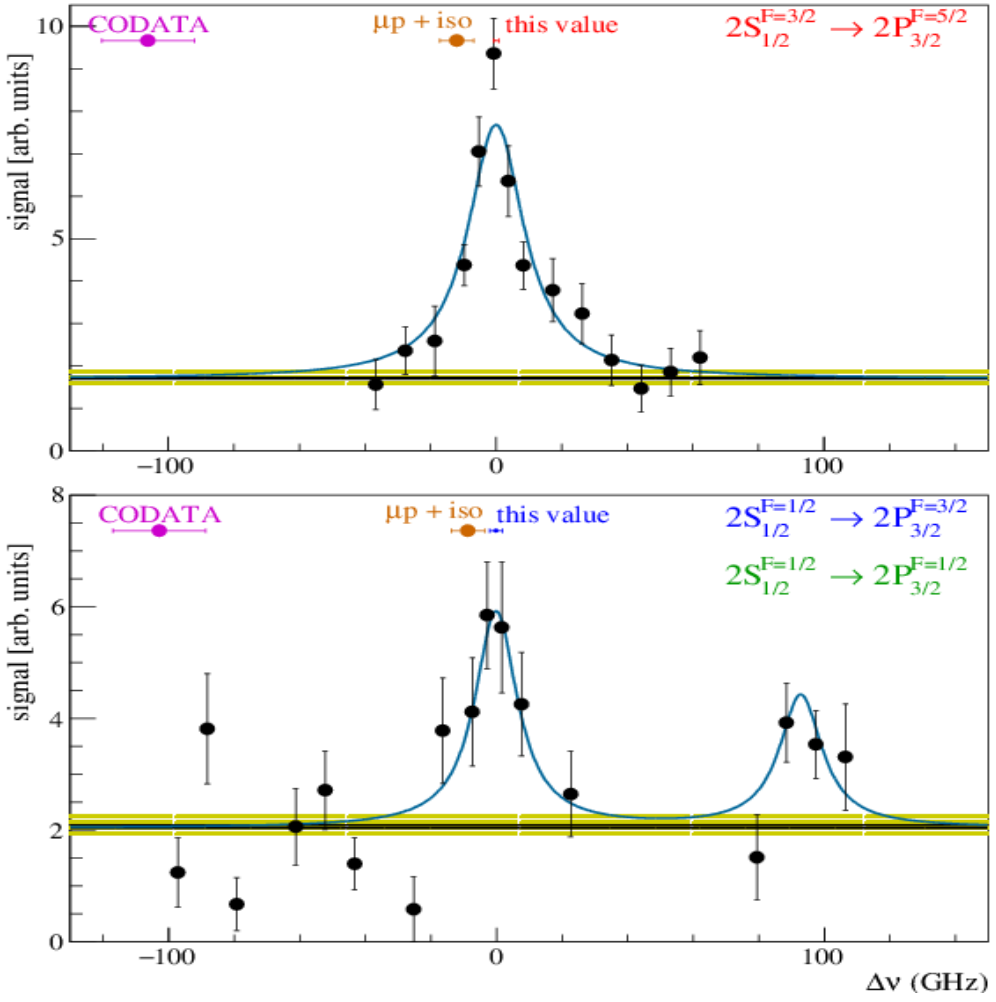

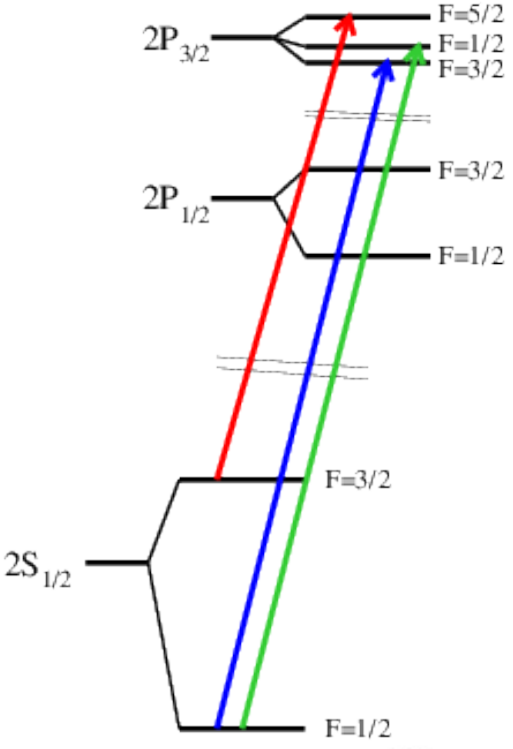

$$\Delta E^{\text{exp}}_{\text{LS}} = 202.8785(31)_{\text{stat}}(14)_{\text{syst}}\,\text{meV}$$

$$\Delta E^{\text{exp}}_{\text{HFS}} = 6.2747(70)_{\text{stat}}(20)_{\text{syst}}\,\text{meV}$$

Pohl et al. (CREMA Coll.), Science 353, 669 (2016)

Theory: Lamb shift in muonic D

$$\Delta E^{\mu D}_{\text{Lamb}} = 228.7740\,(3)\ \text{meV}_{\text{QED}} + 1.7503\,(\mathbf{200})\ \text{meV}_{\text{TPE}} - 6.1074\ \text{meV/fm}^2 * \mathbf{R_d^2}$$

$$\Delta E_{\text{LS}}^{\text{exp}} = 202.8785(31)_{\text{stat}}(14)_{\text{syst}}\ \text{meV}$$

Nuclear structure two (and three!)-photon contributions to the Lamb shift in muonic deuterium.

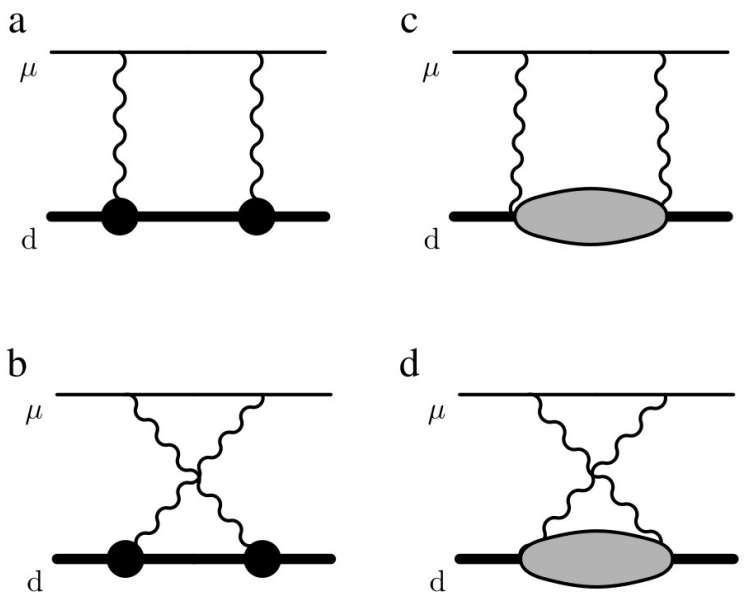

Pachucki, RP et al, arXiv 2212.13782

see also Krauth, RP et al. (2016) using calculations from
Pachucki (2011), Friar (2013), Carlson, Gorchtein, Vanderhaeghen (2014), Hernandez et al. (2014), Pachucki + Wienczek (2015)

+ Pachucki et al., PRA 97, 062511 (2018): Sizeable three-photon !!

+ Hernandez et al., PLB 778, 377 (2018): χEFT

+ Kalinowski (2019): eVP to nucl. struct.

+ Acharya et al., PRC 103, 024001 (2021)
χEFT + Disperson relations

Muonic Deuterium

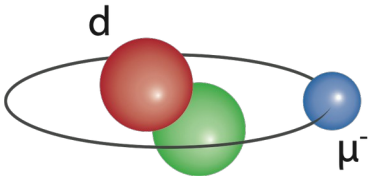

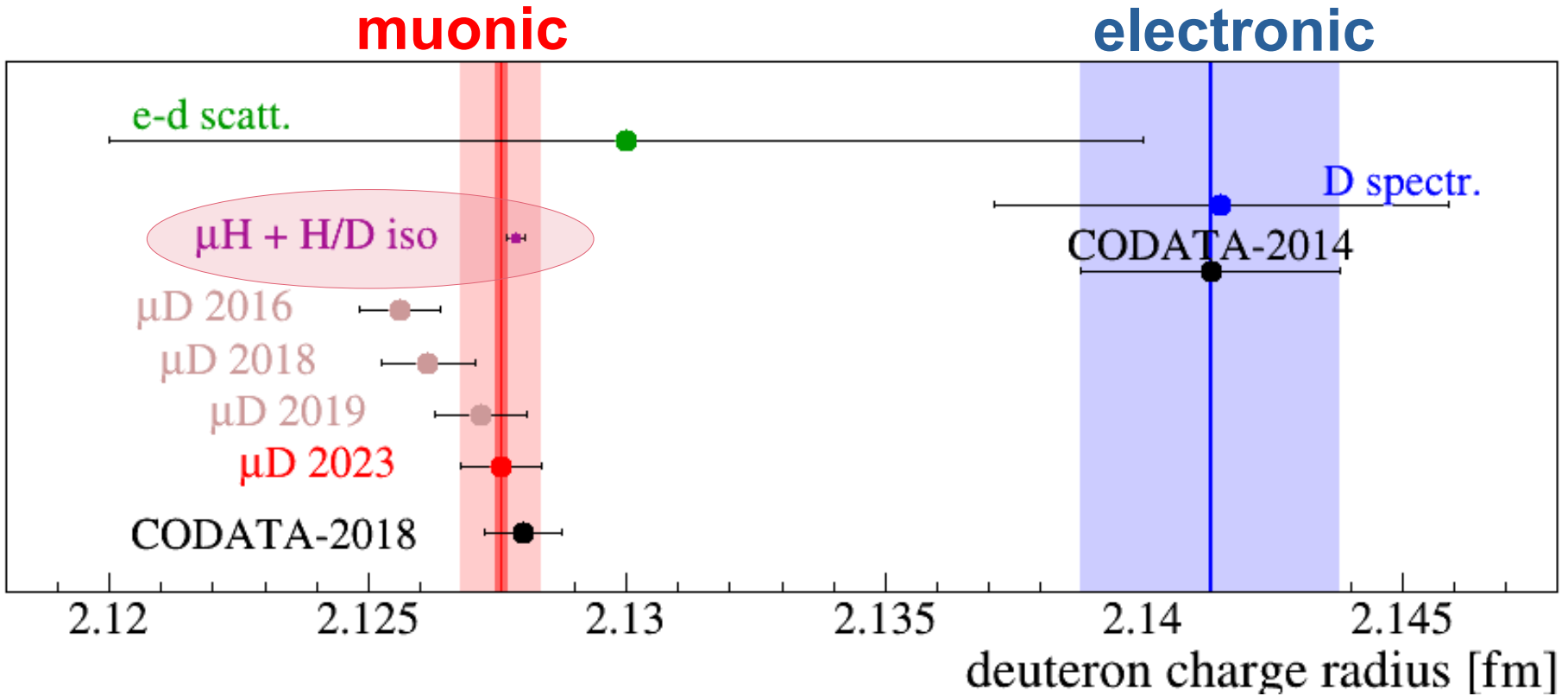

μD: 2.12758 $(13)_{exp}$ $(78)_{theo}$ fm

μH + H/D(1S-2S): 2.12785 (17) fm

$r_d^2 - r_p^2 = 3.8207(3)_{theo}$ fm^2

Theory in muonic D

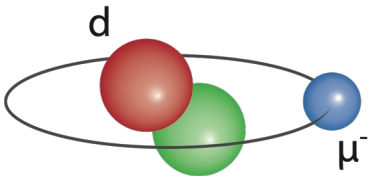

$$\Delta E^{\mu D}_{Lamb} = 228.7740\ (3)\ meV_{QED} + 1.7503\ (\mathbf{200})\ meV_{TPE} - 6.1074\ meV/fm^2 * \mathbf{R_d^2}$$

ΔE_{TPE} (theo) = 1.7503 +- 0.0200 meV Bacca group

vs. +- 0.0034 meV experimental uncertainty

(1) **charge radius**, using **calculated TPE**

r_d (μD) = 2.12758 $(13)_{exp}$ $(78)_{theo}$ fm

(2) **polarizability**, using **charge radius from isotope shift**

ΔE_{TPE} (theo) = 1.7503 (200) meV vs.

ΔE_{TPE} (exp) = 1.7591 (59) meV 3x more accurate

Pachucki, Lensky, Hagelstein, LiMuli, Bacca, Pohl, RMP (2024)

Muonic Deuterium

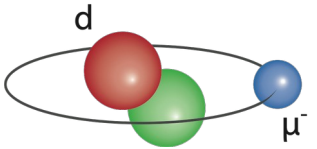

muonic

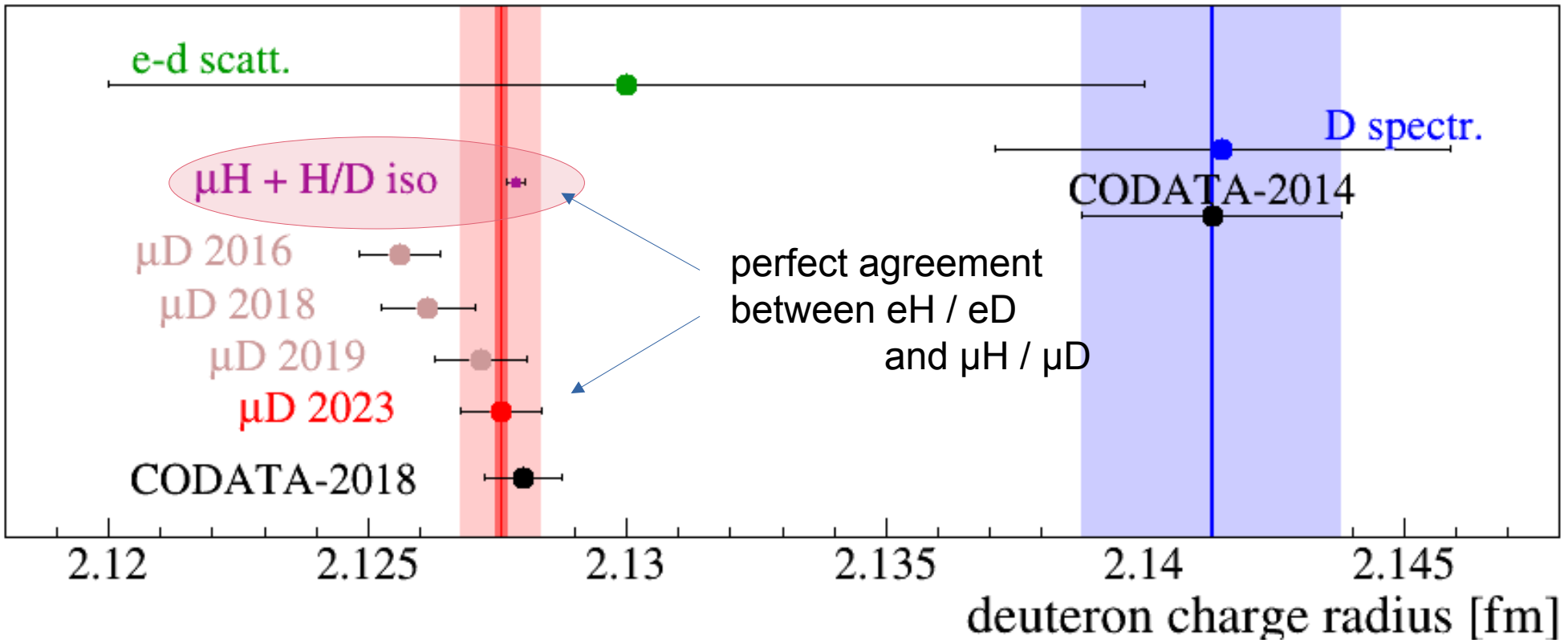

$r_d^2 - r_p^2$ = 3.8207(3) fm² H / D 1S-2S isotope shift

3.8200(31) fm² μH / μD 2S-2P isotope shift (0.2 σ)

H/D isotope shift

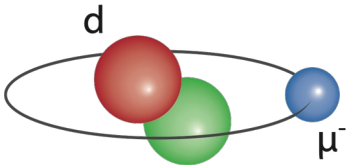

electronic H/D (1S-2S): $r_d^2 - r_p^2 = 3.8207(3)_{theo}$ fm^2

muonic H/D (2S-2P): $r_d^2 - r_p^2 = 3.8200(7)_{exp}(30)_{theo}$ fm^2

→ Best bound on 5th force

T. Sailer *et. al. (Blaum group)*, Nature 606 (2022)

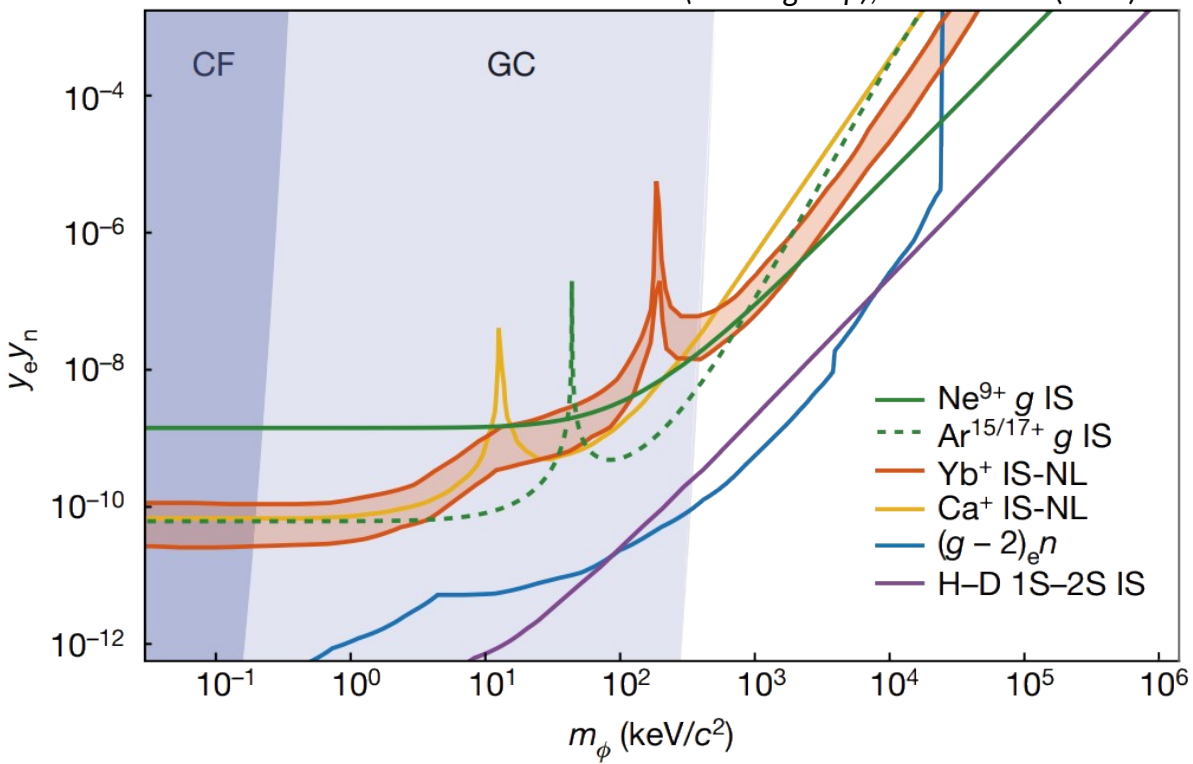

HFS in muonic D

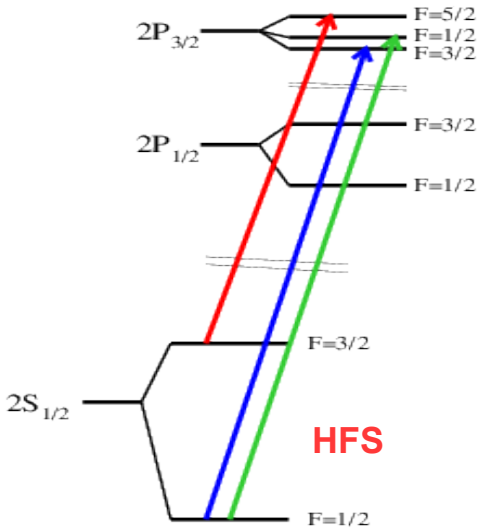

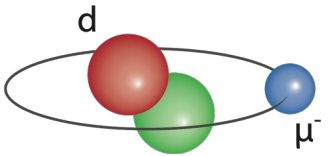

PHYSICAL REVIEW A **98**, 062513 (2018)

Nuclear-structure corrections to the hyperfine splitting in muonic deuterium

Marcin Kalinowski* and Krzysztof Pachucki†
Faculty of Physics, University of Warsaw, Pasteura 5, 02-093 Warsaw, Poland

Vladimir A. Yerokhin
Center for Advanced Studies, Peter the Great St. Petersburg Polytechnic University, 195251 St. Petersburg, Russia

(Received 15 October 2018; revised manuscript received 7 November 2018; published 17 December 2018)

Nuclear structure corrections of orders $Z\alpha\, E_F$ and $(Z\alpha)^2 E_F$ are calculated for the hyperfine splitting of the muonic deuterium. The obtained results disagree with previous calculations and lead to a $5\,\sigma$ disagreement with the current experimental value of the $2S$ hyperfine splitting in muonic deuterium.

5σ disagreement between theory and experiment !!!

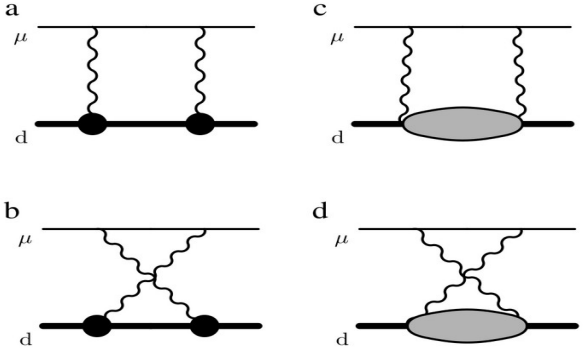

Muonic Helium-3 and -4

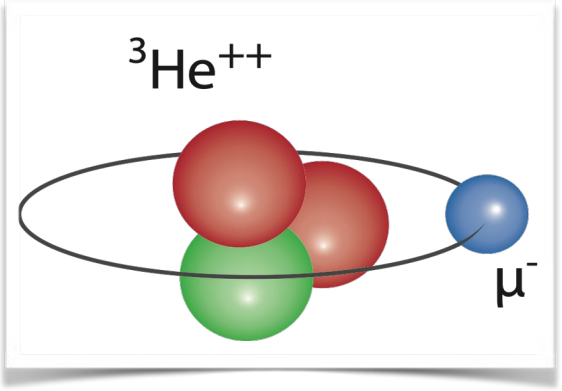

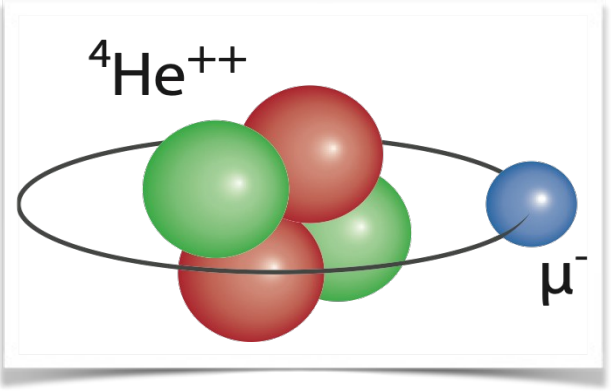

Schuhmann et al. (CREMA)
Science 388, 854 (2025)
arXiv 2305.11679

Krauth et al. (CREMA)
Nature 589, 527 (2021)

Helium-3 – Helium-4 Isotope Shift

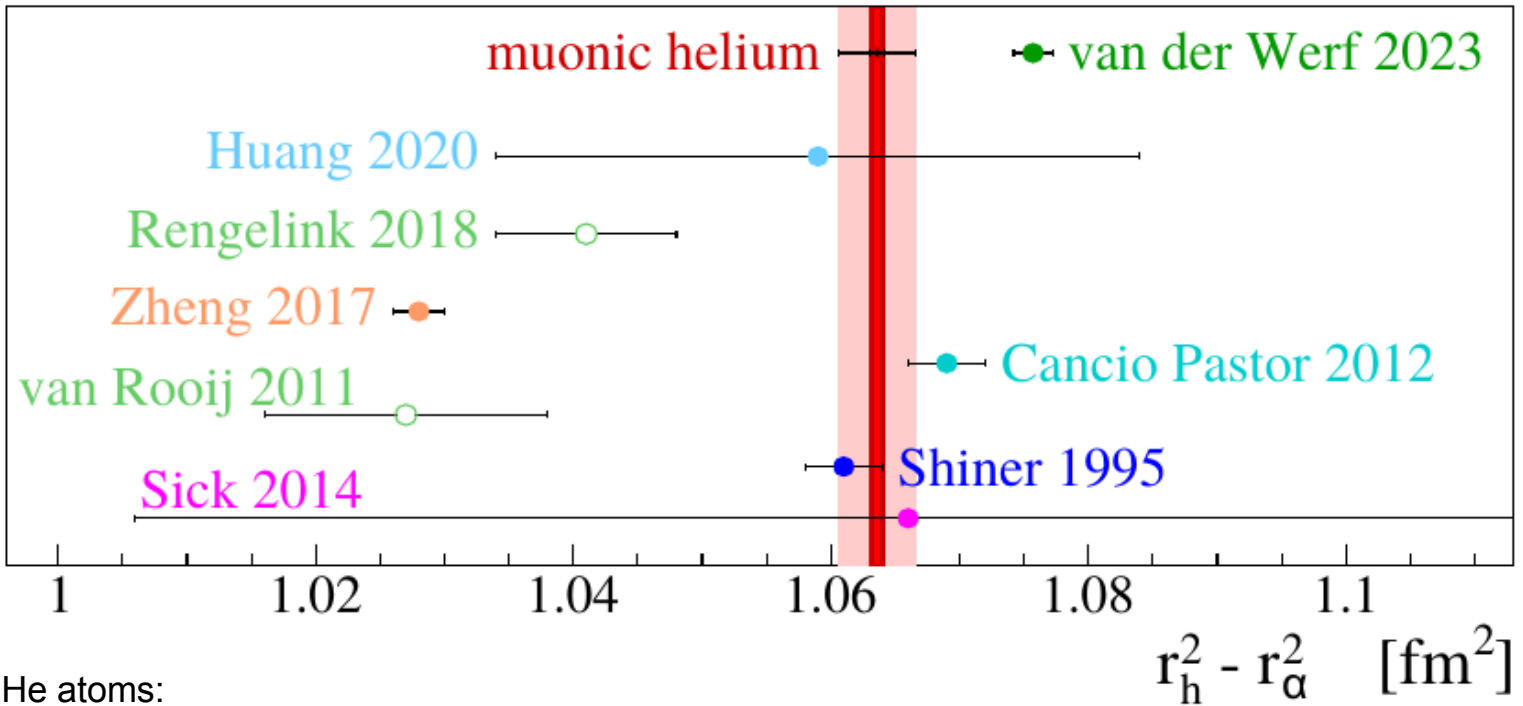

3.6σ !

normal He atoms:

van der Werf et al.: Science (2025 / arXiv 2306.02333
Huang: PRA 101, 062507 (2020)
Rengelink: Nature Physics 14, 1132 (2018)
Zheng: PRL 119, 263002 (2017)
van Rooij: Science 333, 196 (2011)
Cancio Pastor: PRL 108, 143001 (2012)
Shiner: PRL 74, 3553 (1995)

CREMA Coll., Science 388, 852 (2025)

Helium-3 – Helium-4 Isotope Shift

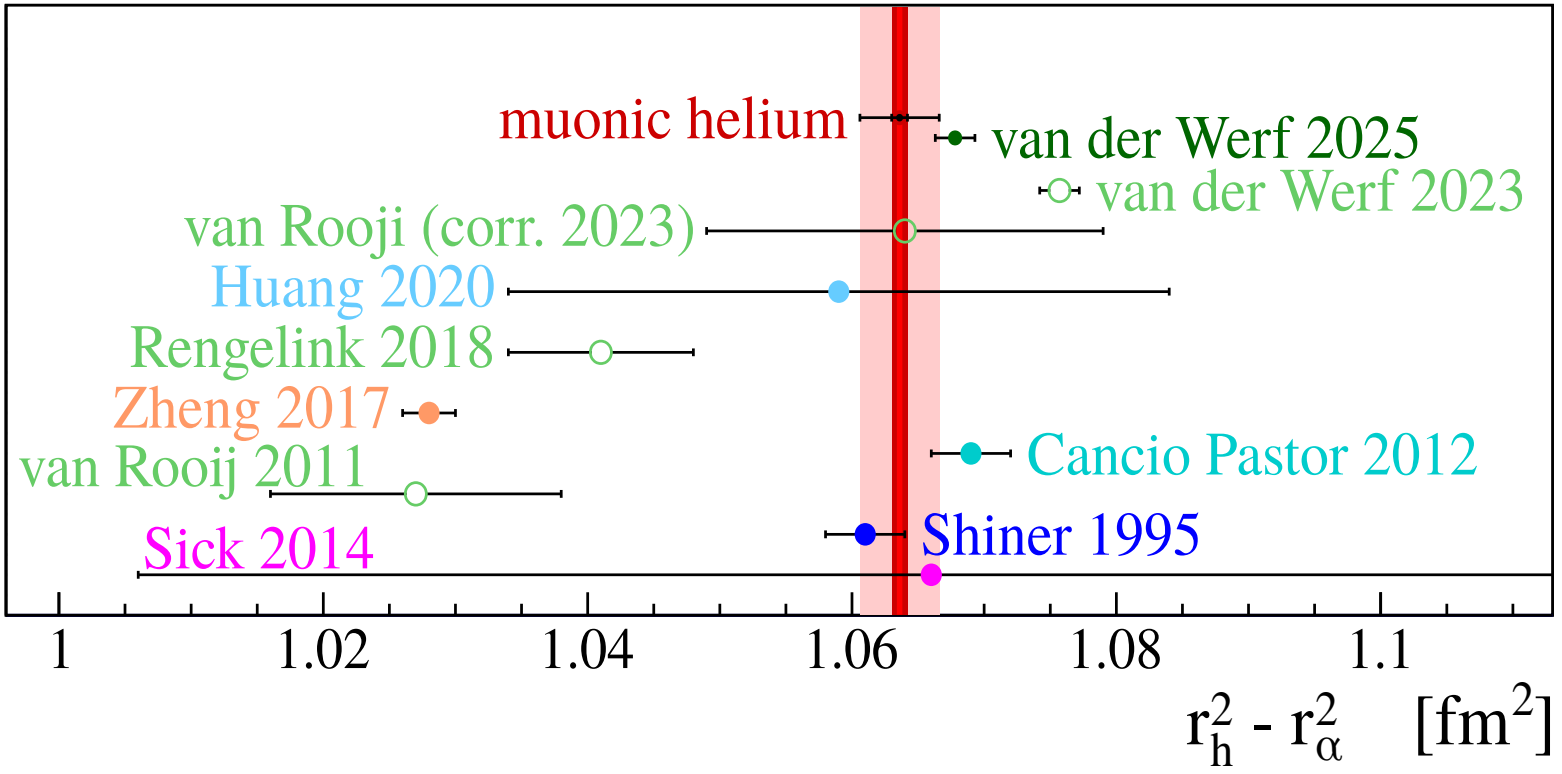

2nd order hyperfine mixing

Qi et al, 2024
Pachucki et al. 2024

CREMA Coll., Science 388, 852 (2025)

Helium-3 – Helium-4 Isotope Shift

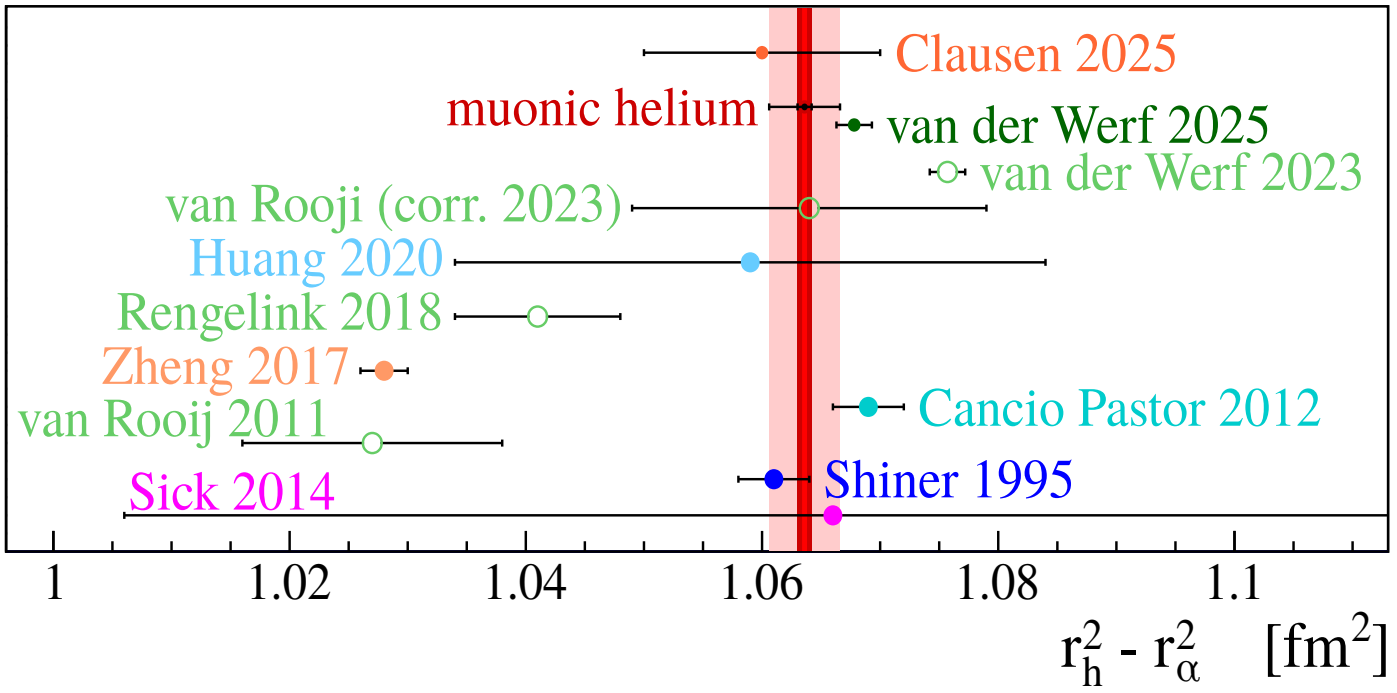

CREMA Coll., Science 388, 852 (2025)

Intermediate conclusions

Muonic atoms / ions provide:

- **~10x more accurate charge radii**, when combined with **calculated polarizability**

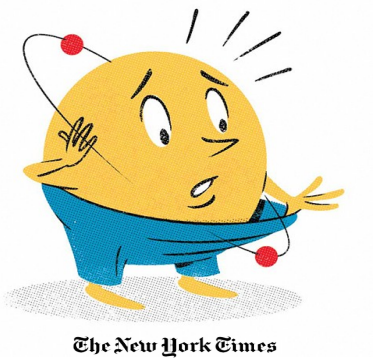

	^{3}He 1.9701*(10) ~~1.9730 (160)~~	^{4}He 1.6786 (12) ~~1.6810 (40)~~
^{1}H 0.8406 (4) ~~0.8751 (61)~~	^{2}D 2.1279 (2) ~~2.1413 (25)~~	^{3}T 1.7550 (860)

Intermediate conclusions

Muonic atoms / ions provide:

- **~10x more accurate charge radii**, when combined with **calculated polarizability**
- few times more accurate **nuclear polarizability (TPE)** ,
- when combined with **charge radius from regular atoms**
- $\Delta E(\text{meas}) = \text{QED} + \text{TPE} - C * R_\alpha^2 / \text{fm}^2$

$$\text{TPE} = 2\text{PE} + 3\text{PE}$$

Muonic atoms are a novel tool for proton and new-nucleon properties!

From Laser to

X-ray spectroscopy

X-ray spectroscopy

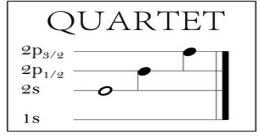

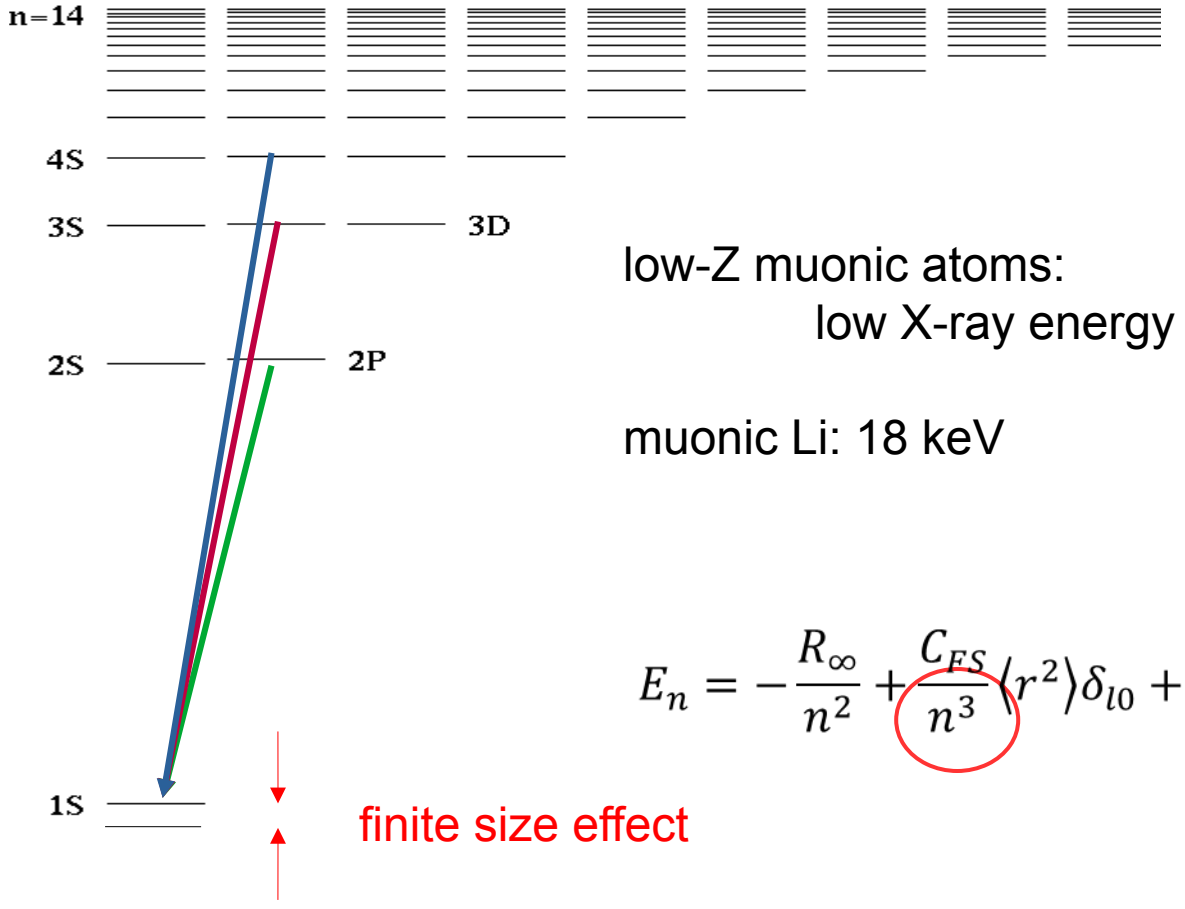

finite size effect

low-Z muonic atoms:

low X-ray energy → difficult!

muonic Li: 18 keV

$$E_n = -\frac{R_\infty}{n^2} + \frac{C_{FS}}{n^3}\langle r^2\rangle\delta_{l0} + \Delta(n,l,j)$$

QUARTET: X-ray spectroscopy

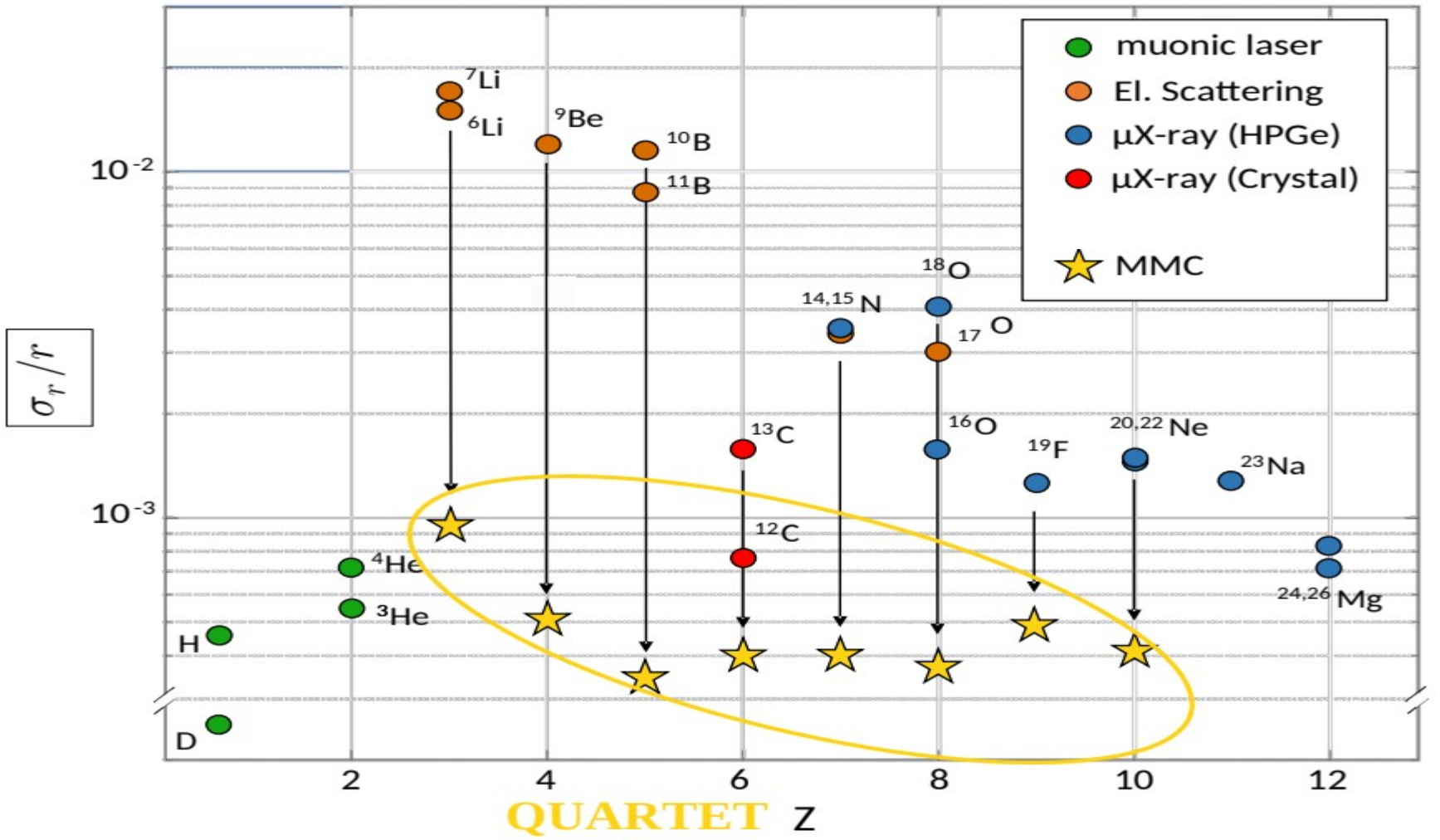

Metallic Magnetic Calorimeters (MMCs)

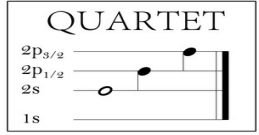

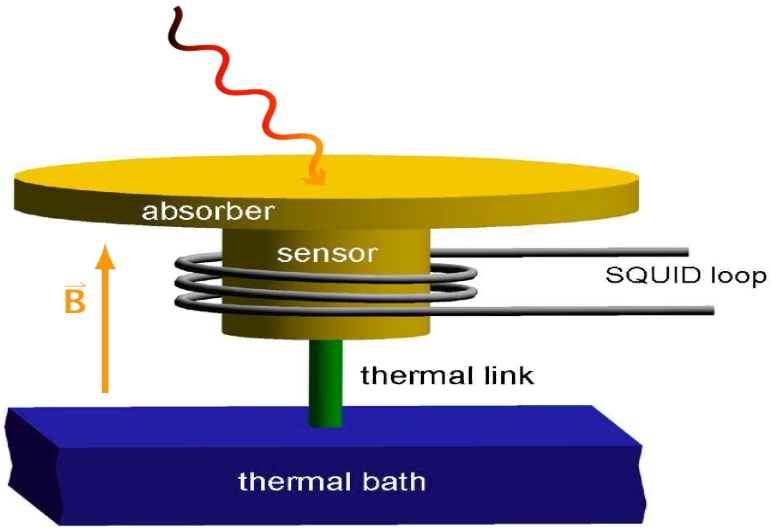

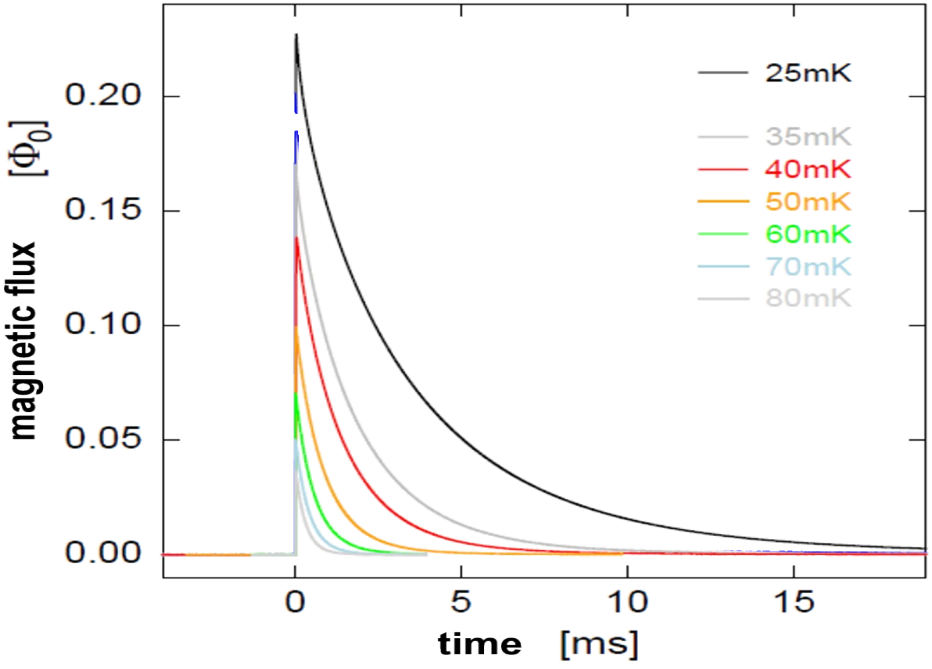

Magnetization of paramagnetic material:

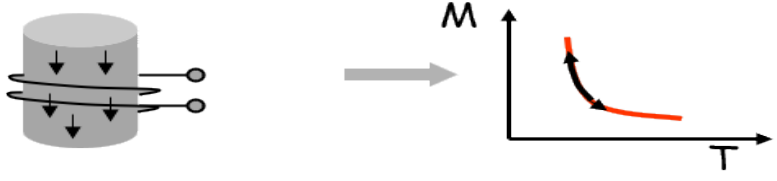

Decay time 3ms@30mK
Keep rates < 10 Hz
per pixel to avoid pileup

Andreas Fleischmann & Loredana Gastaldo, Kirchhoff Institute of Physics (KIP), Heidelberg

Metallic Magnetic Calorimeters (MMCs)

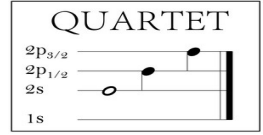

pixel array, area 16mm^2

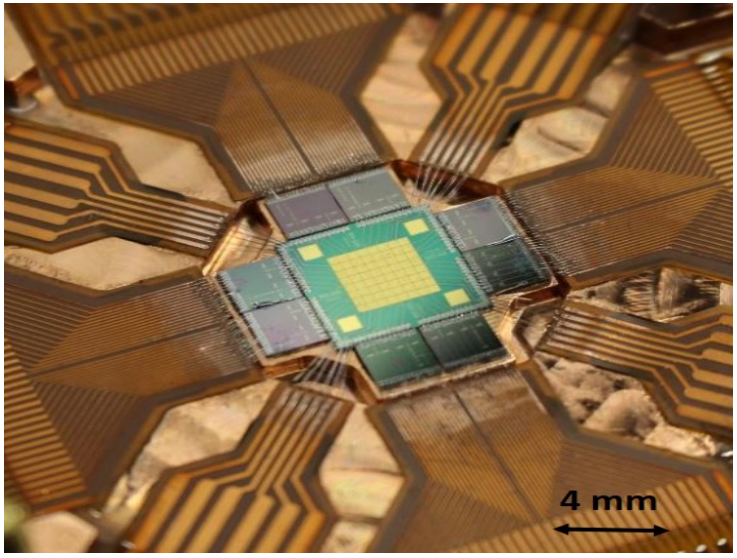

High efficiency (>90%) for photons 10-60 keV

(2025: up to >170keV)

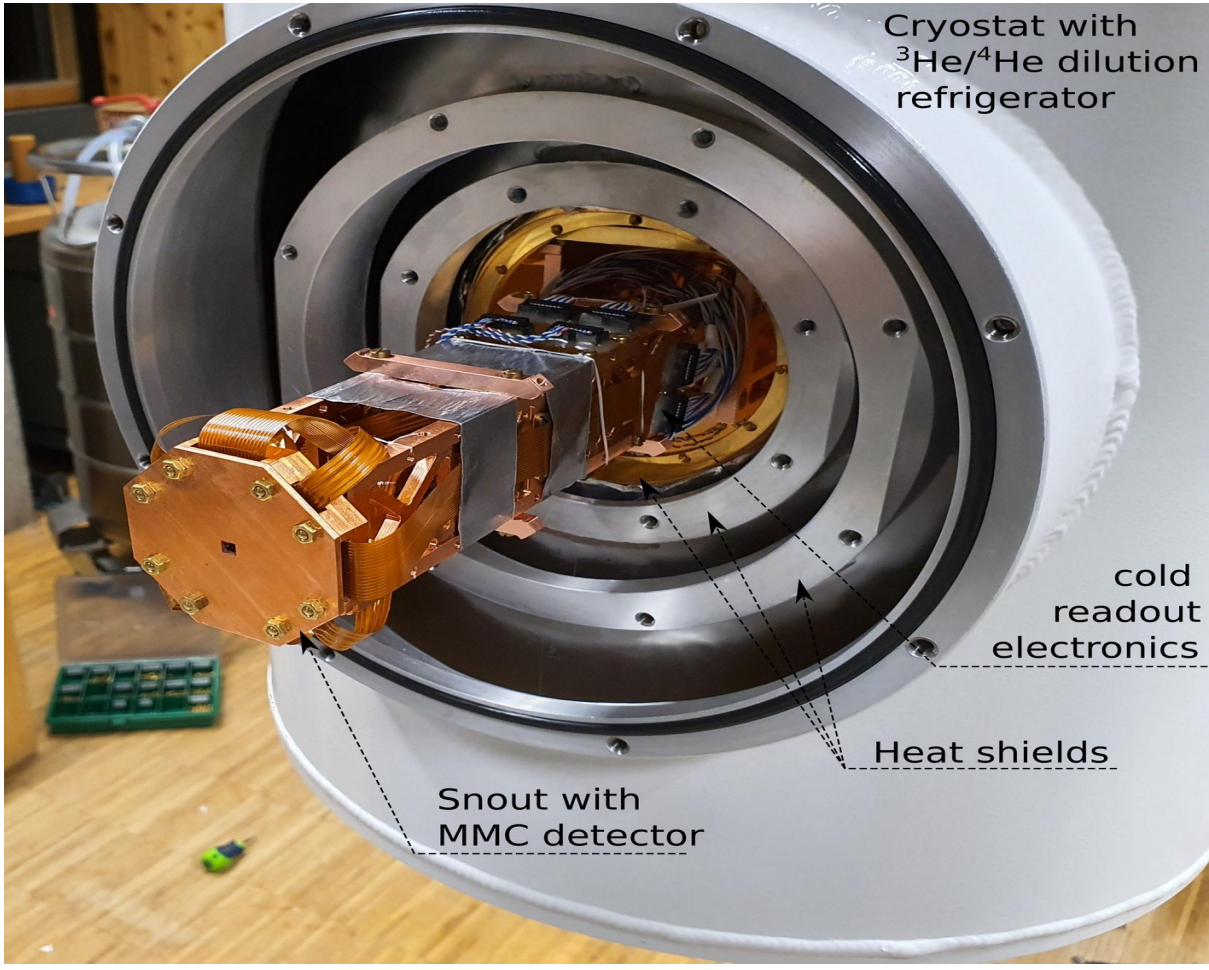

MMC have *excellent* energy resolution

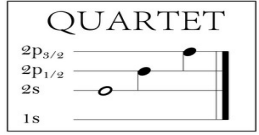

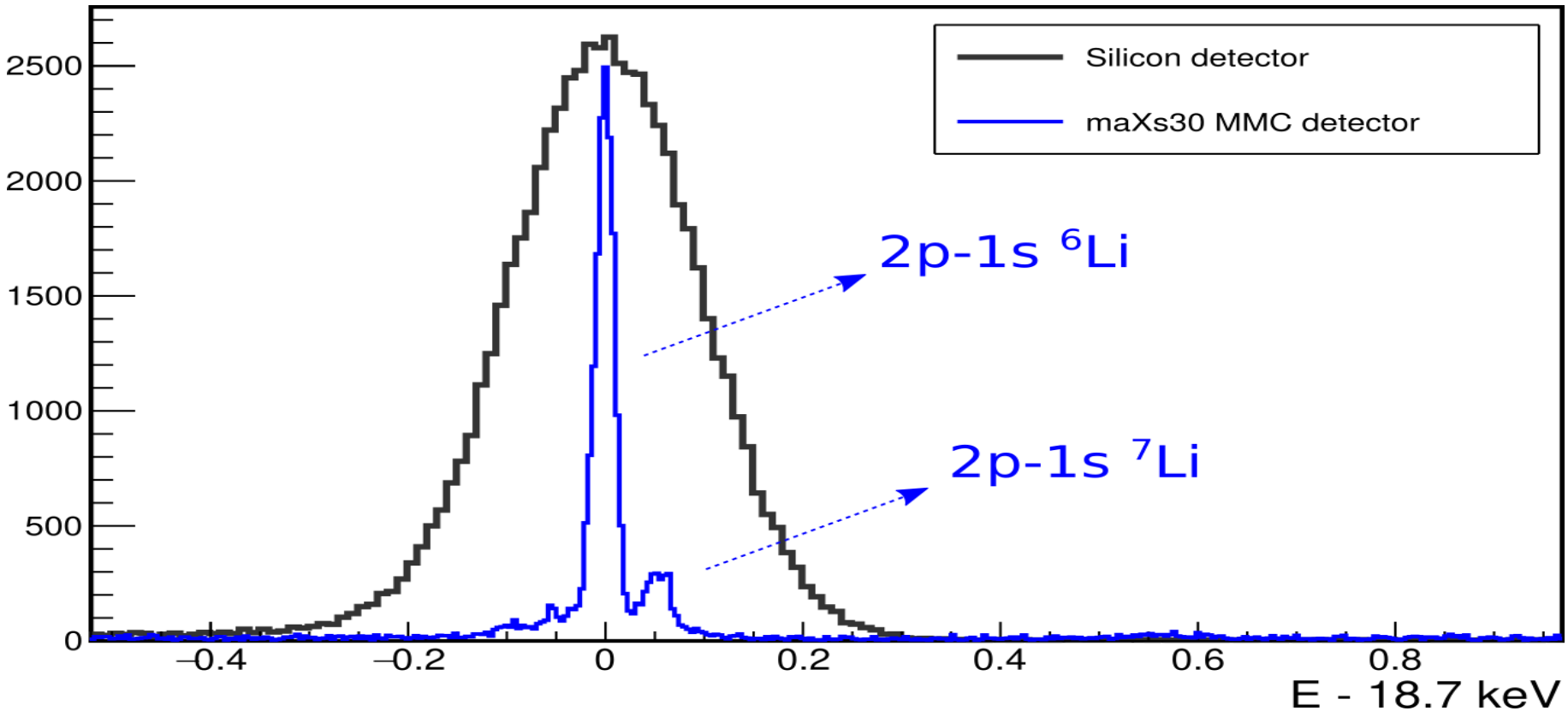

muonic oxygen (2025)

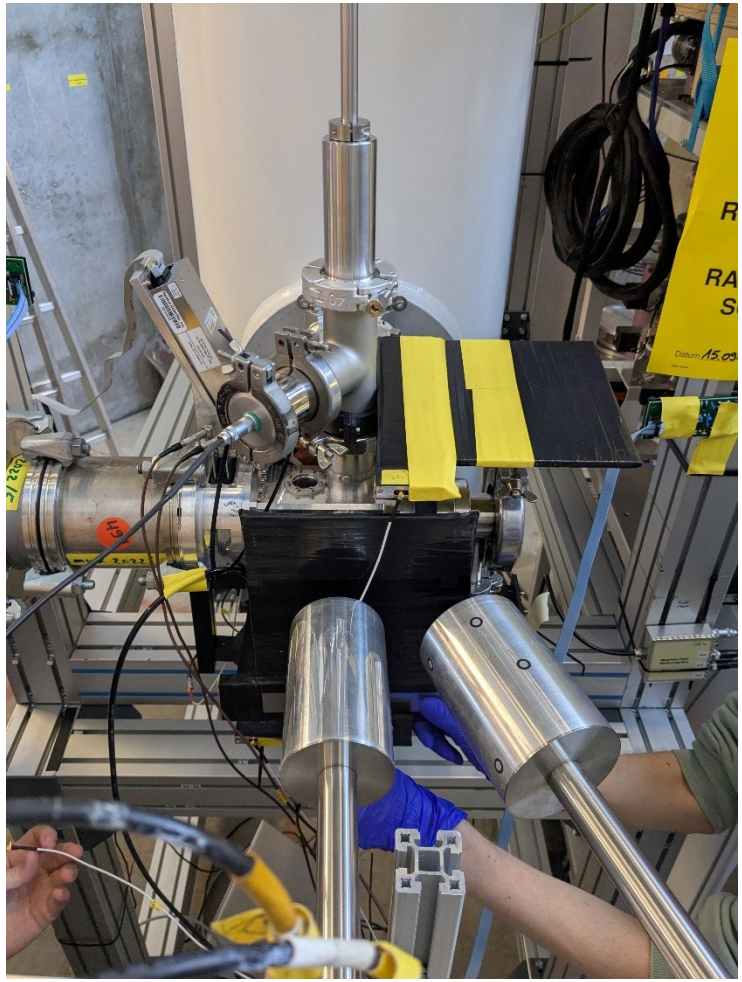

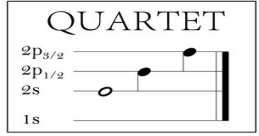

muonic ^{17}O, online spectrum (taken 3 weeks ago)

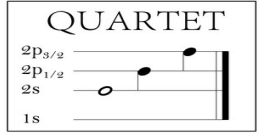

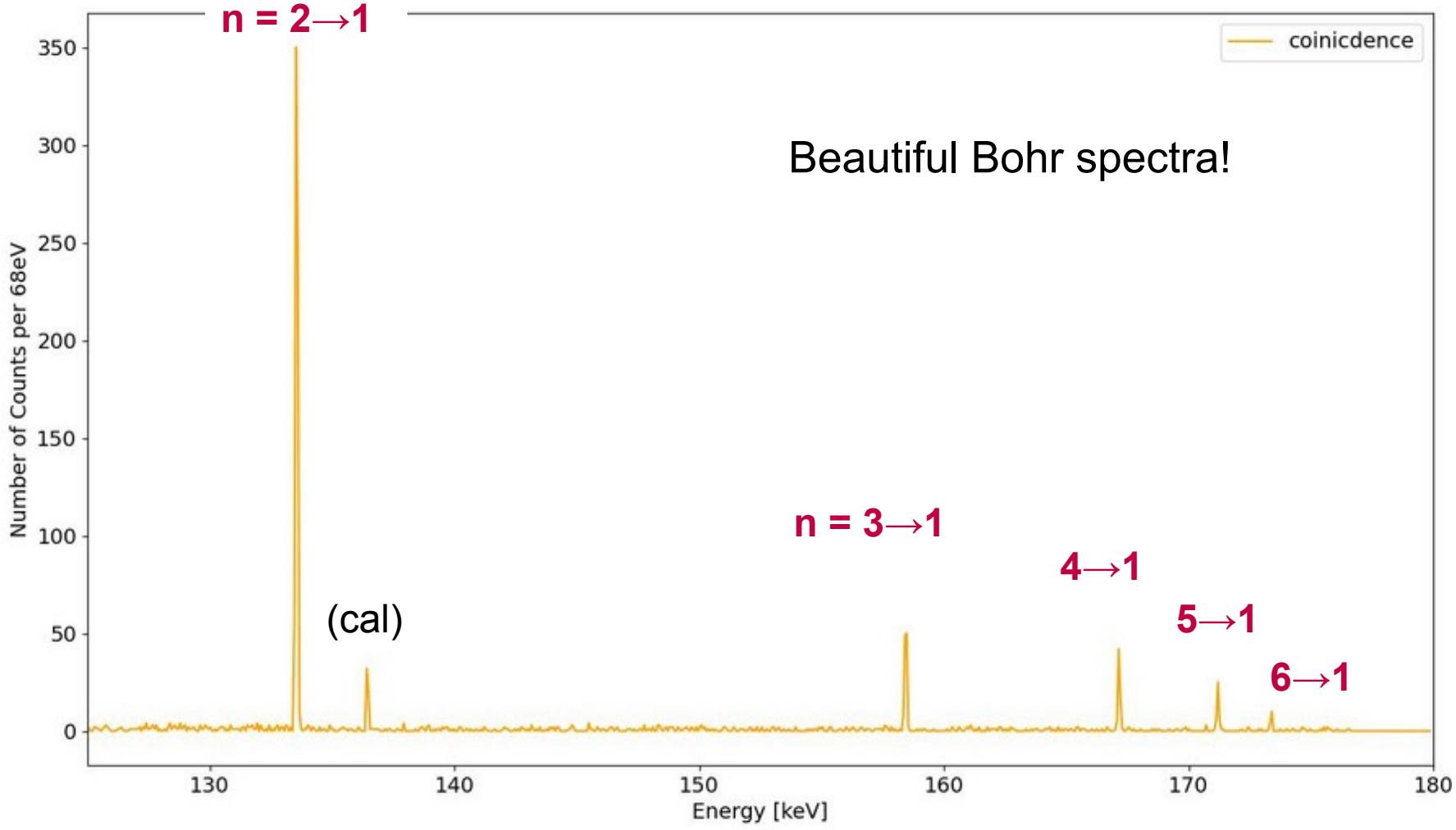

QUARTET: X-ray spectroscopy

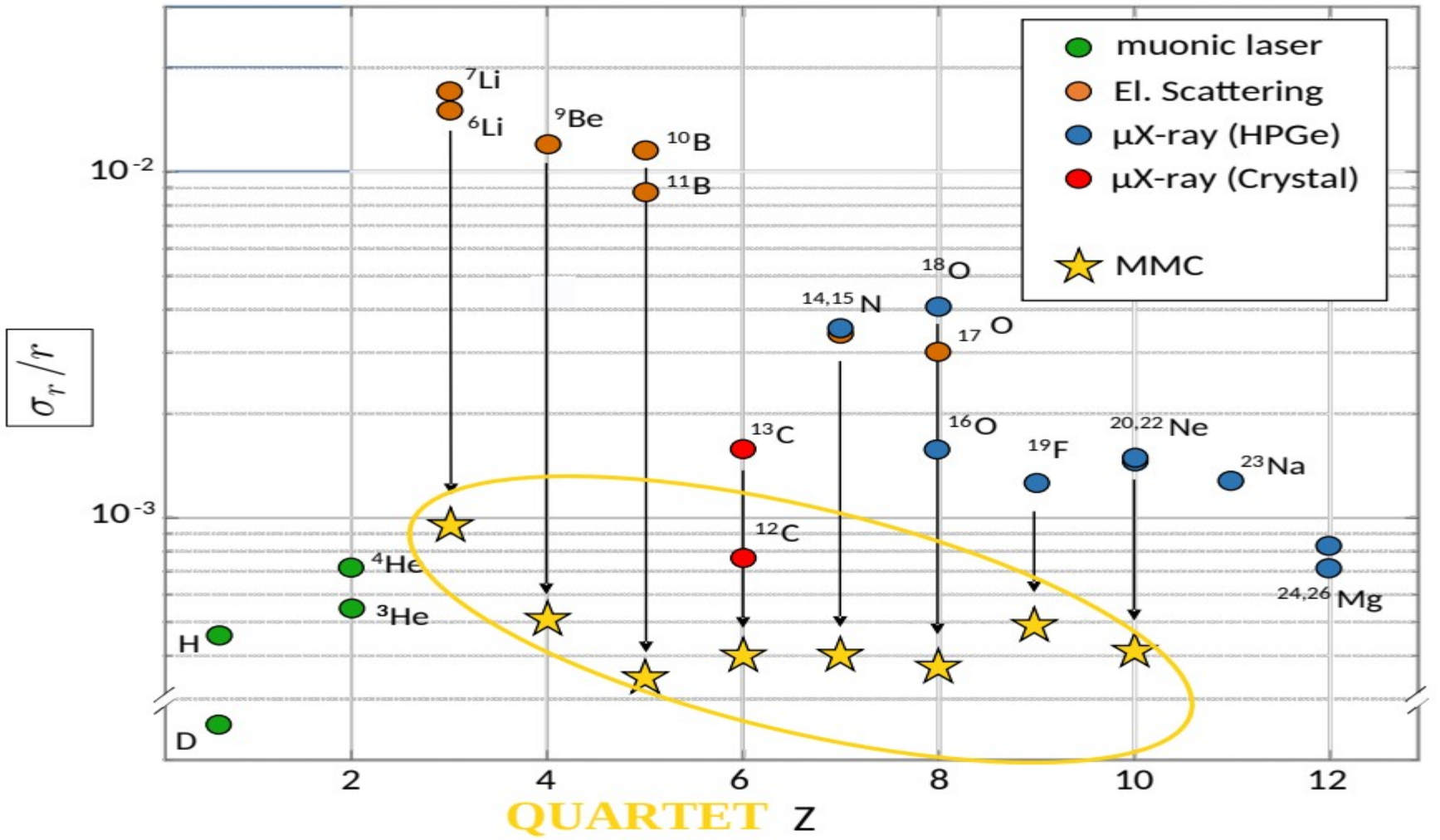

The “missing link”

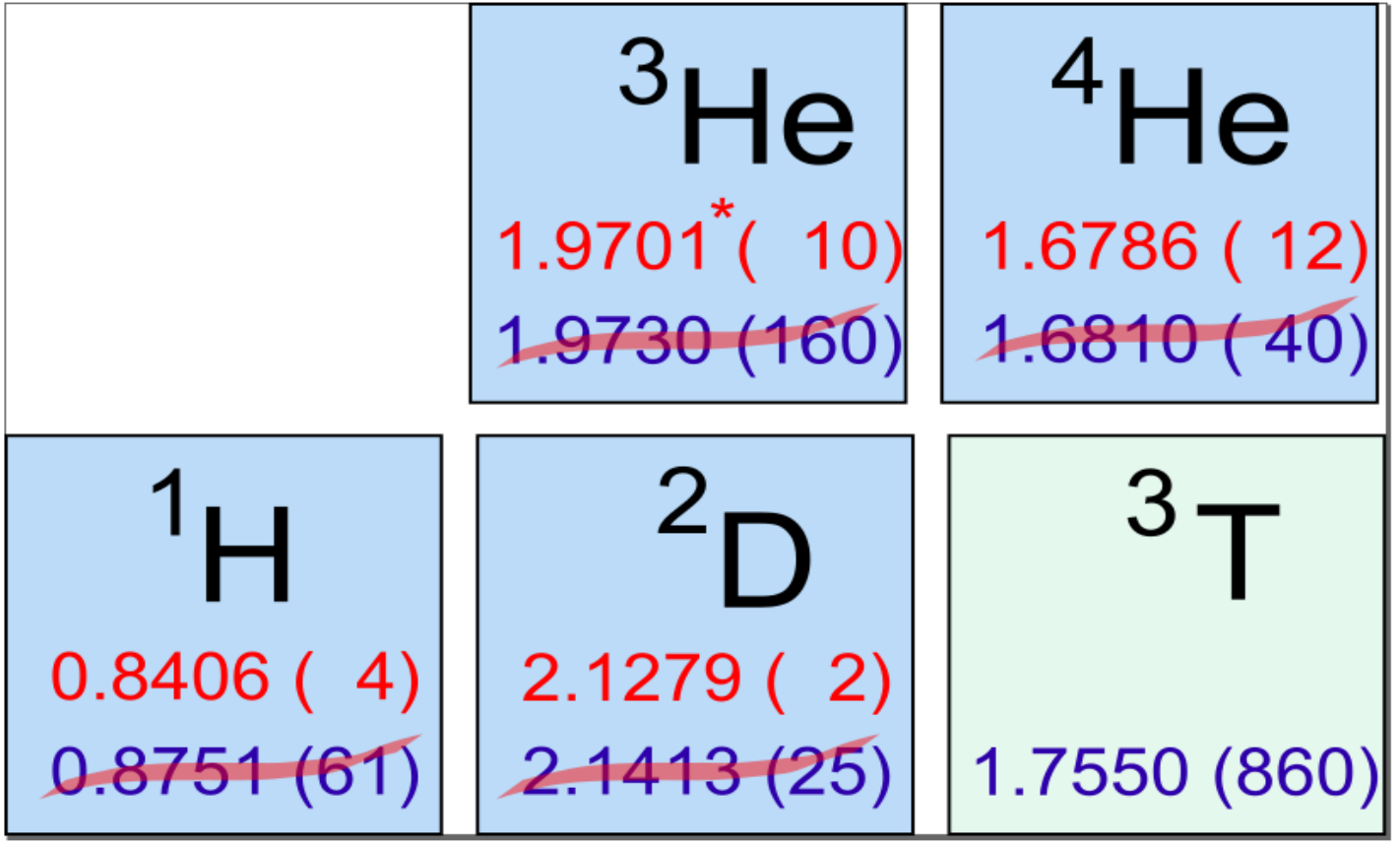

Tritium 1S-2S

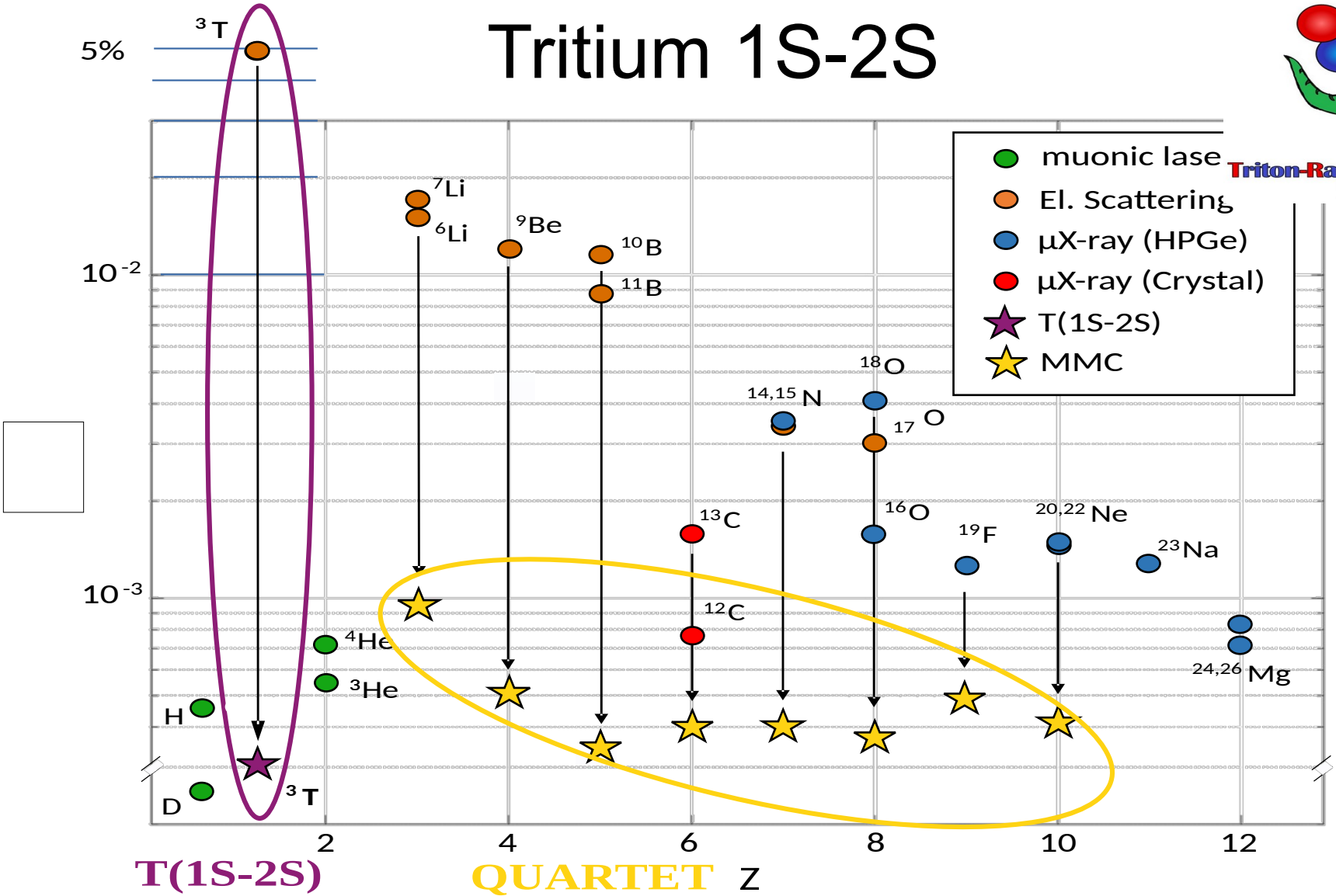

Triton-Radius EXperiment
Mainz

Tritium 1S-2S

measure 1S-2S in **ordinary** tritium to

determine the **isotope H/T shift**

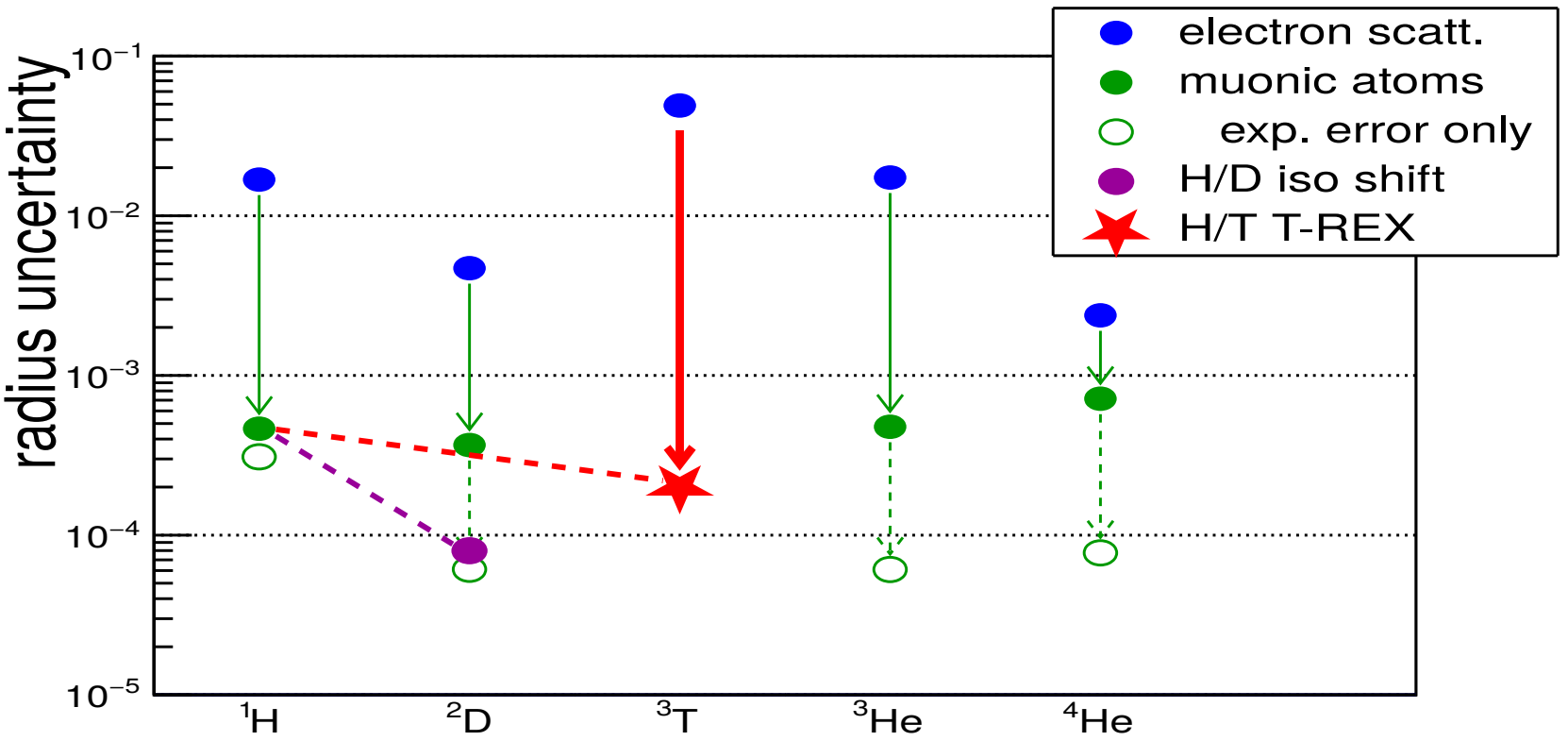

Triton-Radius EXperiment
Mainz

Tritium 1S-2S

400x better triton radius with 1 kHz measurement

(vs. 0.01 kHz for H, D)

- cryogenic H nozzle (4.2K)
- magnetic quadrupole guide
- Li MOT -> cold buffer gas
- magnetic trapping of H/D/T

Triton-Radius EXperiment Mainz

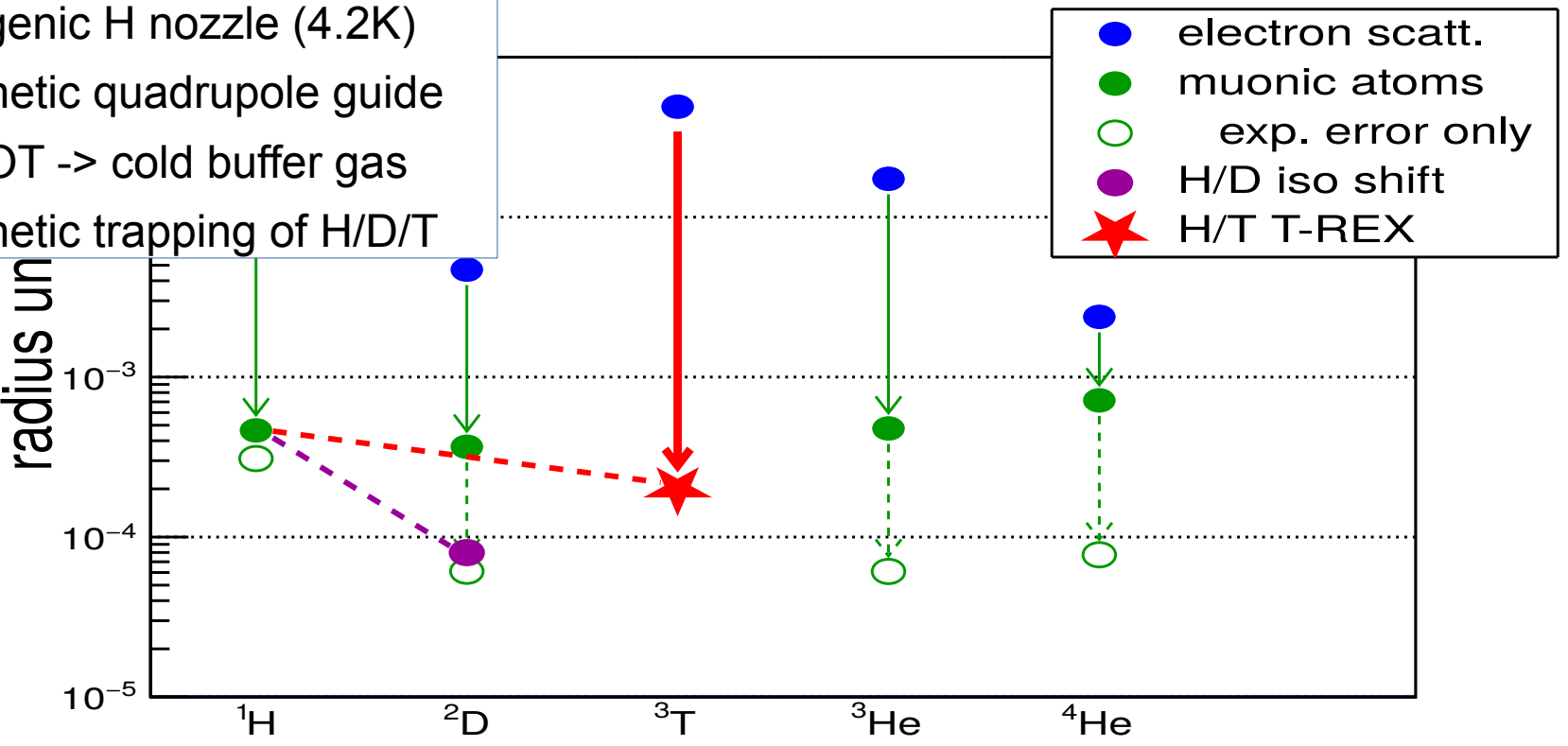

1st step: Somewhat better triton radius

^{3}He 1.9679*(14) ~~1.9730 (160)~~	^{4}He 1.6782 (8) ~~1.6810 (40)~~	
^{1}H 0.8409 (4) ~~0.8751 (61)~~	^{2}D 2.1279 (2) ~~2.1413 (25)~~	^{3}T **1.7xxx (200)** 1.7550 (860)

4x better radius
with 100 kHz measurement
(vs. 0.01 kHz for H, D)

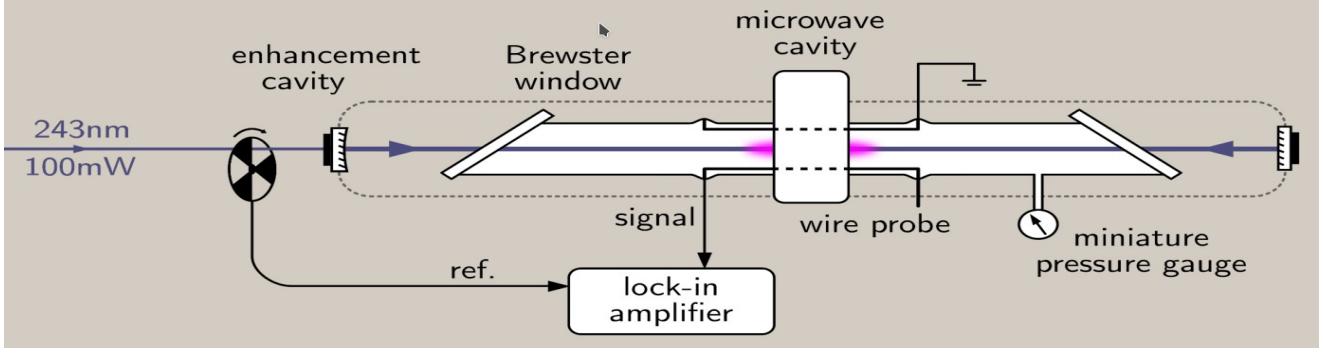

- Optogalvanic spectroscopy in a cell
- Syst. extrapolation w/ H,D
- Tritium confined.

T(1S-2S) in a cell: Optogalvanic spectroscopy

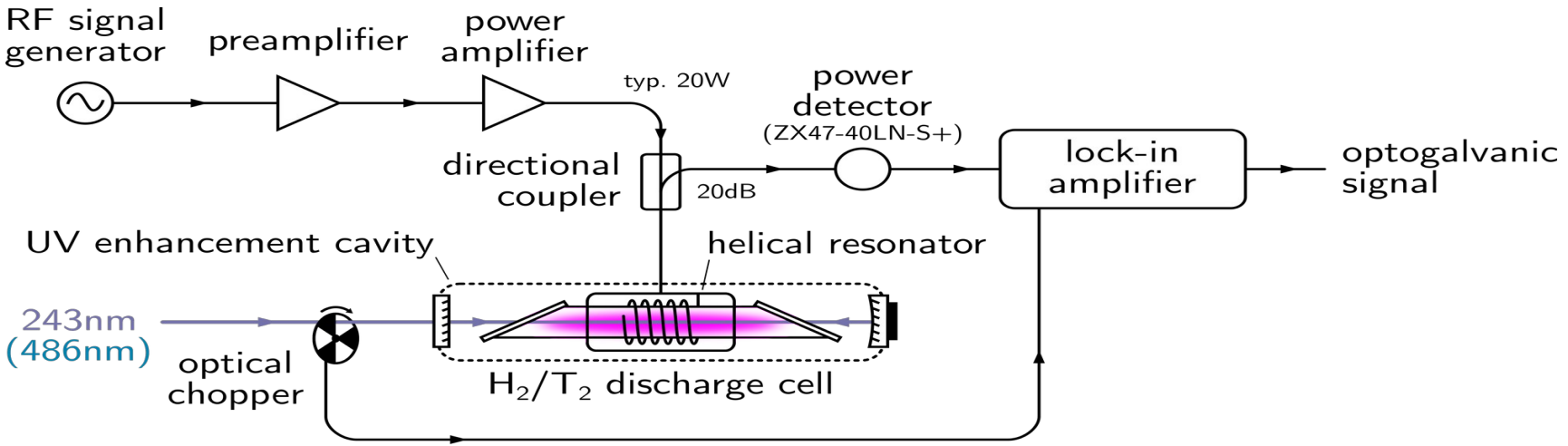

- Optogalvanic spectroscopy in a cell
- → Don't need to observe fluorescence ☺
- → Tritium confined ☺
- → BUT: large systematics! ↓
  - HOWEVER: We KNOW the results for H and D → can test our syst. effects ☺

T(1S-2S) in a cell: Optogalvanic spectroscopy

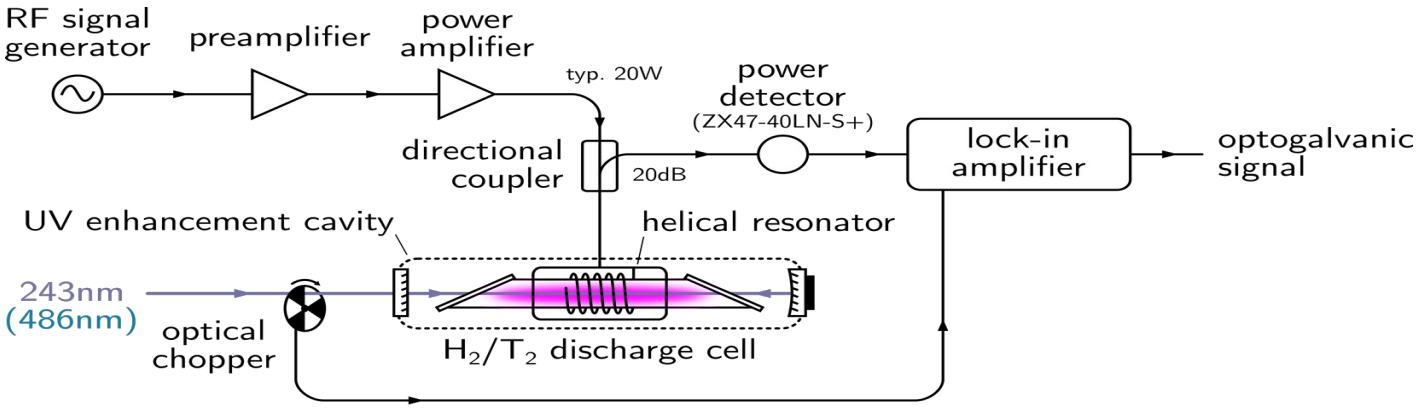

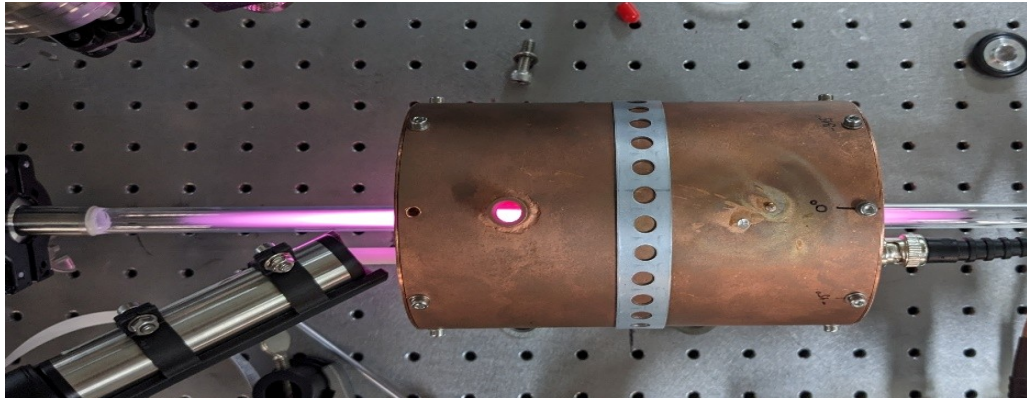

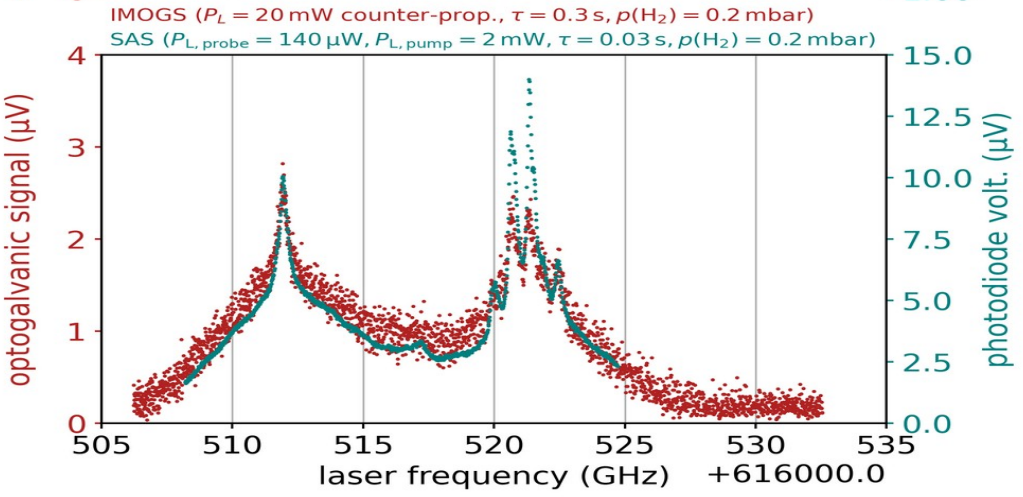

Hydrogen/Tritium Laser Spectroscopy in RF Discharge Cell

Balmer-β Transition / Overview

optogalvanic spectroscopy (OGS)

modulated lin. OGS

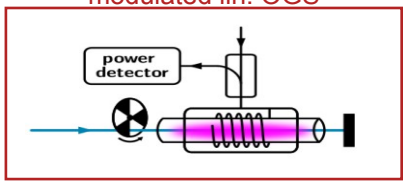

intermodulated OGS (IMOGS)

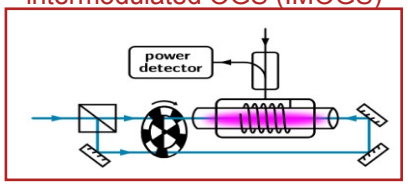

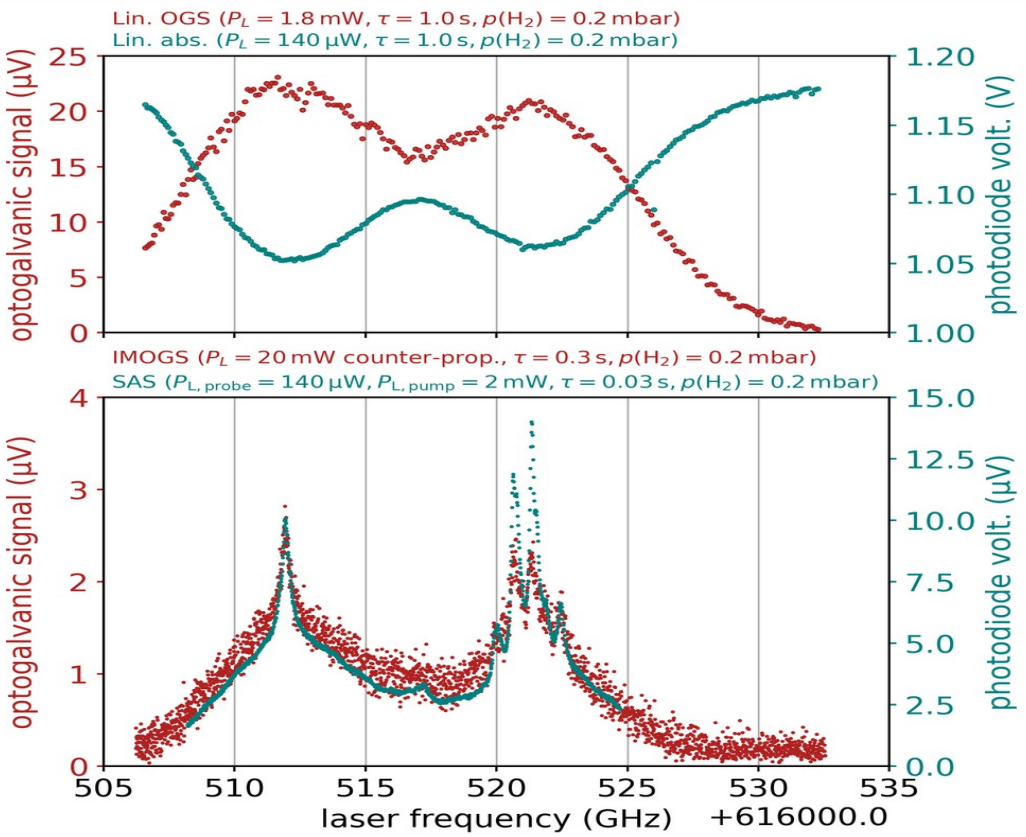

absorption spectroscopy

linear absorption

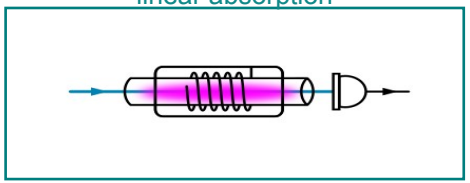

saturated absorption (SAS)

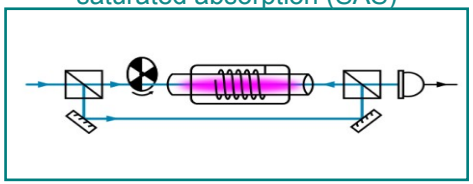

Trapping and spectroscopy

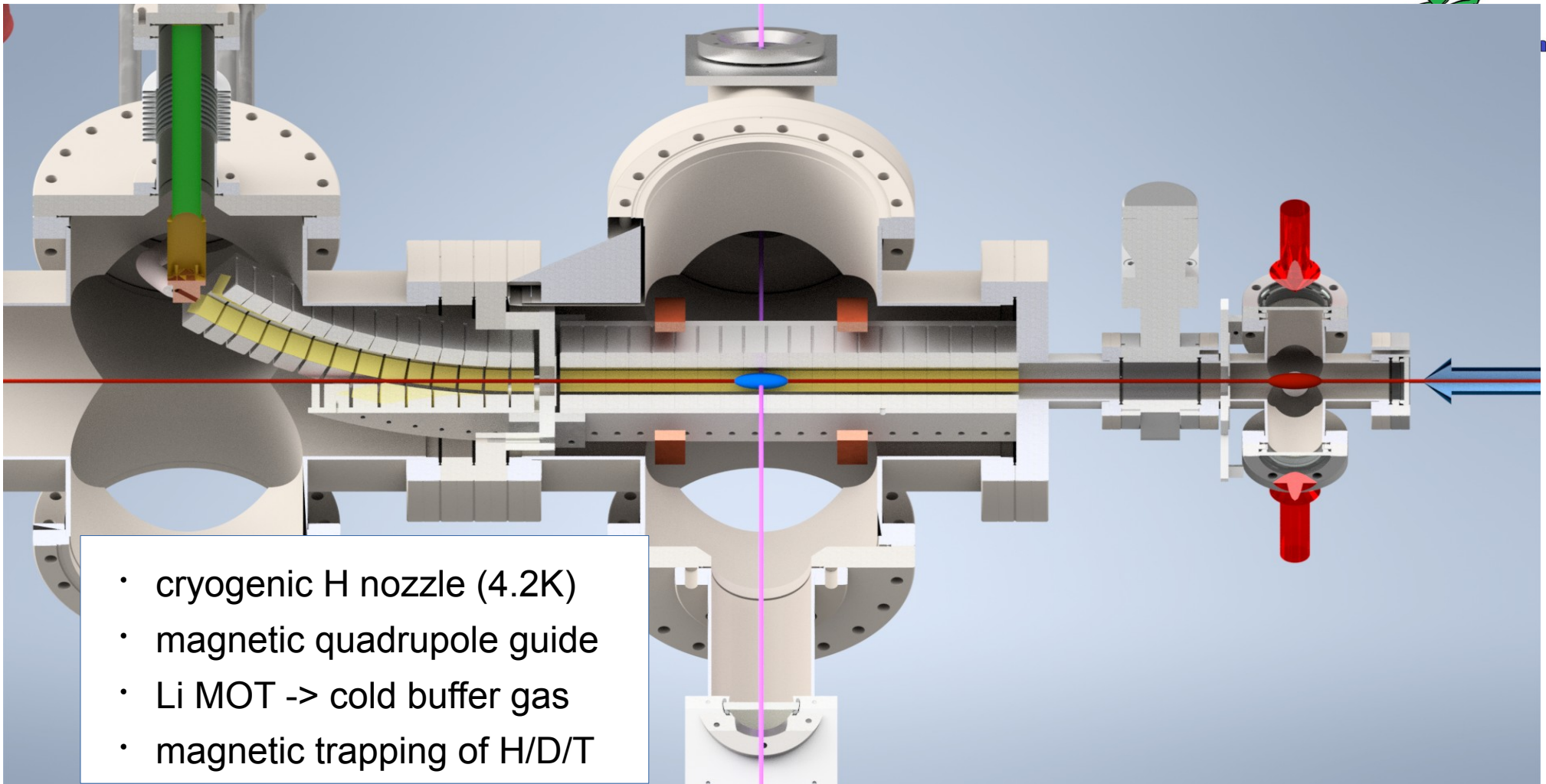

- cryogenic H nozzle (4.2K)
- magnetic quadrupole guide
- Li MOT -> cold buffer gas
- magnetic trapping of H/D/T

Simulated trapping efficiency

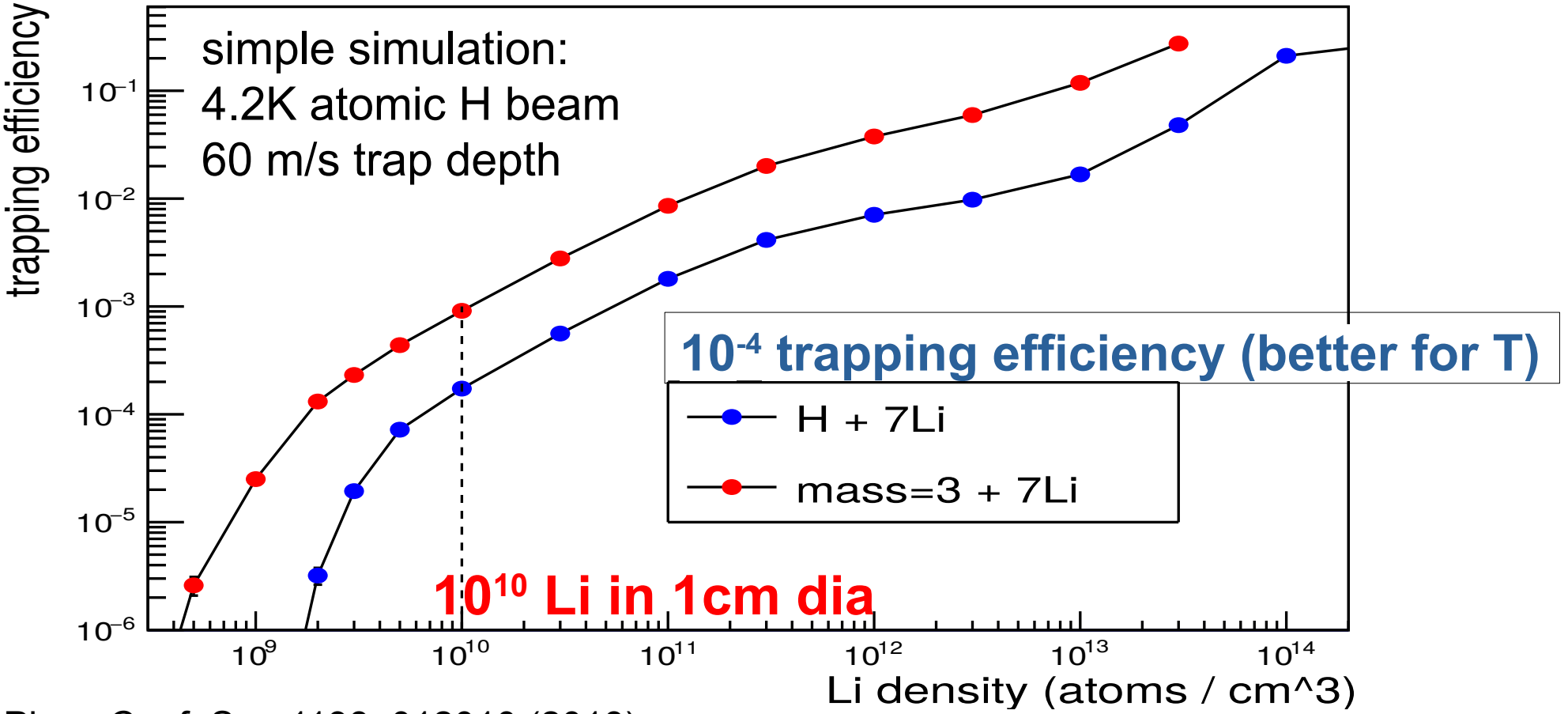

J. Phys. Conf. Ser. 1138, 012010 (2018)

Towards H Beam Characterization

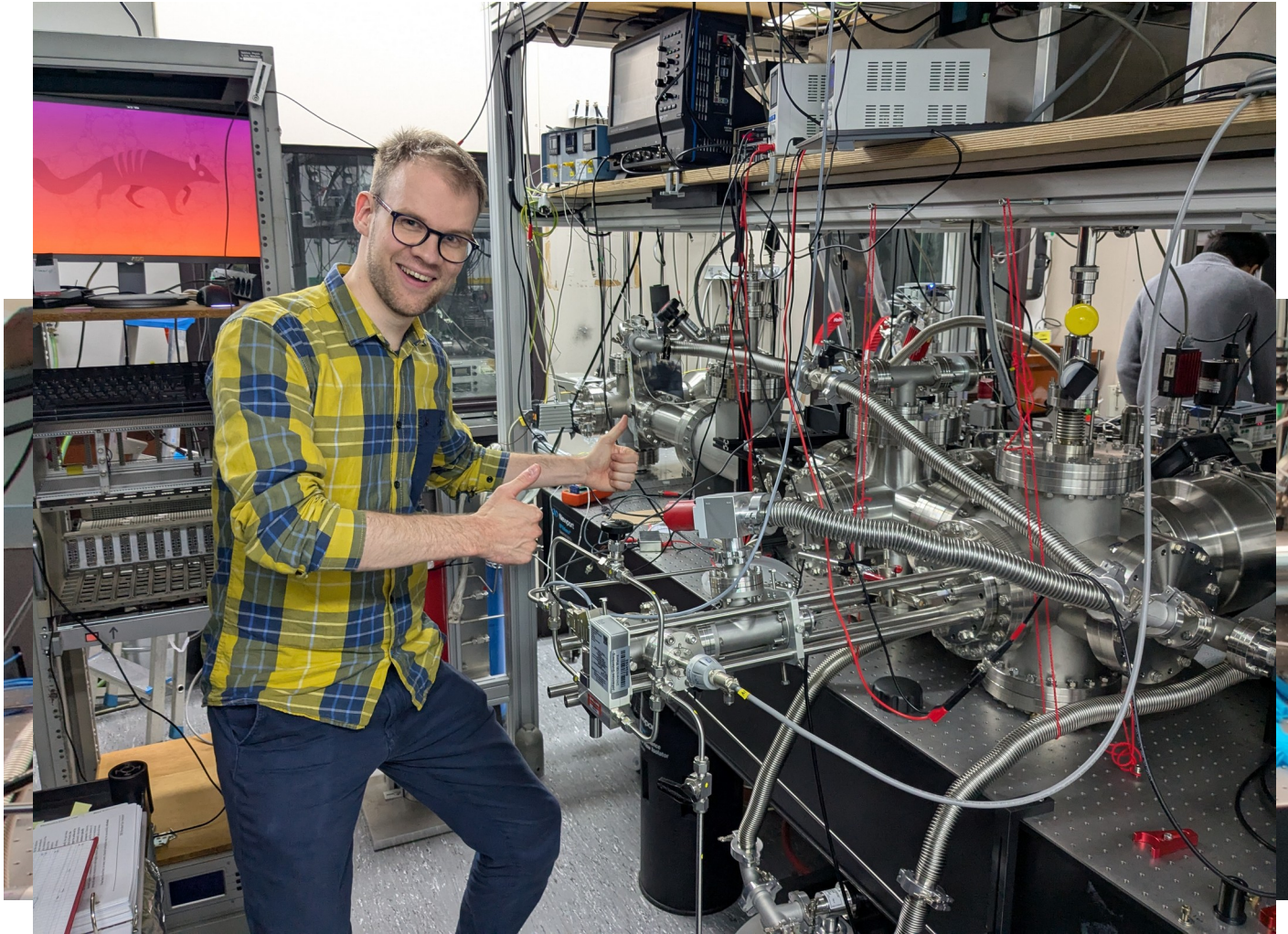

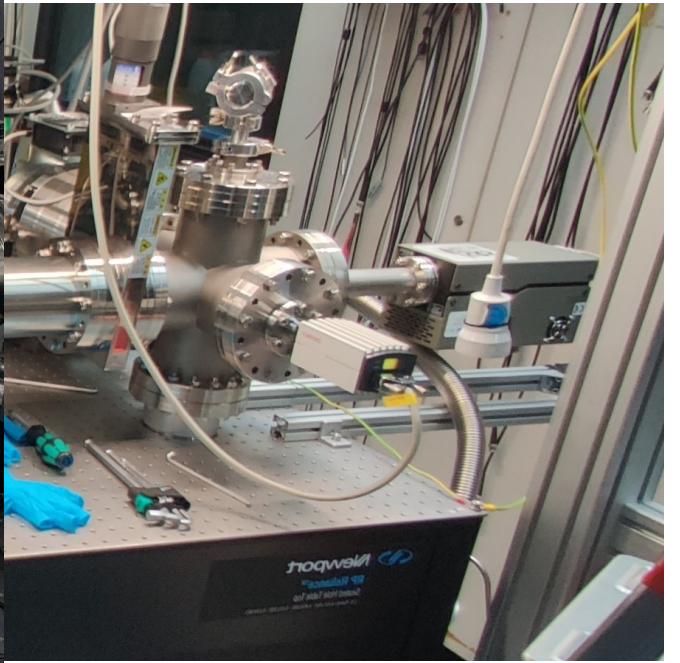

Towards H Beam Characterization

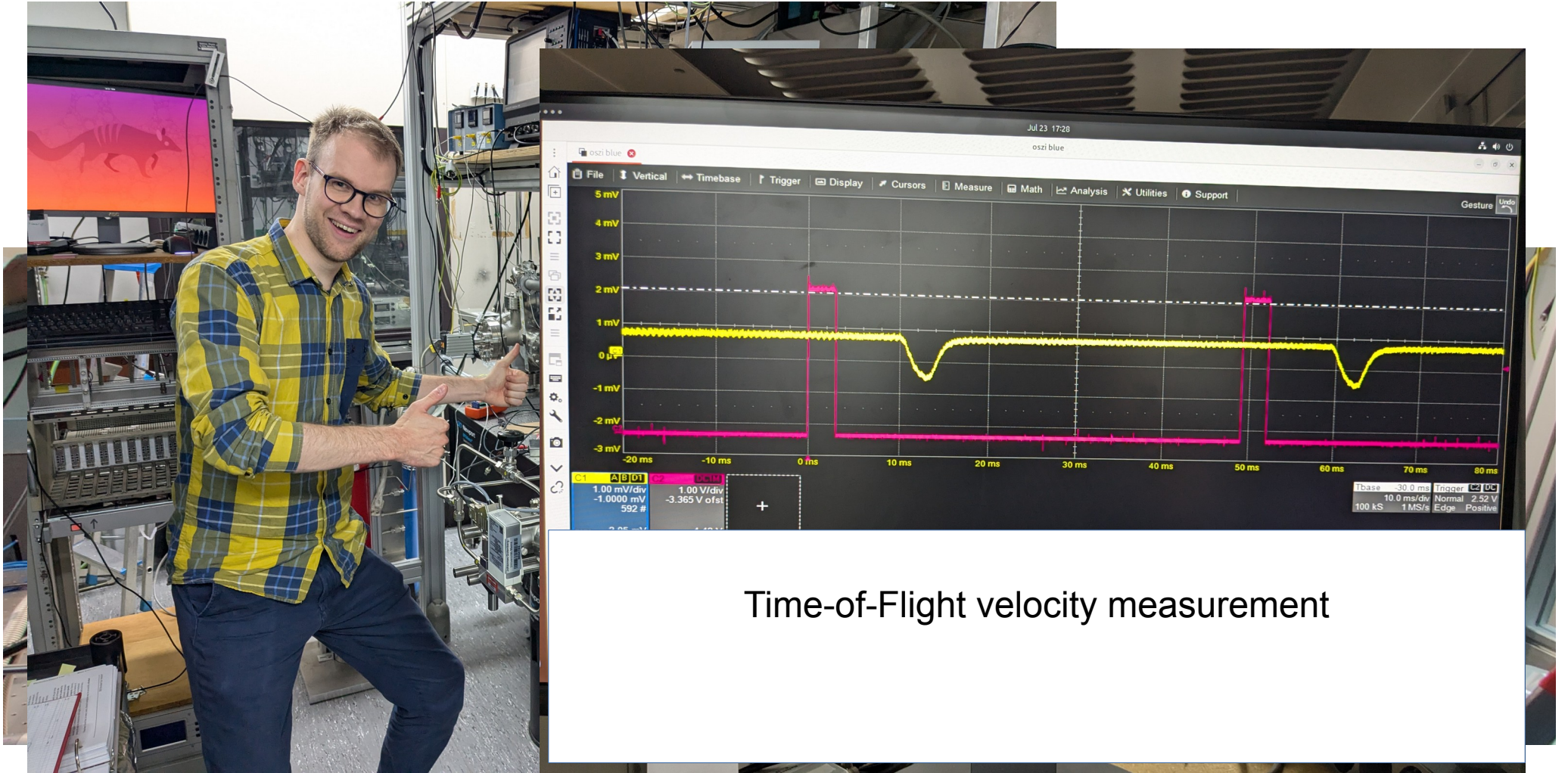

Time-of-Flight velocity measurement

Towards trapping and spectroscopy

Triton-Radius EXperiment
Mainz

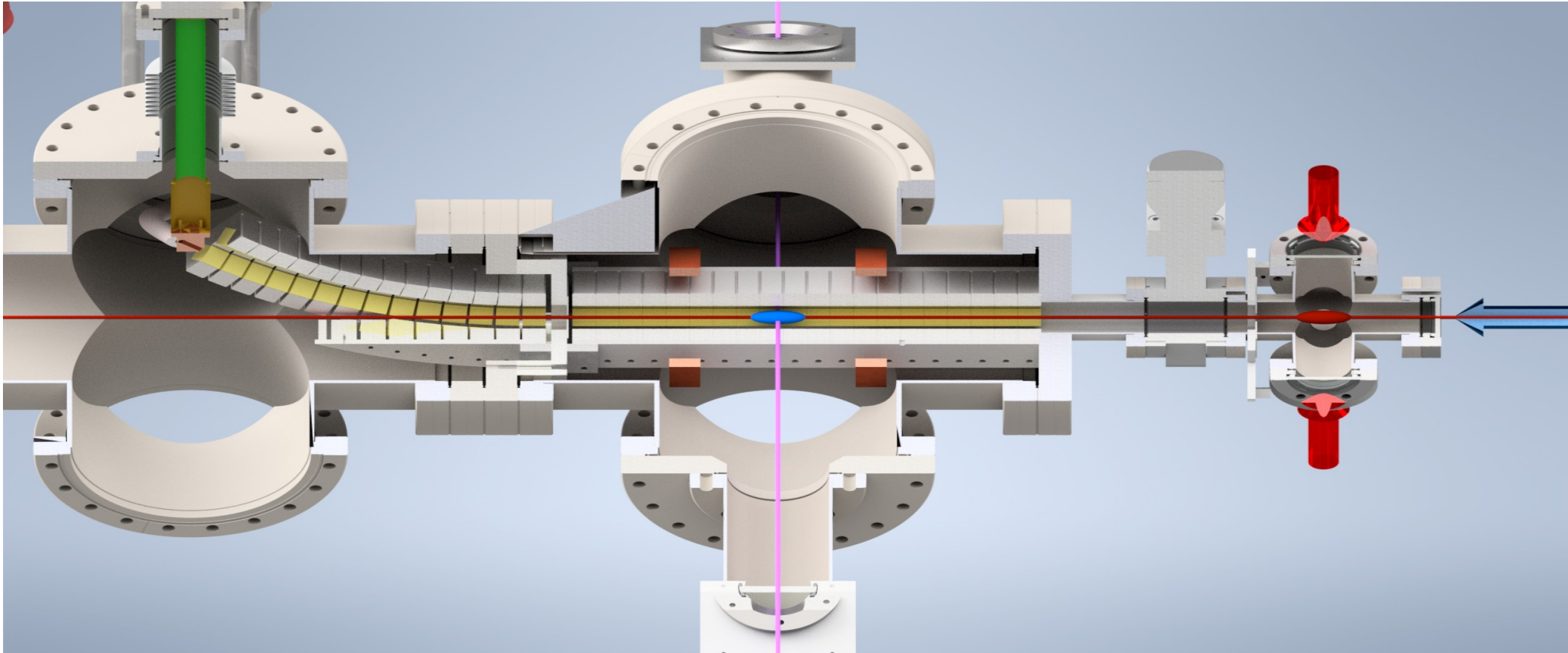

Atomic Lithium

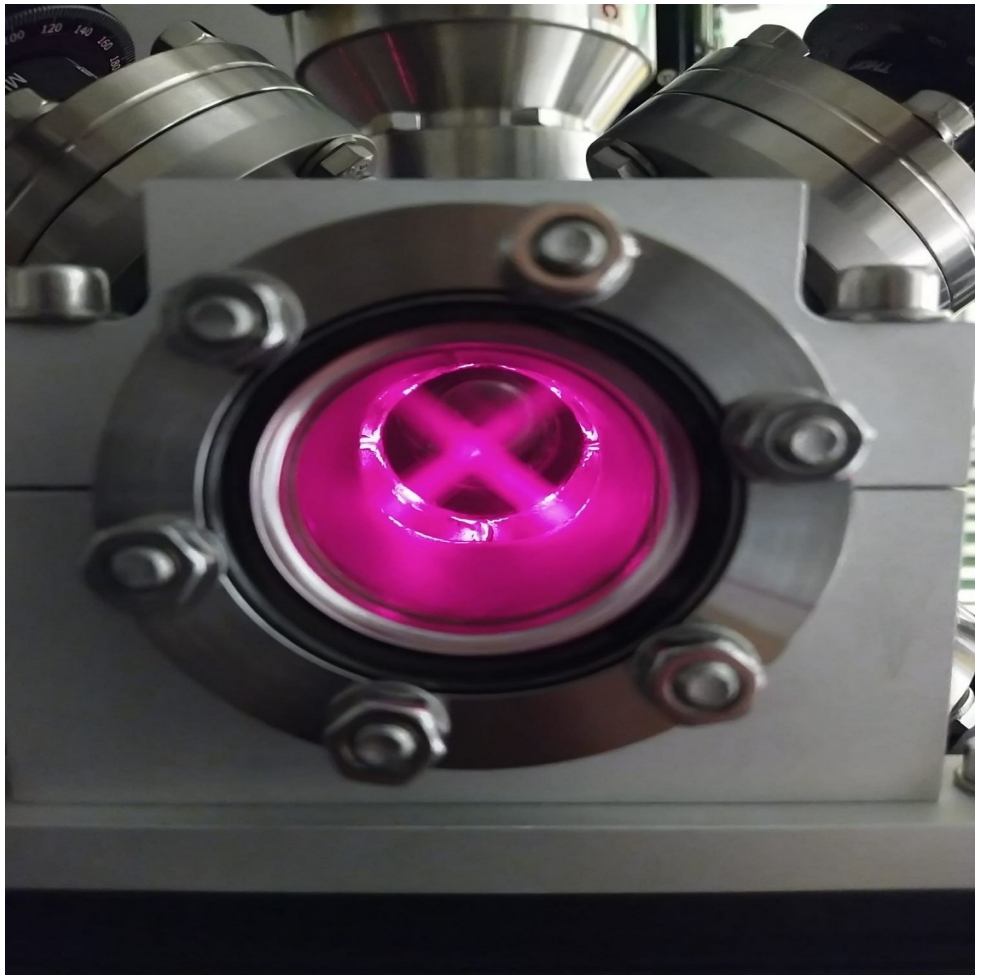

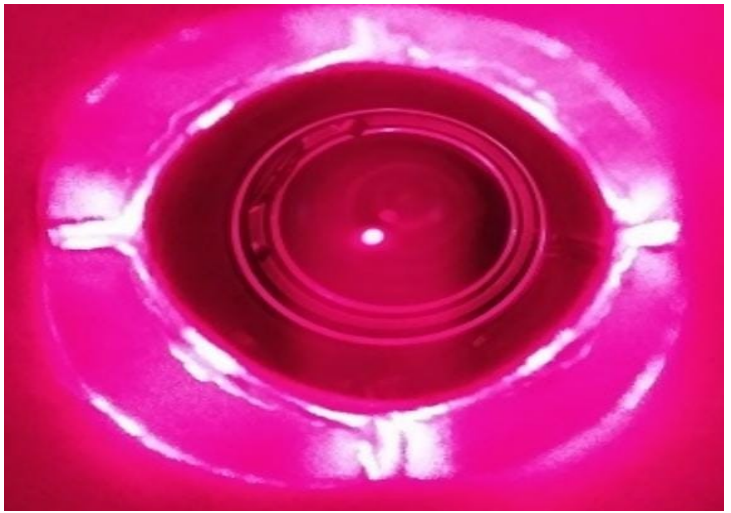

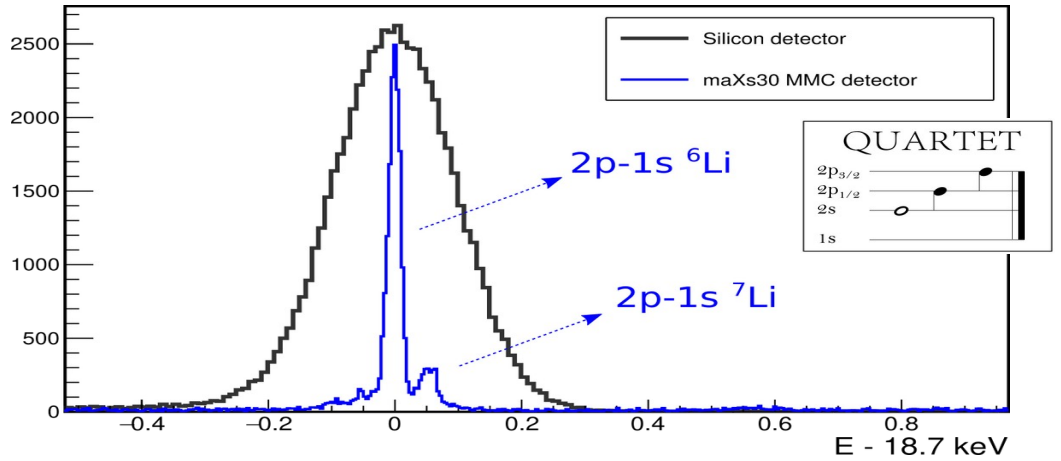

Li-6 Li-7 isotope shift

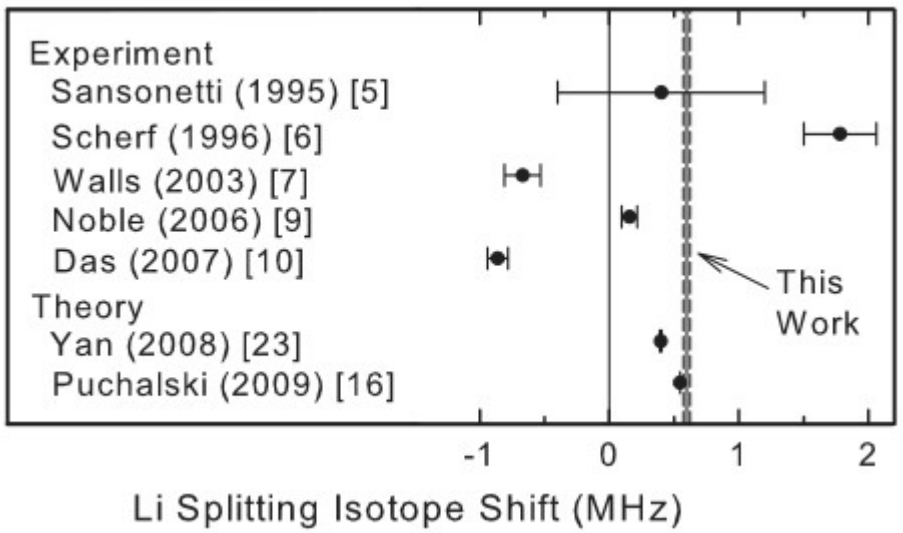

Sansonetti et al., PRL (2011)

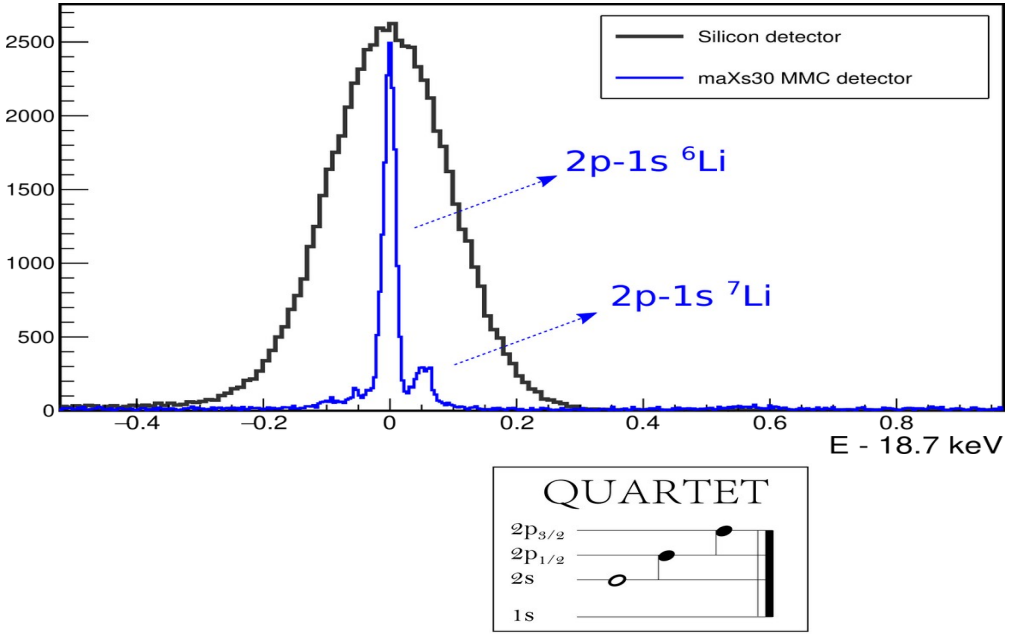

2D MOT + spectroscopy (AFR)

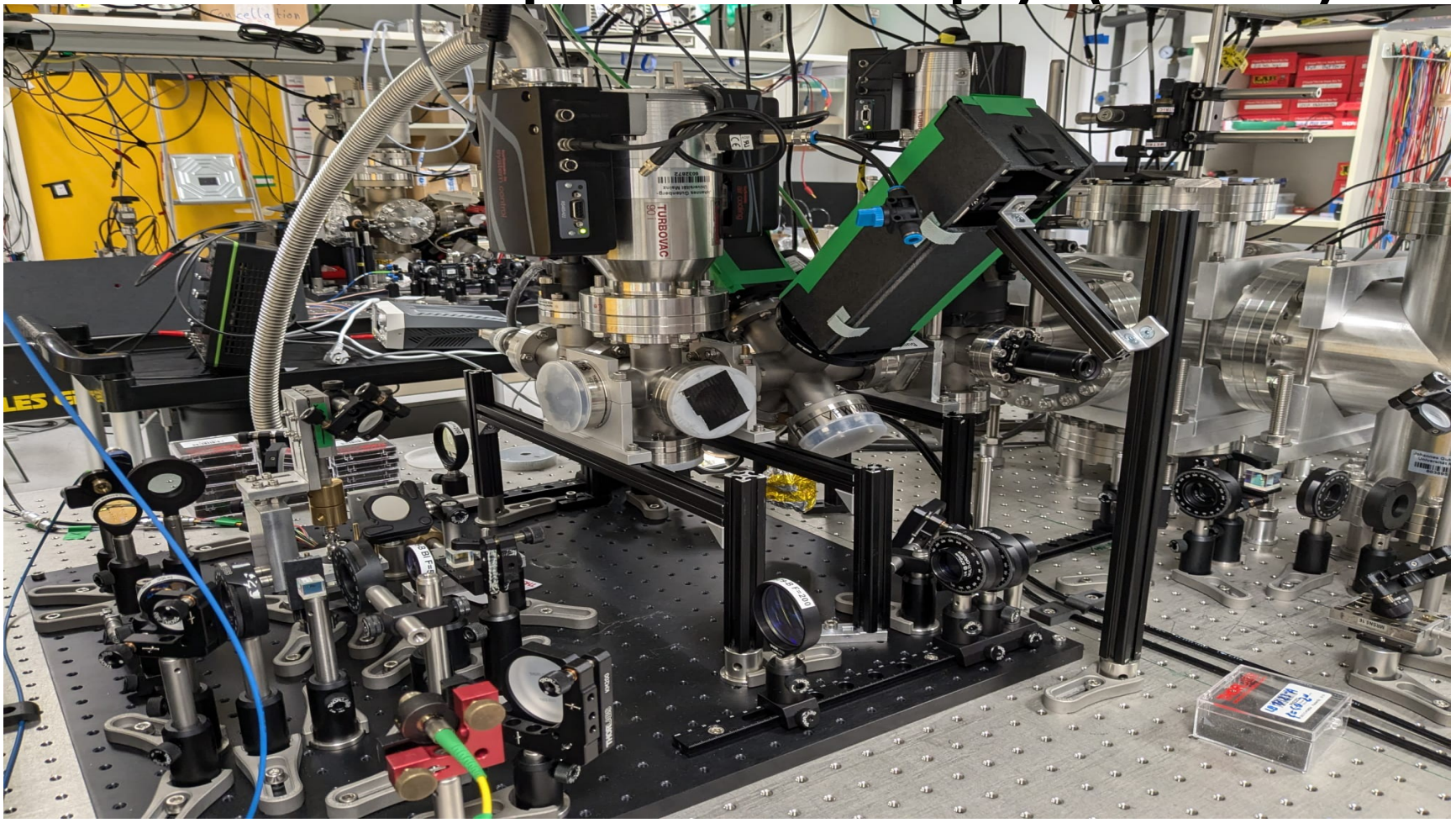

2D-MOT design: Tiecke, Walraven et al, PRA 80, 013409 (2009)

Our 1st spectroscopy on cold ^{6}Li

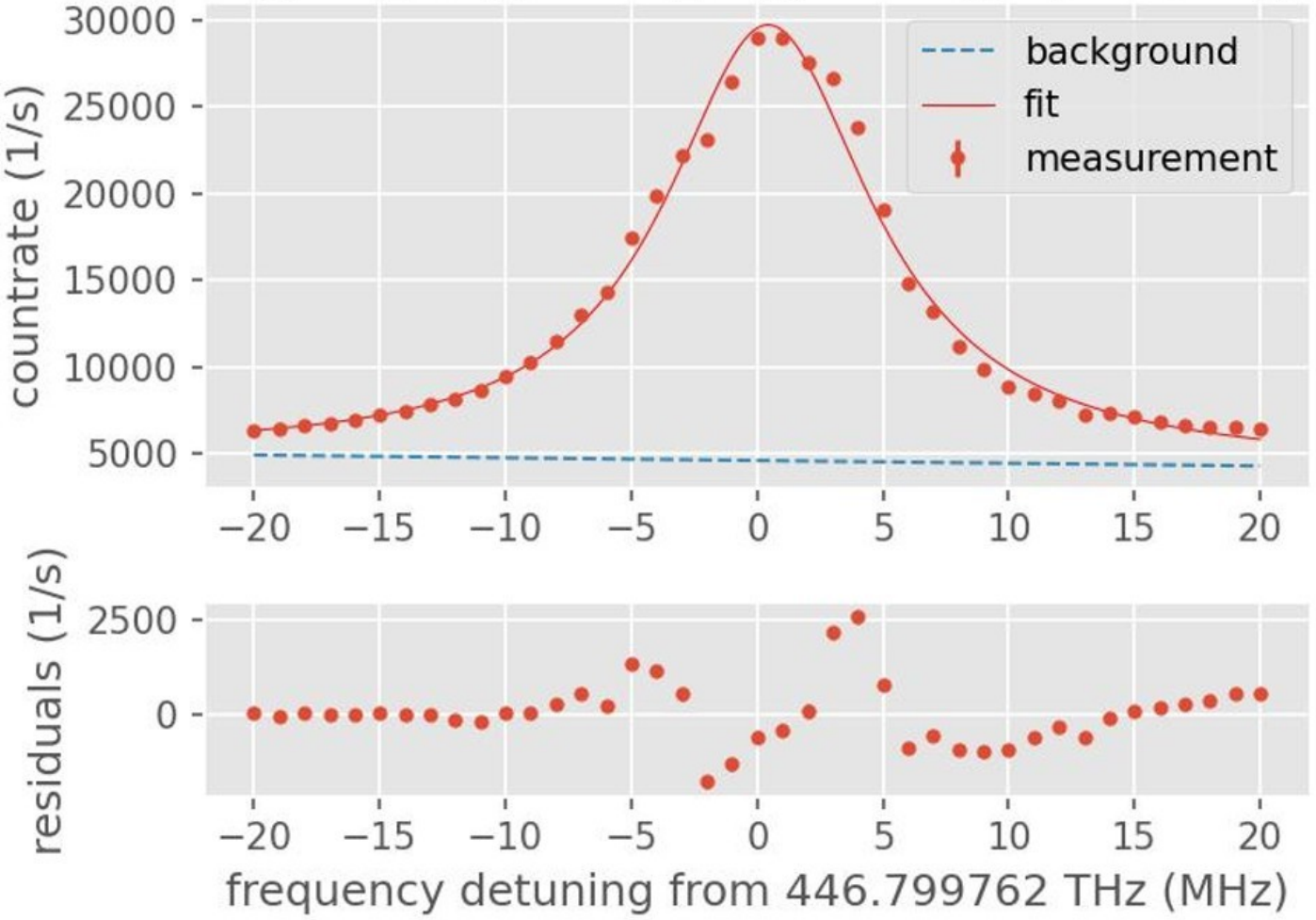

muX

X-rays from **O(10s of µg) target material** using Ge detectors (Miniball)

→ rare, or radioactive

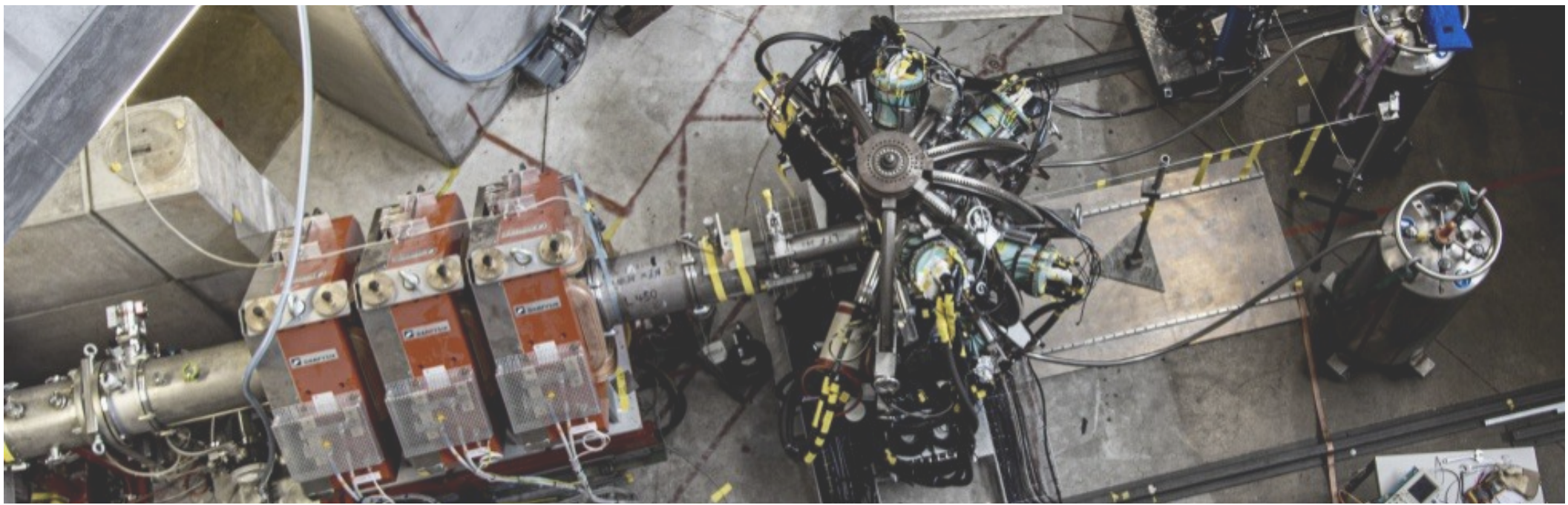

muX: Radii of O(10μg) material

rare stuff, or **radioactive** isotopes

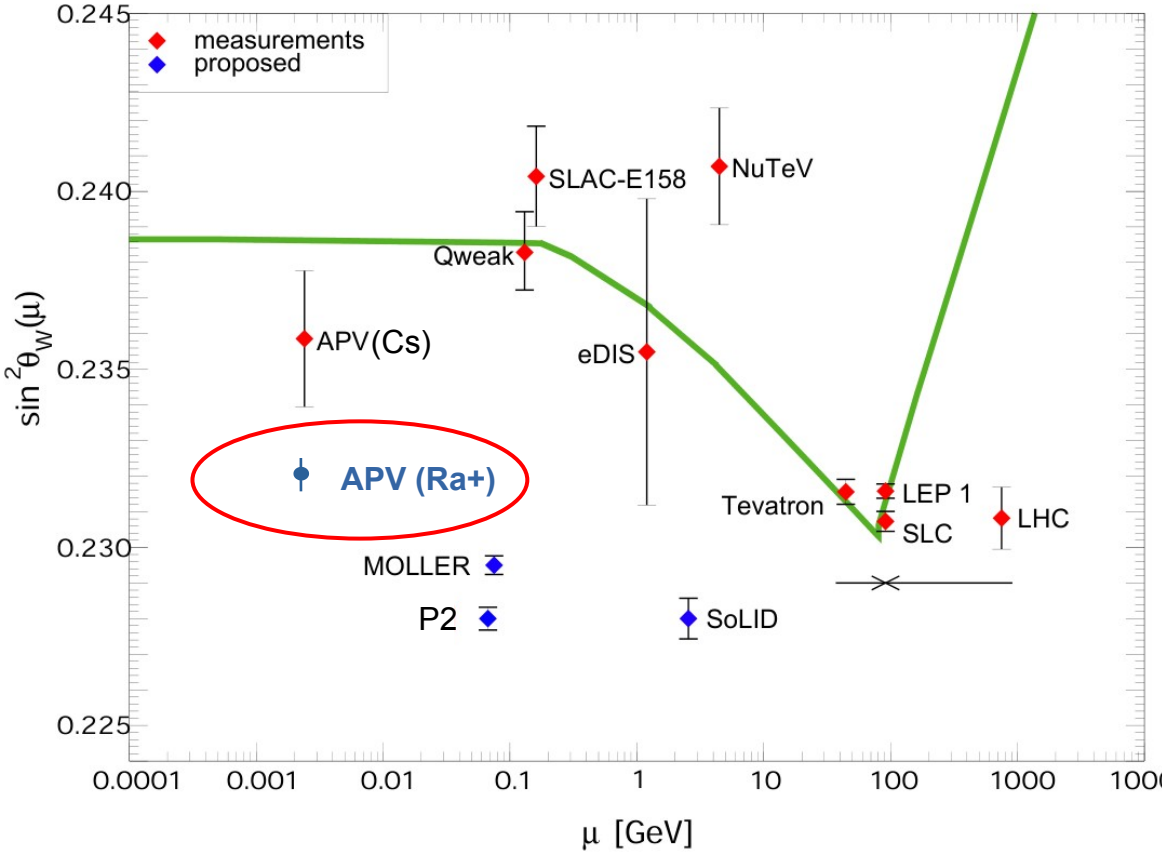

Hyperfine Interact (2011) 199:9–19
DOI 10.1007/s10751-011-0296-6

Atomic parity violation in a single trapped radium ion

O. O. Versolato · L. W. Wansbeek · G. S. Giri · J. E. van den Berg · D. J. van der Hoek · K. Jungmann · W. L. Kruithof · C. J. G. Onderwater · B. K. Sahoo · B. Santra · P. D. Shidling · R. G. E. Timmermans · L. Willmann · H. W. Wilschut

INPUT: need δR to 0.2%

$$E1_{PNC} = K_r Z^3 Q_W$$

muX Setup

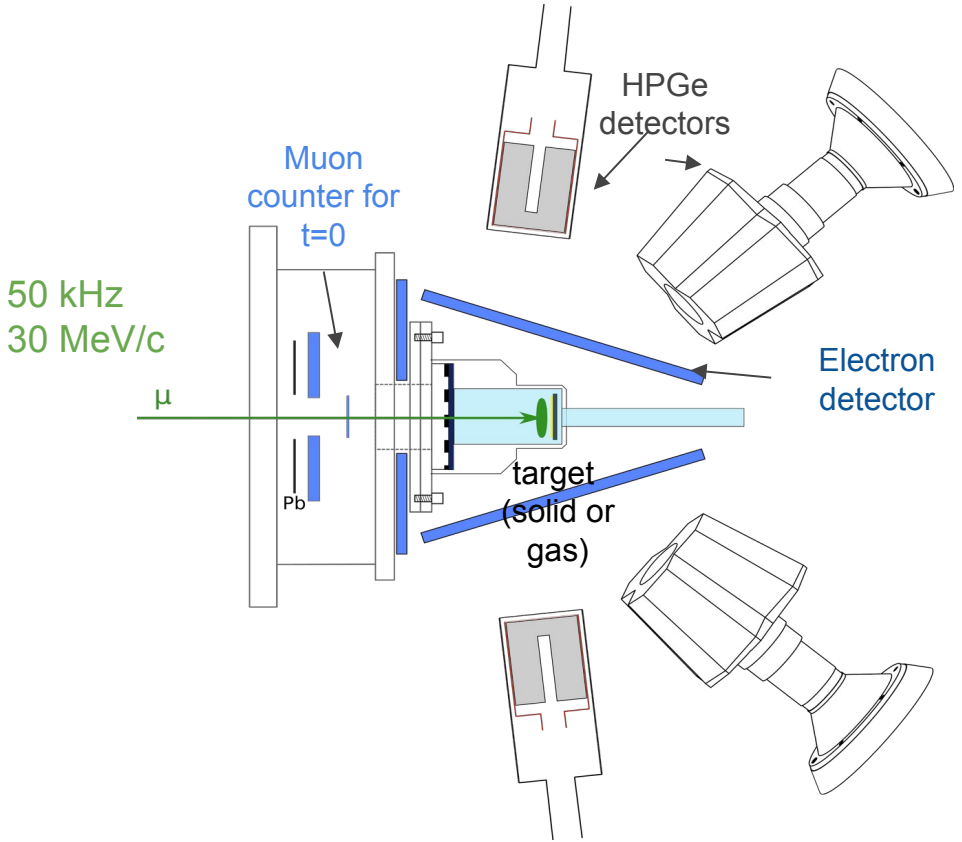

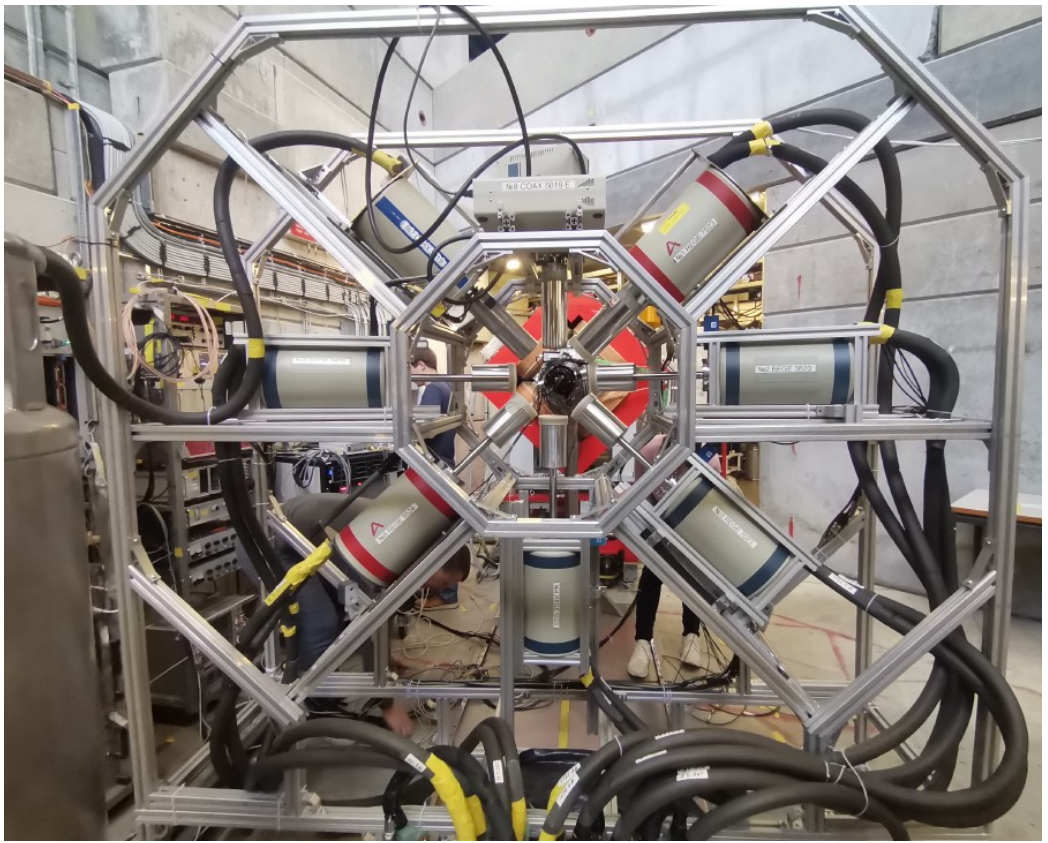

Miniball detector array

Muon transfer to microgram targets

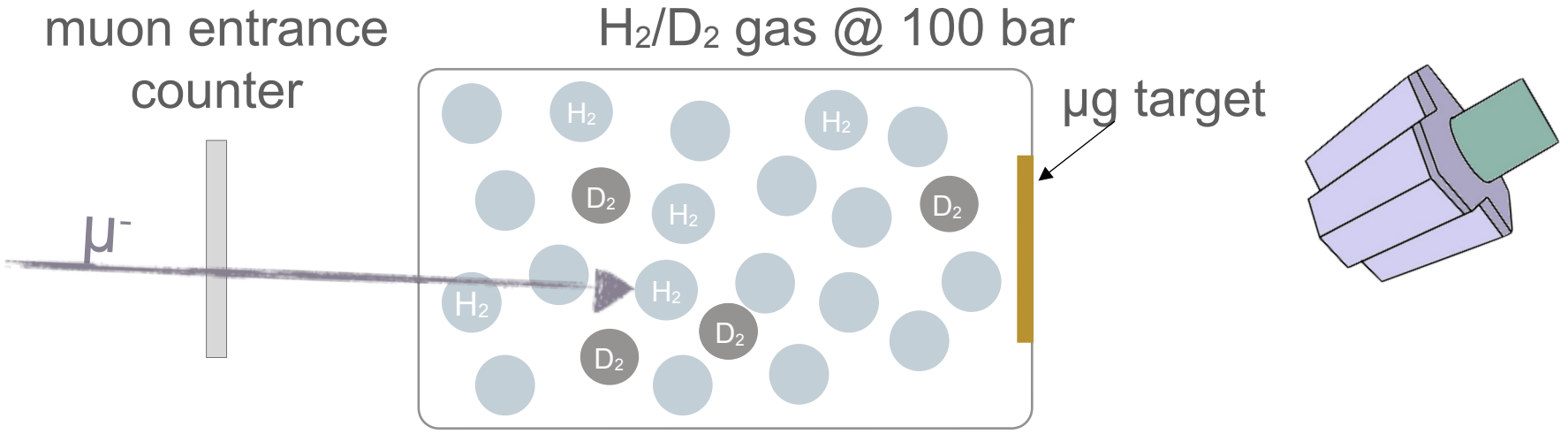

1. μ^- stops in 100 bar of H_2 + 0.25% D_2 & forms muonic hydrogen μp
2. transfer to deuterium μp → μd
3. μd moves almost freely in the H_2 gas
4. transfer to high-Z element μd → μZ when hitting target & emission of x rays during the atomic cascade

Muon transfer to microgram targets

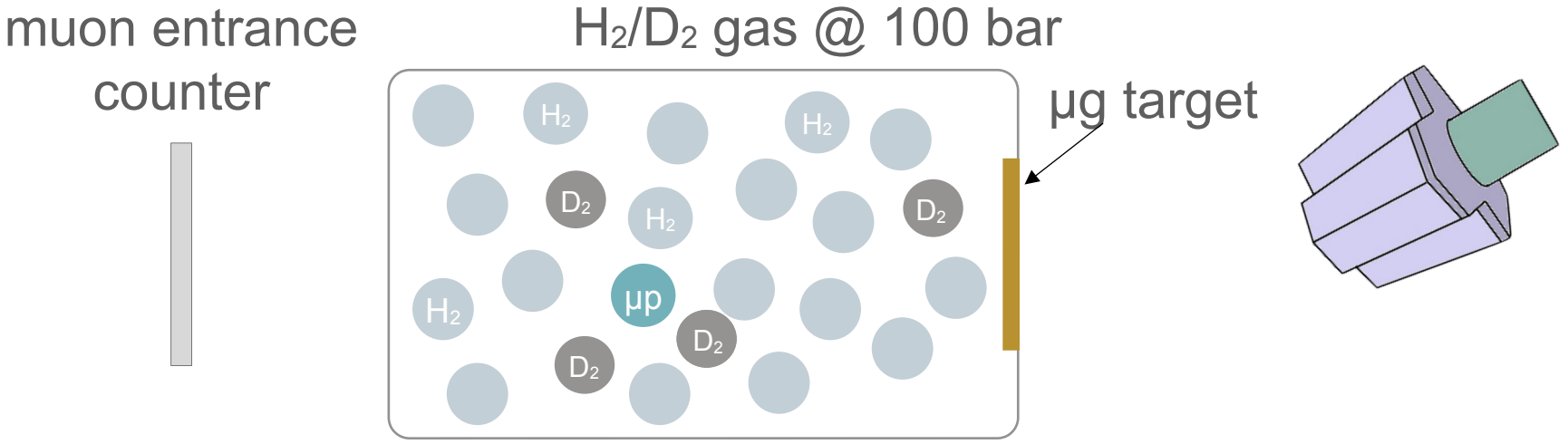

1. μ^- stops in 100 bar of H_2 + 0.25% D_2 & **forms muonic hydrogen μp**
2. transfer to deuterium μp → μd
3. μd moves almost freely in the H_2 gas
4. transfer to high-Z element μd → μZ when hitting target & emission of x rays during the atomic cascade

Muon transfer to microgram targets

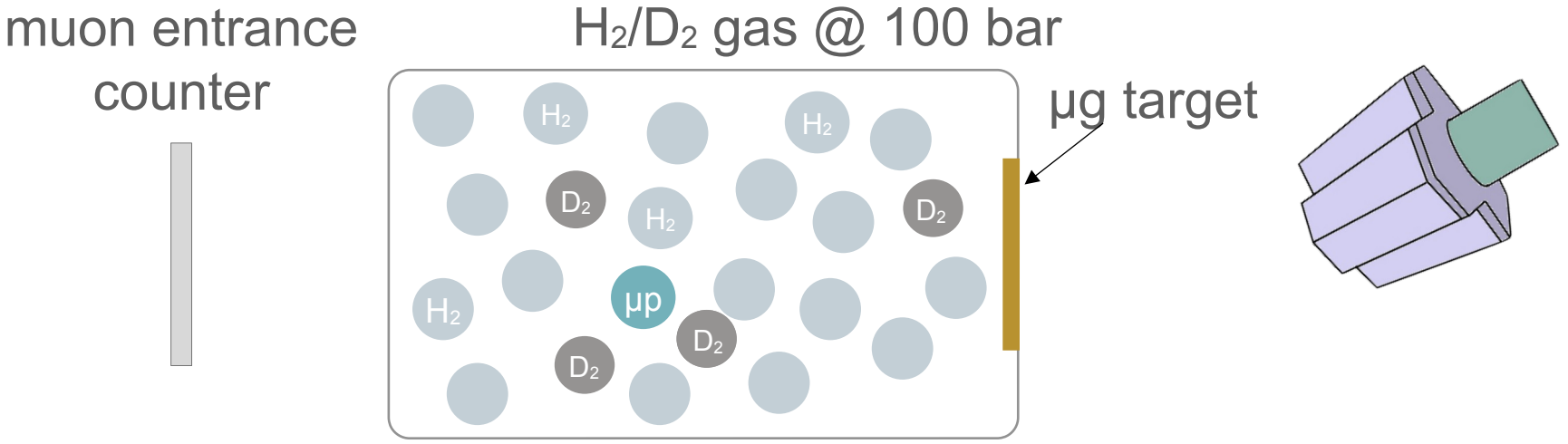

1. μ^- stops in 100 bar of H_2 + 0.25% D_2 & **forms muonic hydrogen μp**
2. transfer to deuterium μp → μd
3. μd moves almost freely in the H_2 gas
4. transfer to high-Z element μd → μZ when hitting target & emission of x rays during the atomic cascade

Muon transfer to microgram targets

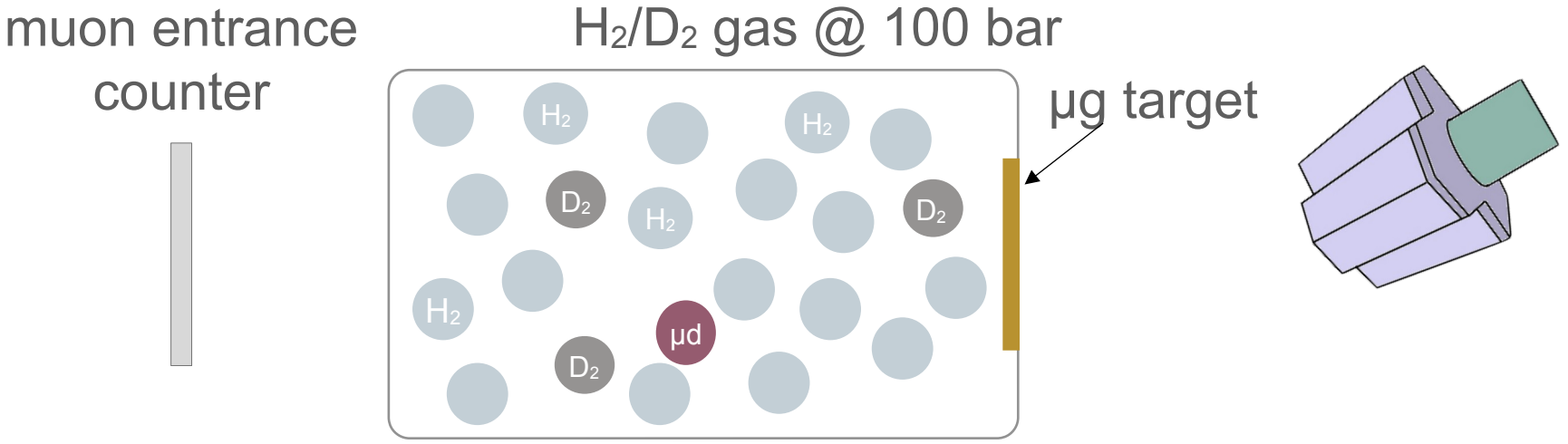

1. μ^- stops in 100 bar of H_2 + 0.25% D_2 & **forms muonic hydrogen μp**
2. transfer to deuterium μp → μd
3. μd moves almost freely in the H_2 gas
4. transfer to high-Z element μd → μZ when hitting target & emission of x rays during the atomic cascade

Muon transfer to microgram targets

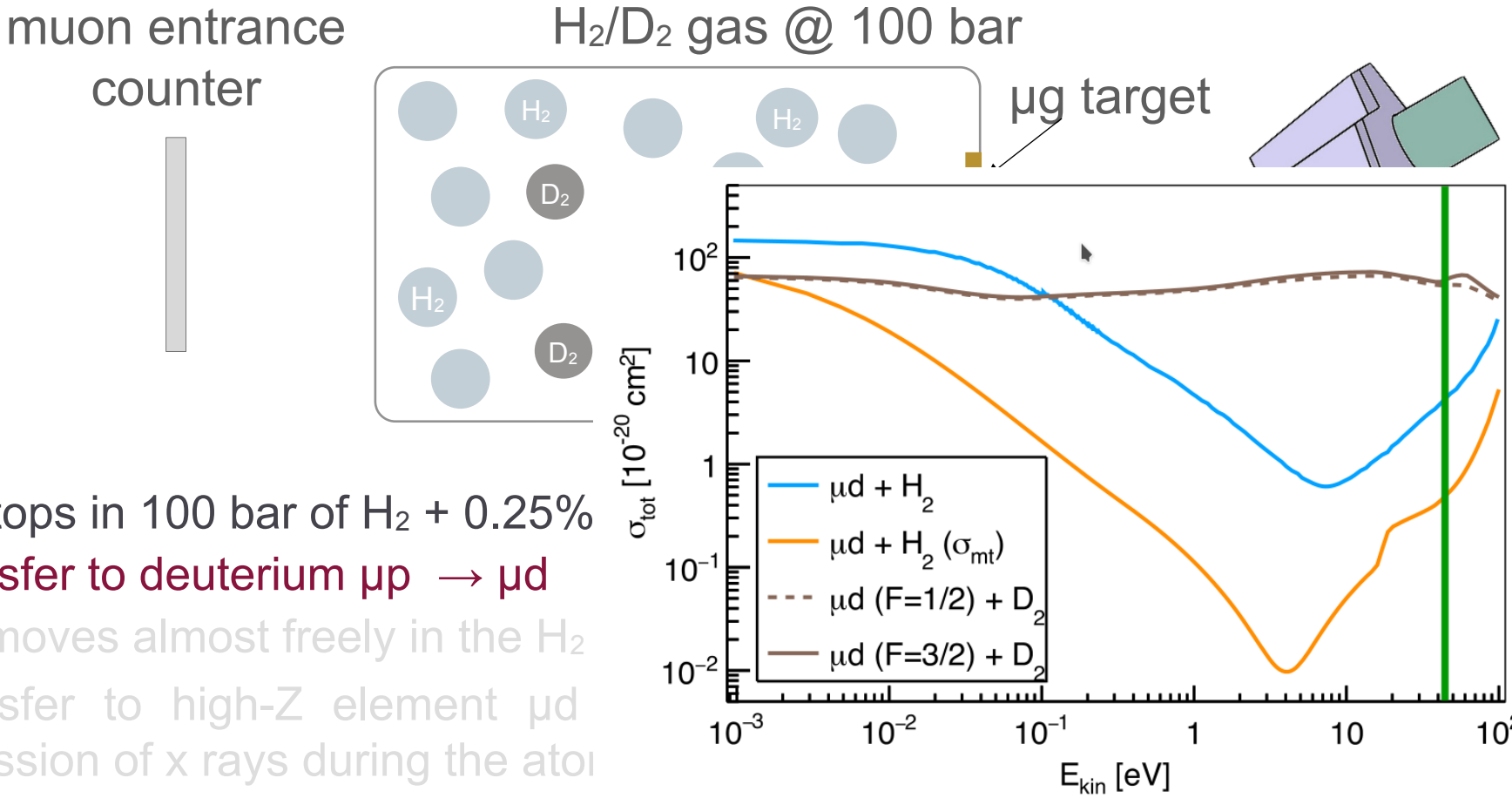

1. μ^- stops in 100 bar of H_2 + 0.25%
2. transfer to deuterium μp → μd
3. μd moves almost freely in the H_2
4. transfer to high-Z element μd emission of x rays during the ato

Muon transfer to microgram targets

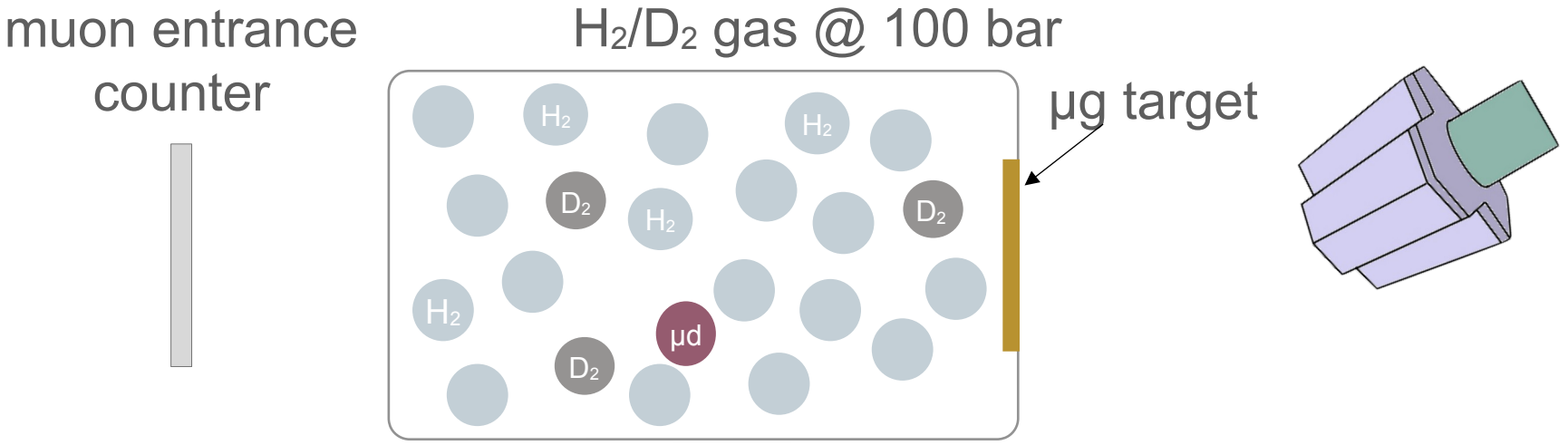

1. μ^- stops in 100 bar of H_2 + 0.25% D_2 & **forms muonic hydrogen μp**
2. transfer to deuterium μp → μd
3. μd moves almost freely in the H_2 gas
4. transfer to high-Z element μd → μZ when hitting target & emission of x rays during the atomic cascade

Muon transfer to microgram targets

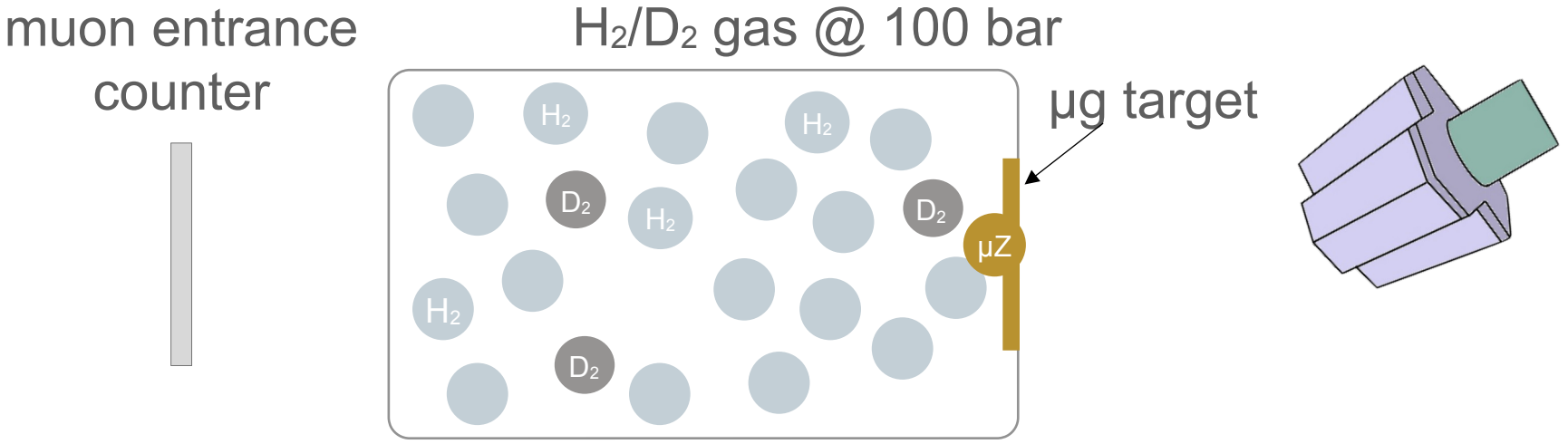

1. μ^- stops in 100 bar of H_2 + 0.25% D_2 & **forms muonic hydrogen μp**
2. transfer to deuterium μp → μd
3. μd moves almost freely in the H_2 gas
4. transfer to high-Z element μd → μZ when hitting target & emission of x rays during the atomic cascade

Muon transfer to microgram targets

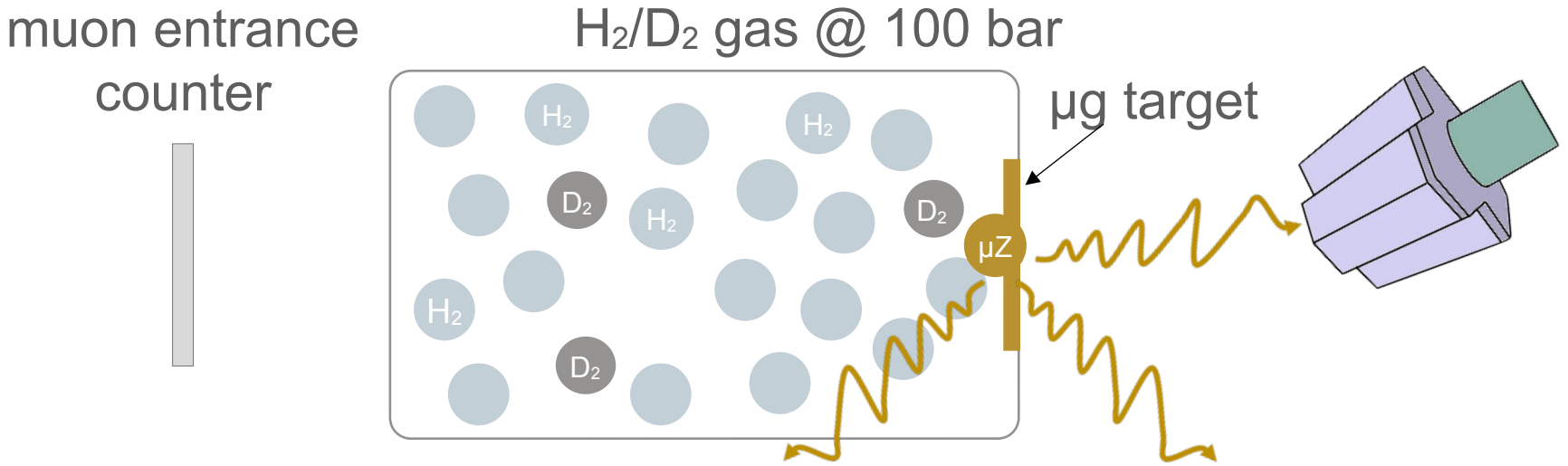

1. μ^- stops in 100 bar of H_2 + 0.25% D_2 & **forms muonic hydrogen μp**
2. transfer to deuterium μp → μd
3. μd moves almost freely in the H_2 gas
4. transfer to high-Z element μd → μZ when hitting target & emission of x rays during the atomic cascade

Proof-of-principle

So far problems with the uniformity of Ra target.

Measured Re and Cm

$Q(^{185}Re) = 2.07(5)$ b
$Q(^{187}Re) = 1.94(5)$ b

First physics result:
PRC 101, 054313 (2020)

15 µg of ^{248}Cm

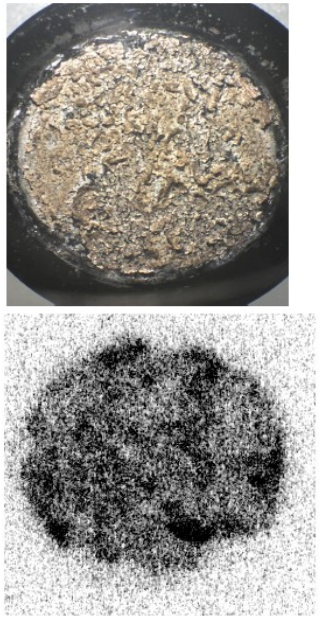

4 µg of ^{226}Ra

Nuclear charge radius in ^{185,187}Re

The extraction of the nuclear charge radius from the analysis of the 2p1s hyperfine transitions

Preliminary results:

$R(^{185}Re) = 5.297(2)_{stat}(6)_{sys}$ fm

$R(^{187}Re) = 5.288(2)_{stat}(4)_{sys}$ fm

Not all the systematics are taken into account.

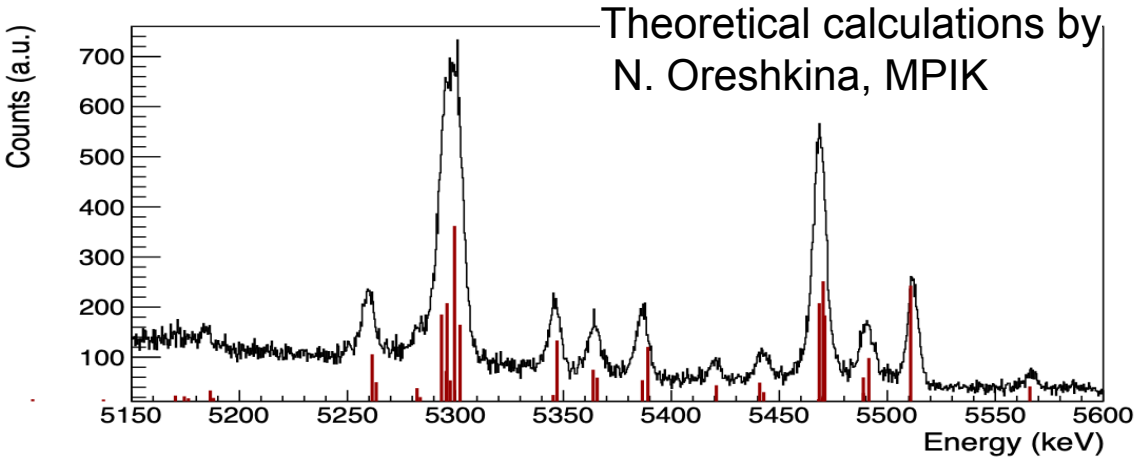

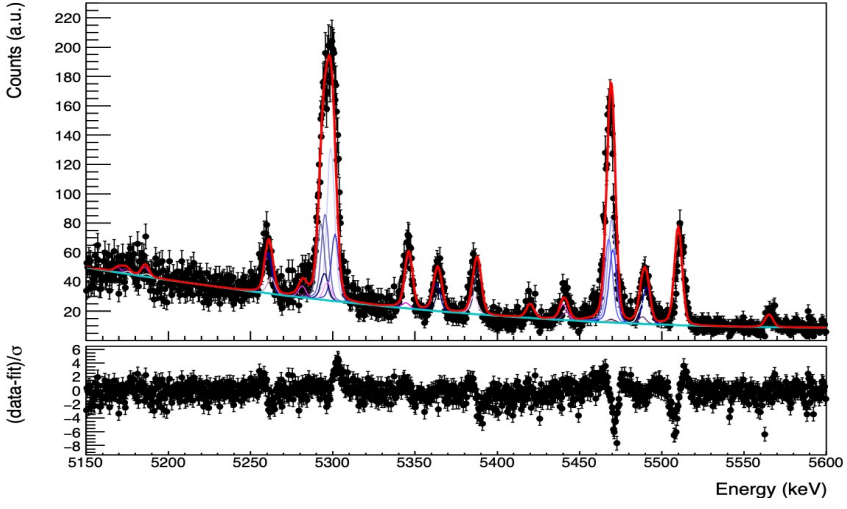

Conclusions

muonic H, D, ^{3}He, ^{4}He by laser done → improved charge radii
nuclear polarizability

muonic Li, Be, …. → better charge radii by QUARTET X-rays and MMCs

muonic high-Z , also for rare or radioactive nuclei! → muX

^{3}T charge radius: missing link Z=1 → 2
T_2^+ molecular ions (F. Schmid) or T(1S-2S) in Mainz

^{6,7}Li isotope shift: new effort in Mainz using cold Li beams + AFR

Thanks a lot for your attention

Backup

Hyperfine structure in muonic H

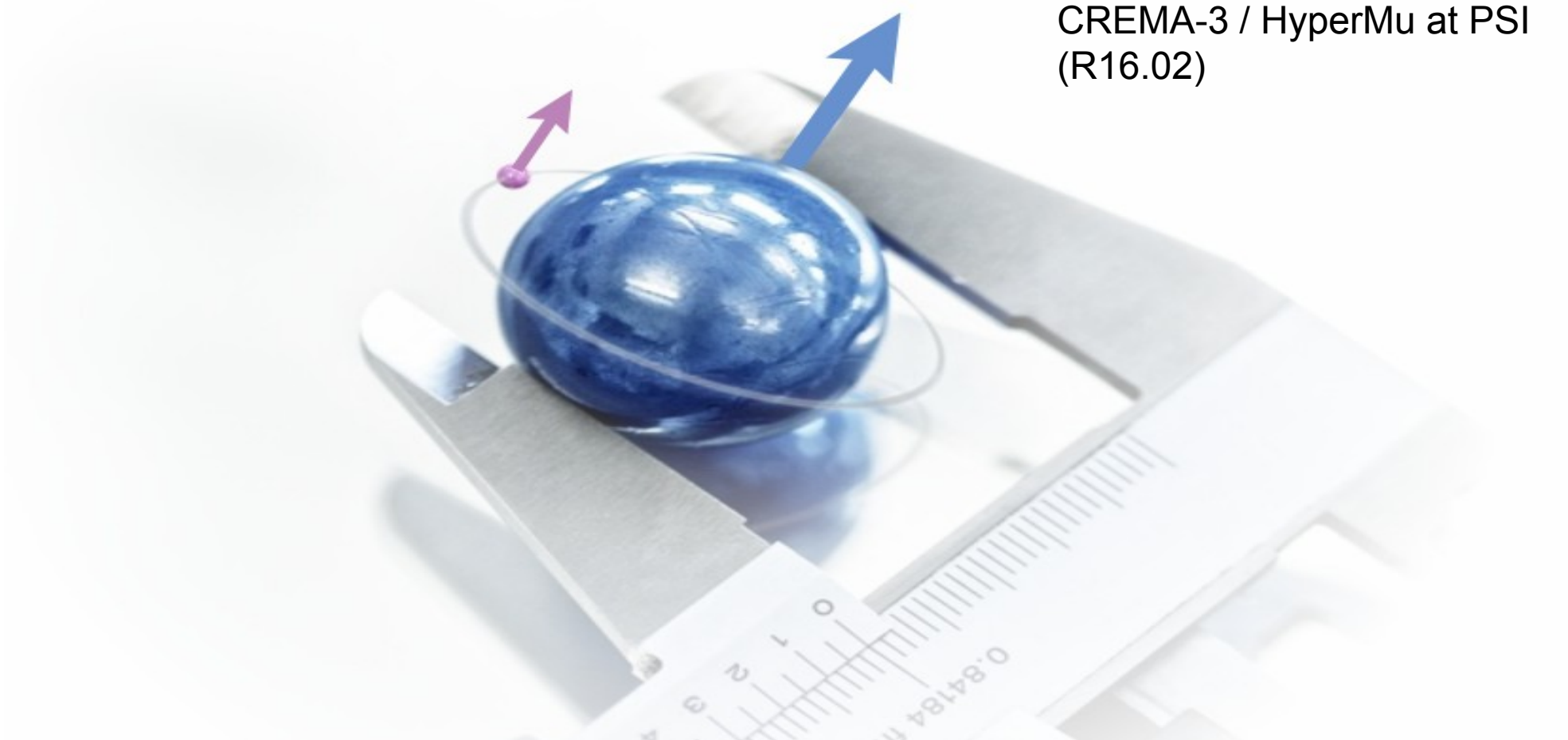

CREMA-3 / HyperMu at PSI
(R16.02)

The sky in hydrogen

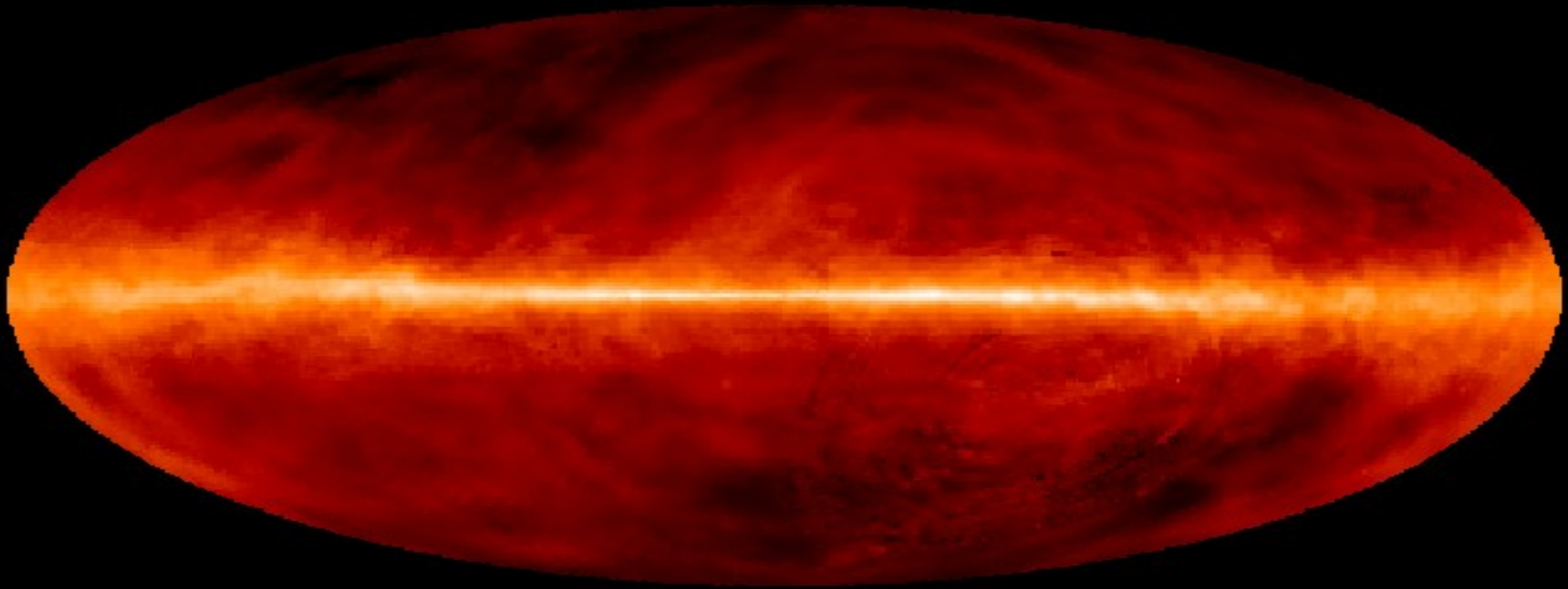

Hyperfine structure in H / μp

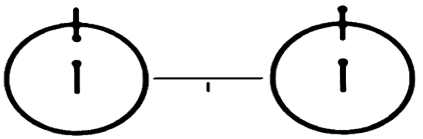

The 21 cm line in hydrogen (1S hyperfine splitting) has been **measured** to 12 digits (0.001 Hz) in 1971:

$$\nu_{exp} = 1\,420\,405.\,751\,766\,7 \pm 0.000\,001\ \text{kHz}$$

Essen et al., Nature 229, 110 (1971)

QED test is limited to 6 digits (800 Hz) because of proton structure effects:

$$\nu_{theo} = 1\,420\,403.\,1 \pm 0.6_{\text{proton size}} \pm 0.4_{\text{polarizability}}\ \text{kHz}$$

Eides et al., Springer Tracts 222, 217 (2007)

Proton Zemach radius

HFS depends on “Zemach” radius:

$$\Delta E = -2(Z\alpha)m\langle r\rangle_{(2)} E_F$$

$$\langle r\rangle_{(2)} = \int d^3r\, d^3r'\, \rho_E(r)\,\rho_M(r')\,|r-r'|$$

Zemach, Phys. Rev. 104, 1771 (1956)

$$\Delta E = \frac{8(Z\alpha)m}{\pi n^3} E_F \int_0^\infty \frac{dk}{k^2}\left[\frac{G_E(-k^2)\,G_M(-k^2)}{1+\kappa}\right]$$

Form factors and momentum space

From charge to magnetic properties

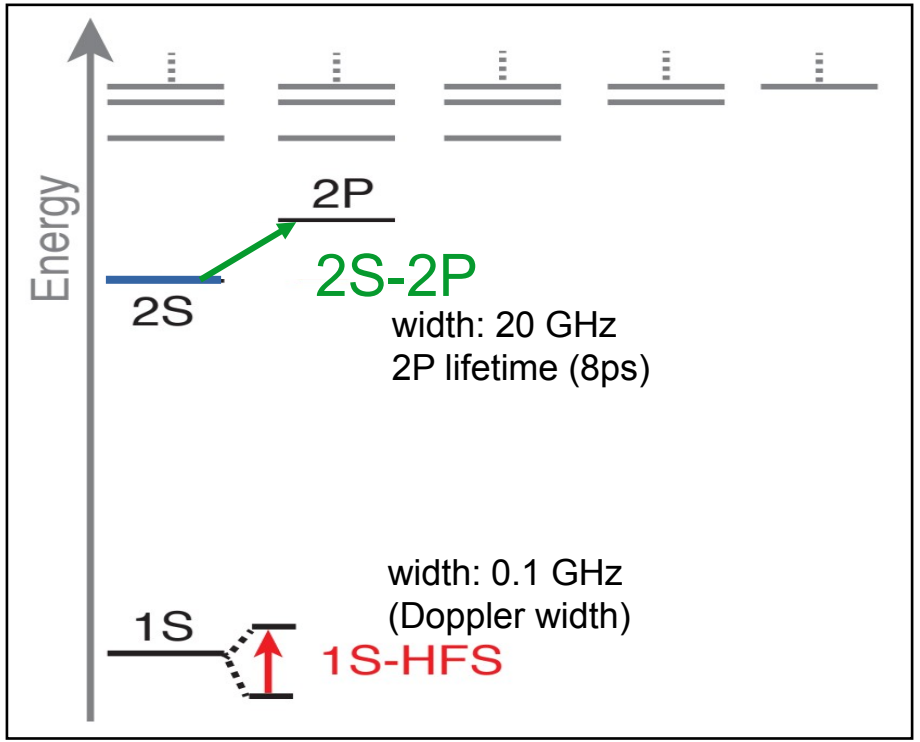

2S-2P = Lamb shift

is sensitive to CHARGE radius

1S-HFS = Hyperfine splitting

is sensitive to ZEMACH radius

Amaro et al [CREMA], 2112.00138

Proton Zemach radius from μp

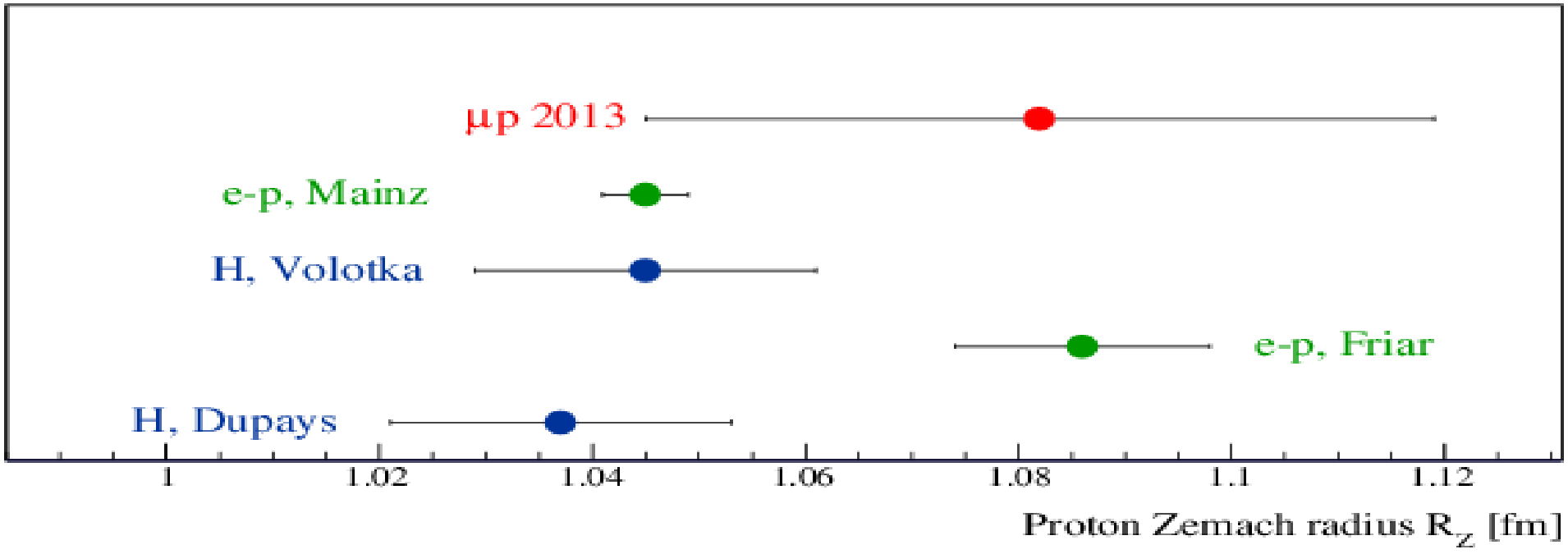

μp 2013: Antognini et al. (CREMA Coll.), Science 339, 417 (2013)

Proton Zemach radius from μp

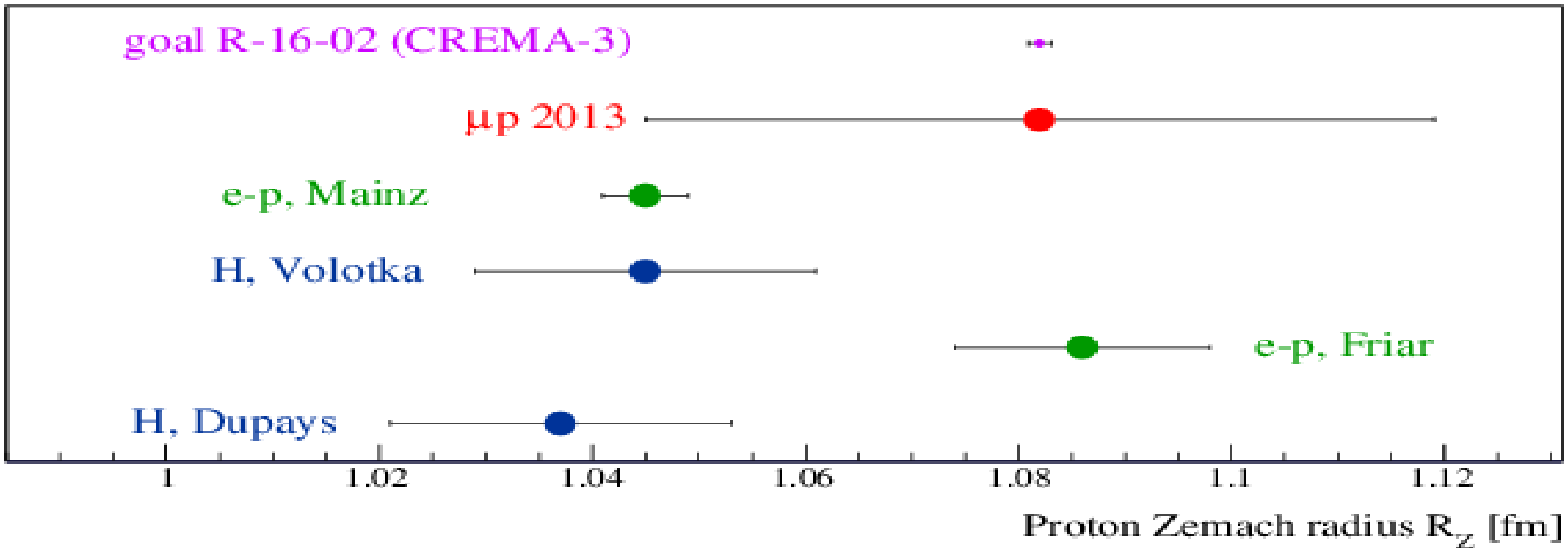

PSI Exp. R-16-02: Antognini, RP et al. (CREMA-3 / HyperMu)
see e.g. Schmidt, RP et al., J. Phys. Conf. Ser 1138, 012010 (2018); arXiv 1808.07240

also: FAMU @ RIKEN/RAL, and a Collaboration at J-PARC

AFR: Active Fiber-based Retroreflector

- Use of Active fiber-based Retroreflector:

  → Reduction of Doppler effect

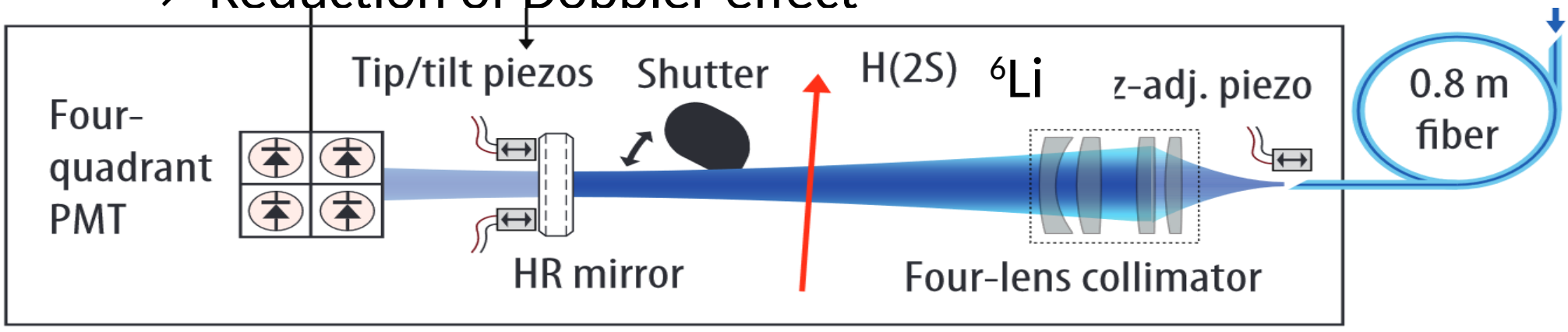

[A. Beyer, "Active fiber-based retroreflector providing phase-retracing anti-parallel laser beams for precision spectroscopy", 2016]

[V. Wirthl, "Improved active fiber-based retroreflector with intensity stabilization and a polarization monitor for the near UV", 2022]

AFR: Actively stabilized Fiber-based Retro-Reflector

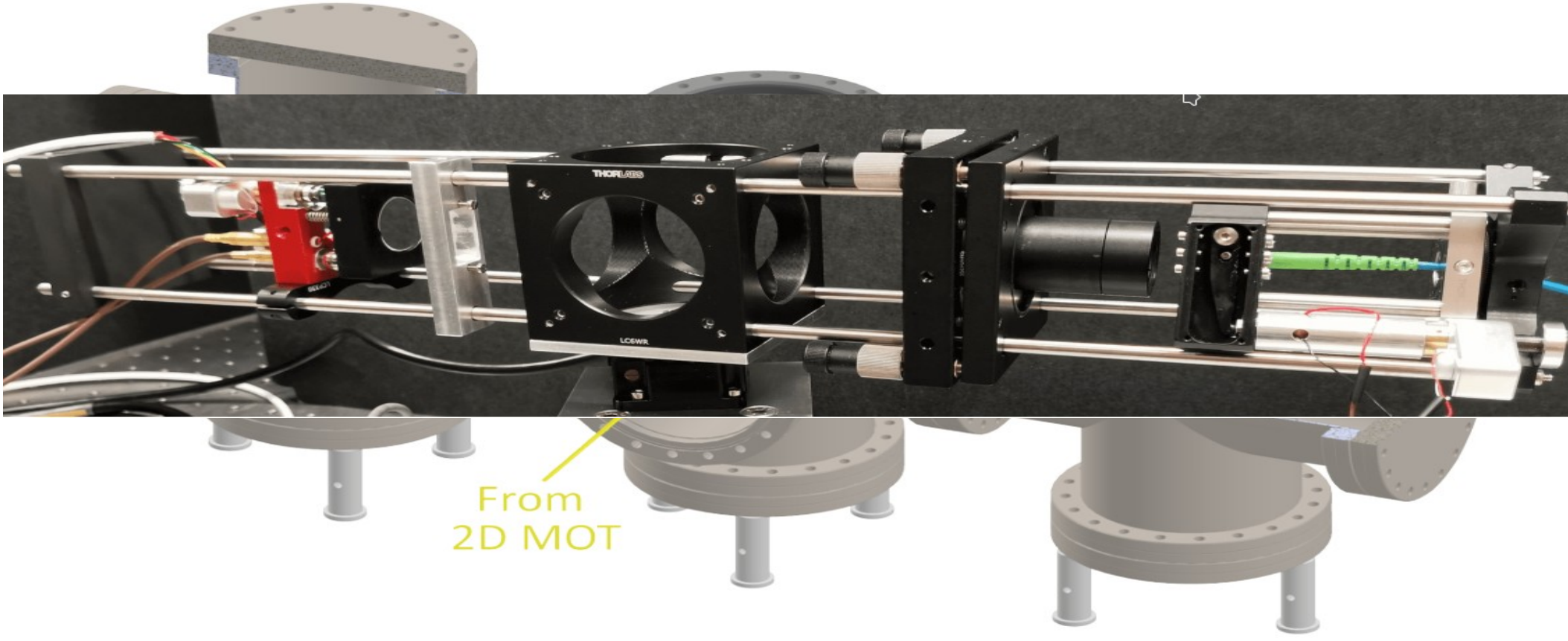

Electron scattering

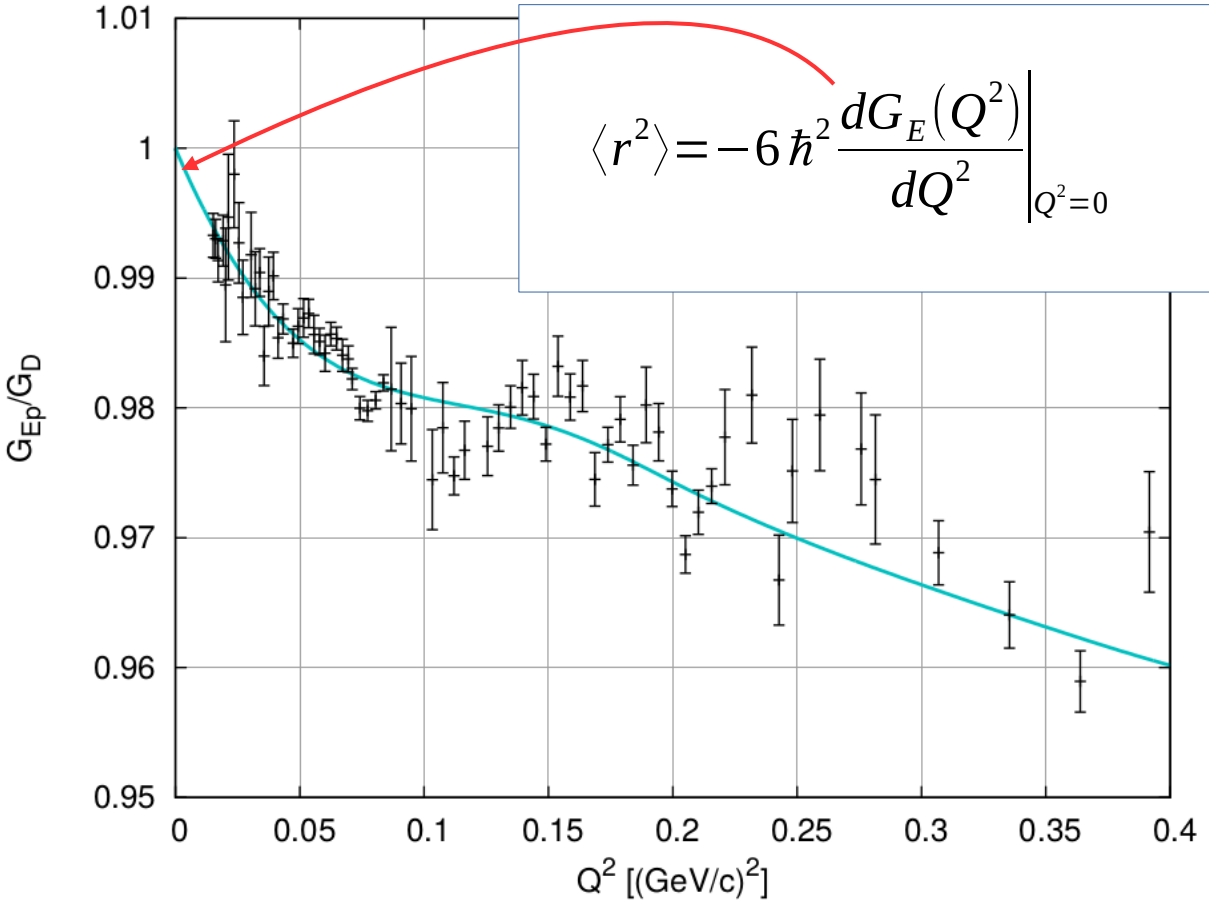

$$\langle r^2 \rangle = -6\hbar^2 \frac{dG_E(Q^2)}{dQ^2}\bigg|_{Q^2=0}$$

extrapolation to $Q^2 = 0$ required

Vanderhaeghen, Walcher: 1008.4225

Mainz MAMI data 2010

Correlation between R_∞ and R_p / R_d

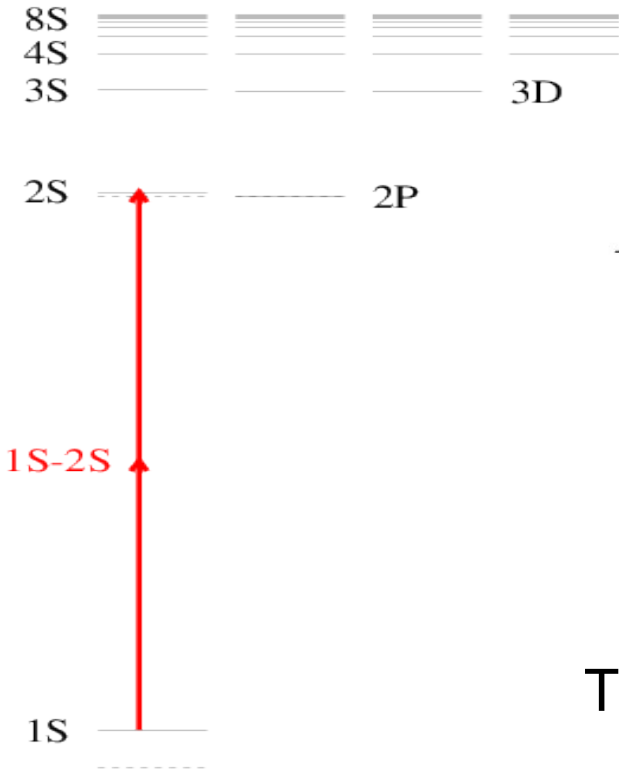

$$E(n,\ell,j)/h = -\frac{cR_\infty}{n^2}\frac{m_{\rm red}}{m_e} + \frac{E_{NS}}{n^3}\delta_{\ell 0} + \Delta(n,\ell,j). \quad (7)$$

$$\nu(1S-2S) \approx \frac{3}{4}R_\infty - \frac{7}{8}E_{NS}$$

10^{-15} = 10 Hz 10^{-12} = 20 kHz

The source of the 98.91% correlation of R_∞ and R_p

[Pohl et al., Metrologia 54, L1 (2017)]

Hydrogen 2S-6P: which contributions are being tested

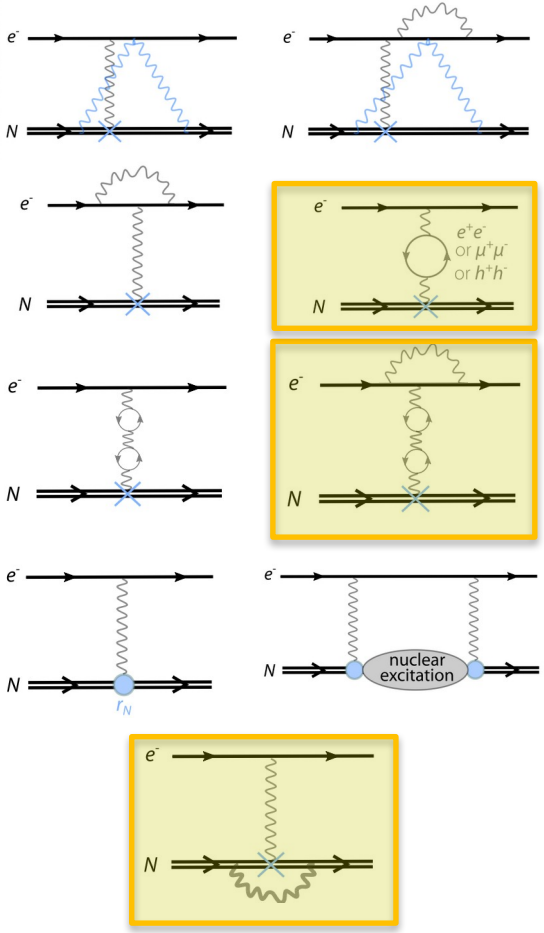

	Hydrogen $2S_{1/2}$-$6P_{1/2}$ (Hz)
Dirac (with $m_e \to m_{\rm red}$)	730 691 021 696 054
Rel. nuclear recoil	1 129 173
Radiative recoil	1540
1-loop QED	
self-energy	−1 071 679 859
vacuum-polarization	26 853 088
$\mu^+\mu^-$ vacuum-pol.	634
hadronic vacuum-pol.	425
2-loop QED	−90 477
3-loop QED	−236
Finite nuclear size	
$\propto \alpha^4$	−138 394
$\propto \alpha^5$	5
$\propto \alpha^6$	−74
Nuclear polarizability	
$\propto \alpha^5$	8
$\propto \alpha^6$	−49
Nuclear self-energy	−584
Total	730 689 977 771 255
Theory uncertainty	199

Our 2S-6P meas. uncert.:
490 Hz

Start seeing muons and hadrons in vacuum

Start seeing 3-loop bound-state vacuum effects

Start seeing Nuclear self-energy

Quantum Interference in 2S-nP

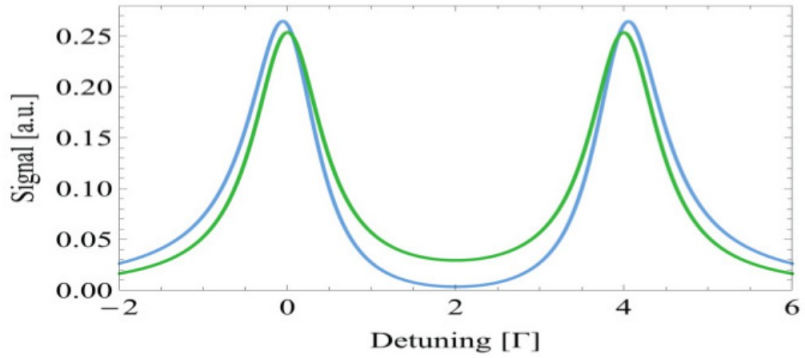

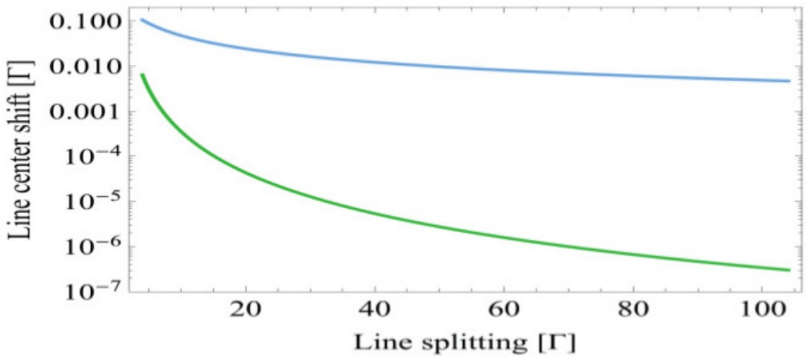

Fitting this with 2 Lorentzians creates

line shifts

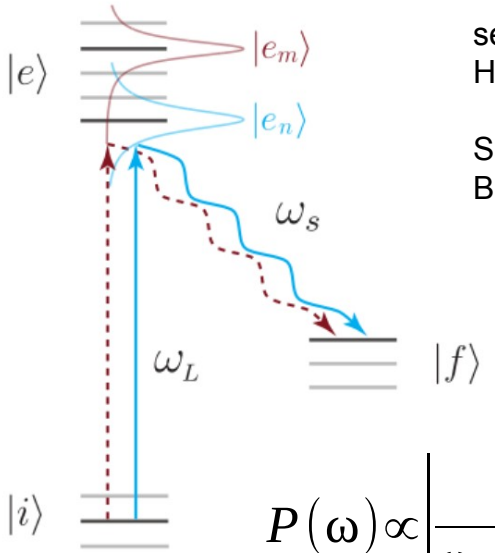

see
Horbatsch, Hessels, PRA 82, 052519 (2010);
PRA 84, 032508 (‘11); PRA 86 040501 (‘12)
Sansonetti et al., PRL 107, 021001 (2011)
Brown et al., PRA 87, 032504 (2013)

$$P(\omega) \propto \left| \frac{(\vec{d}_1 \vec{E}_0)\vec{d}_1}{\omega_1 - \omega_L + i\,\gamma_1/2} + \frac{(\vec{d}_2 \vec{E}_0)\vec{d}_2 e^{i\Delta\Phi}}{\omega_2 - \omega_L + i\,\gamma_2/2} \right|^2$$

= Lorentzian(1) + Lorentzian(2)

+ cross-term (QI)

Studying Quantum Interference in 2S-4P

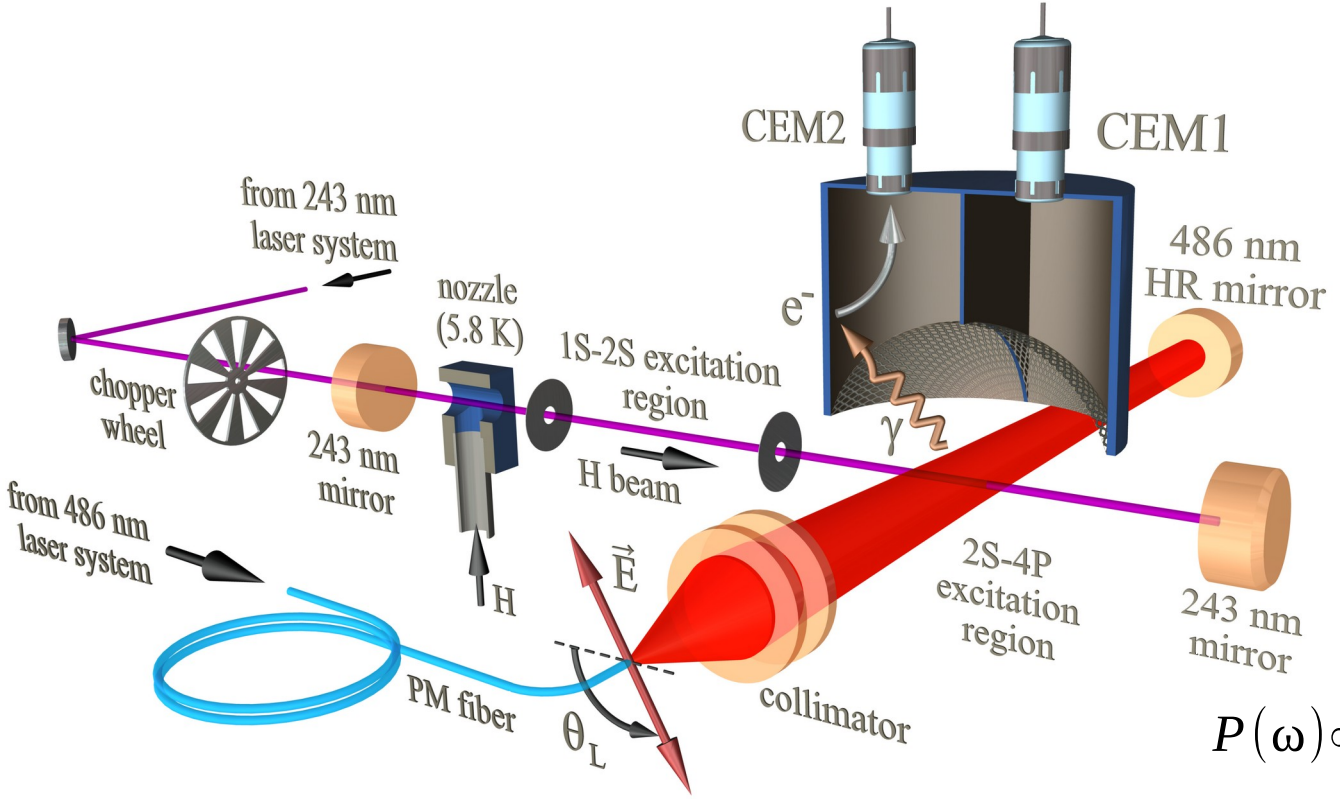

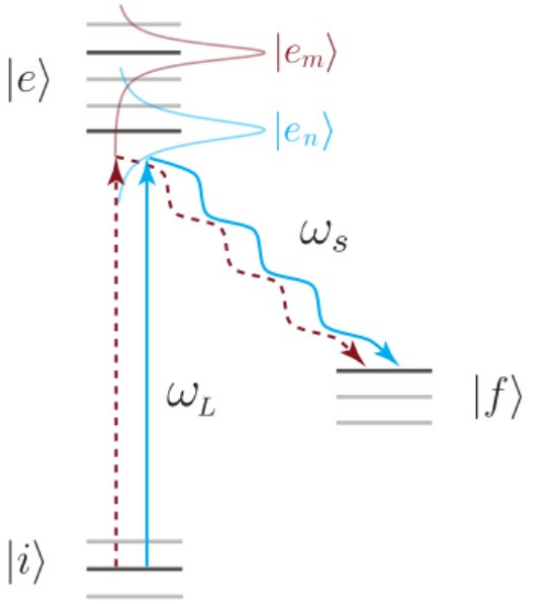

$$P(\omega) \propto \left| \frac{(\vec{d}_1 \vec{E}_0)\vec{d}_1}{\omega_1 - \omega_L + i\gamma_1/2} + \frac{(\vec{d}_2 \vec{E}_0)\vec{d}_2 e^{i\Delta\Phi}}{\omega_2 - \omega_L + i\gamma_2/2} \right|^2$$

= Lorentzian(1) + Lorentzian(2)

+ cross-term (QI)

Beyer, Maisenbacher, RP et al, Science 358, 79 (2017)

Studying Quantum Interference in 2S-4P

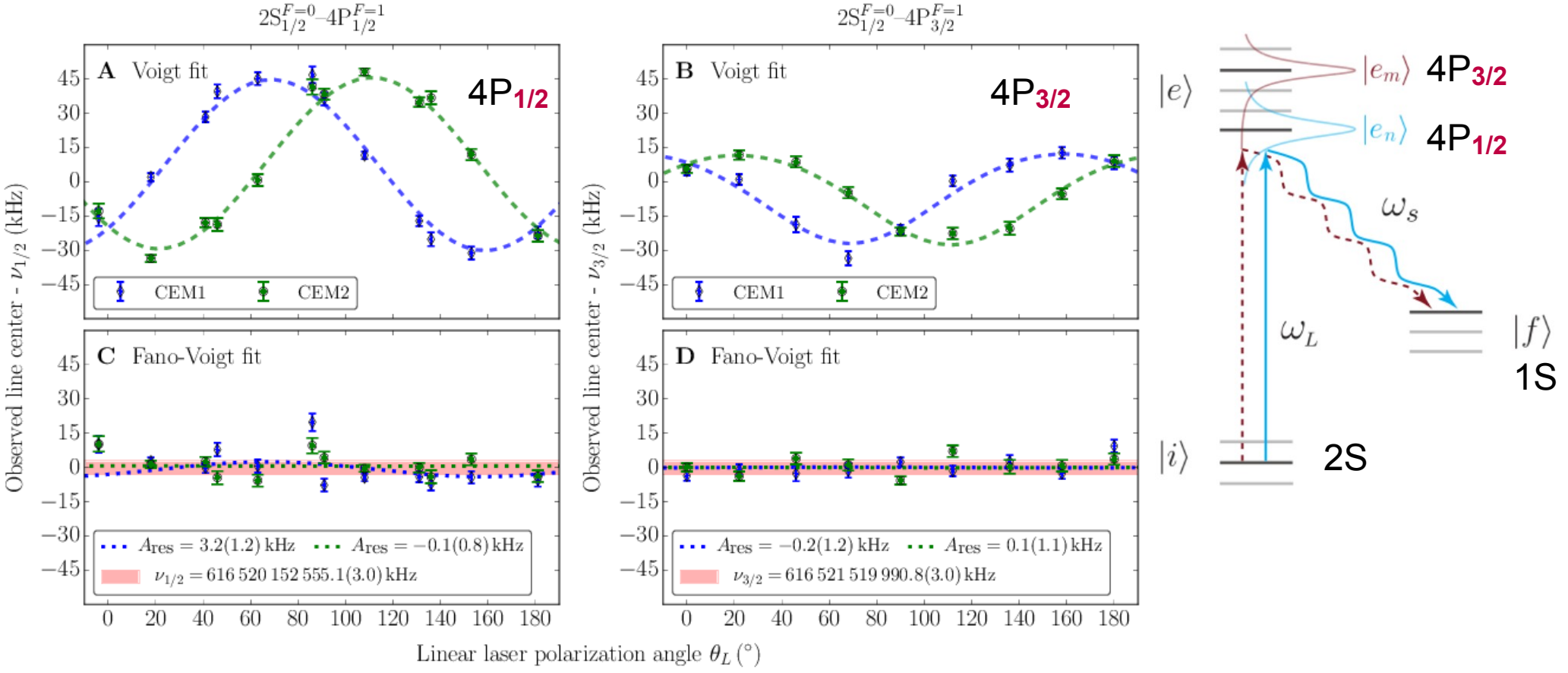

Beyer, Maisenbacher, RP et al, Science 358, 79 (2017)

muonic ^{4}He ions

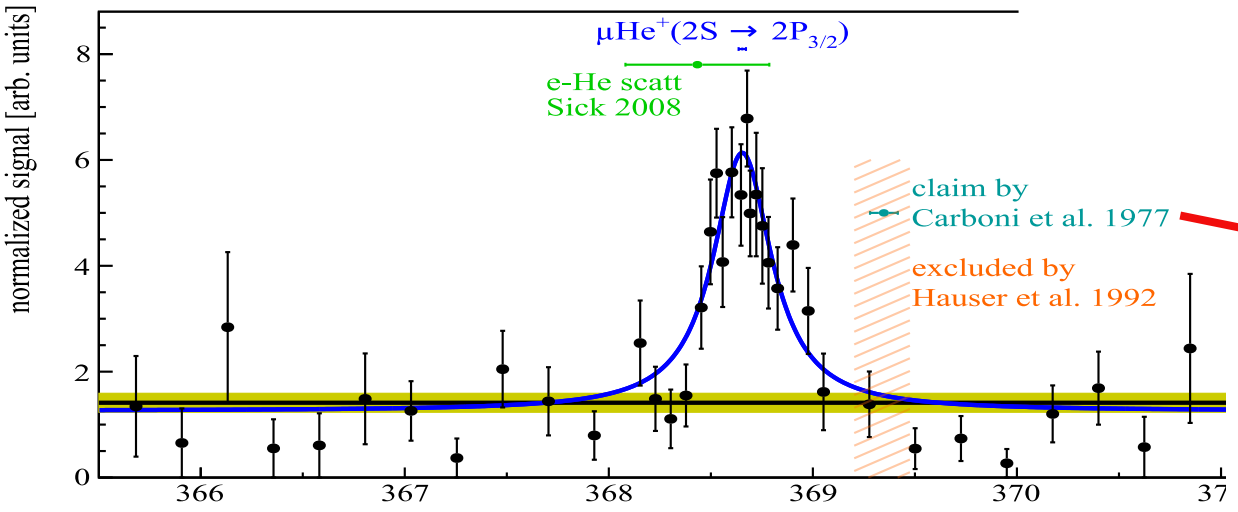

$2P_{3/2}$: ±17 GHz

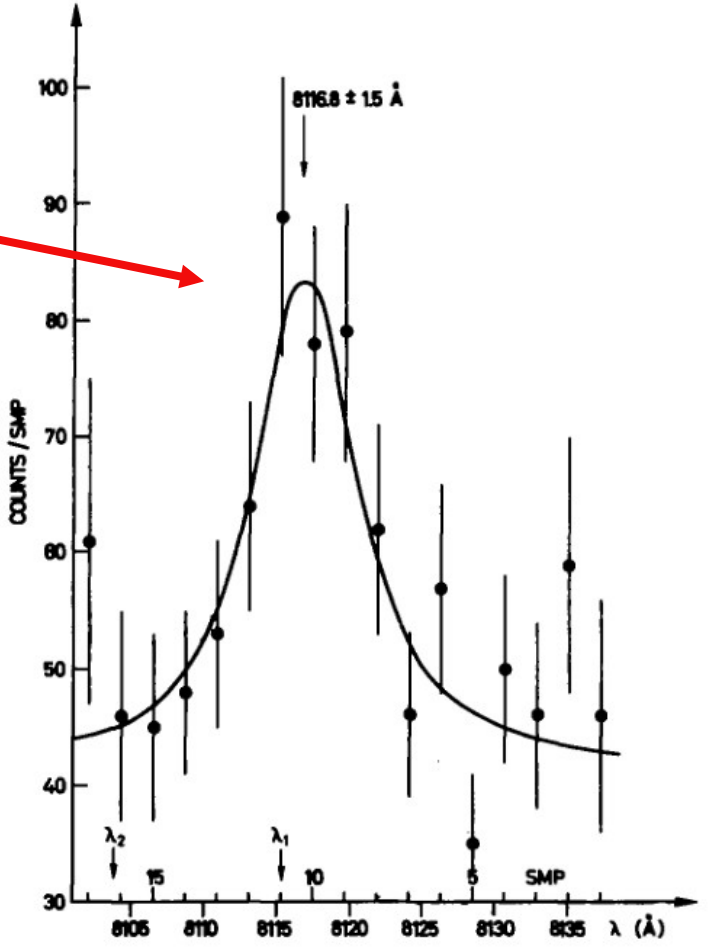

muonic ^{4}He ions

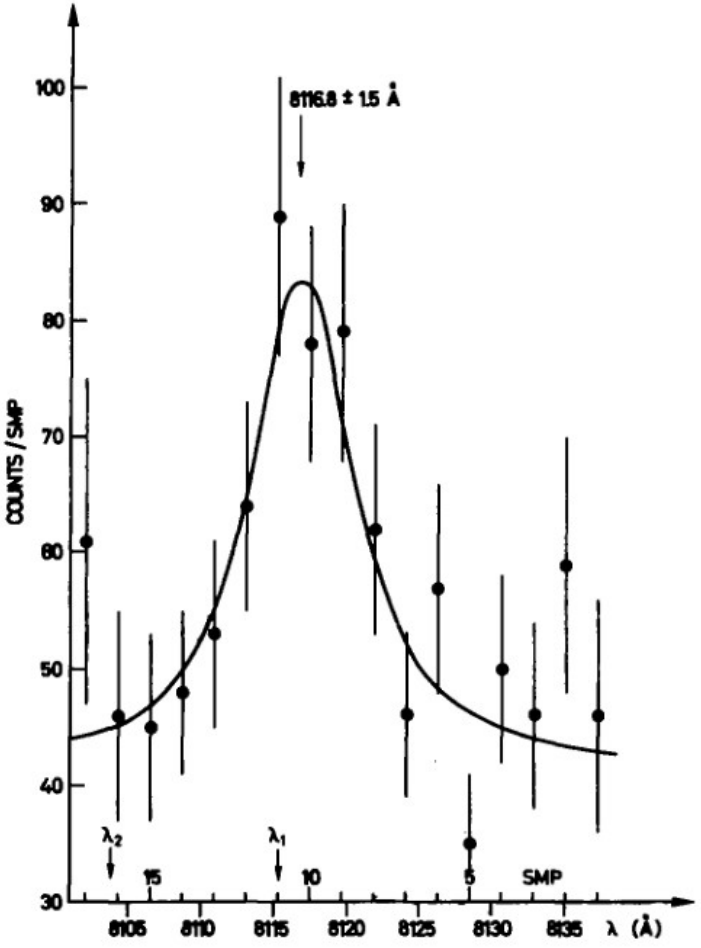

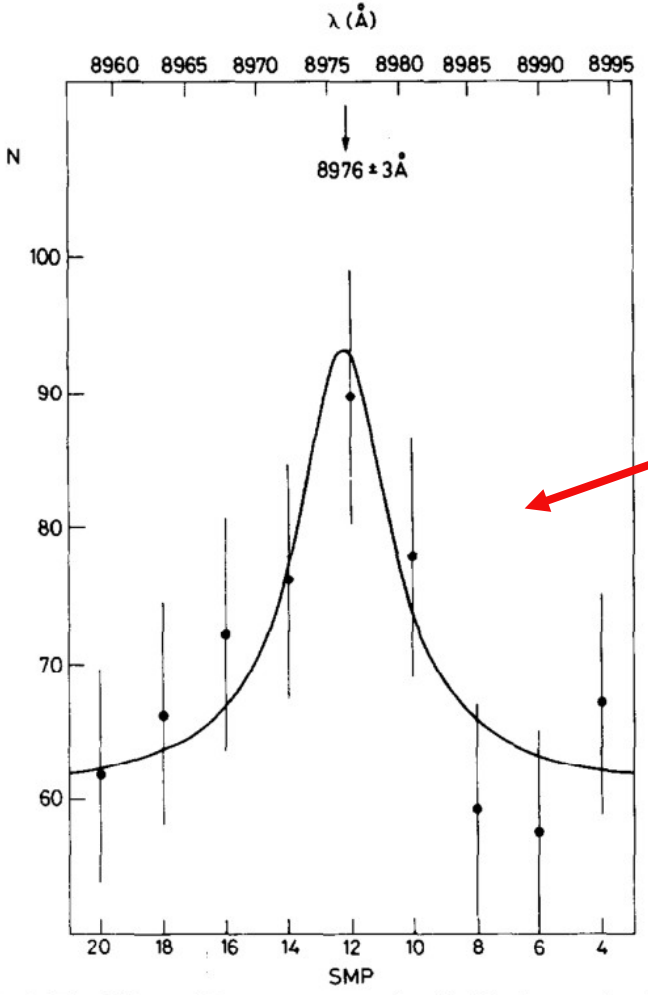

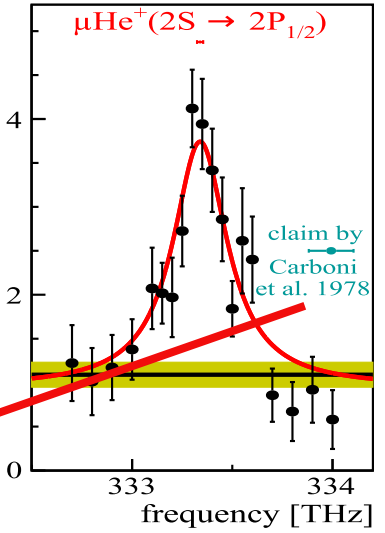

$2P_{1/2}$: ±15 GHz

ReferenceRadii

muX with lighter nuclei

absolute radii and Kir

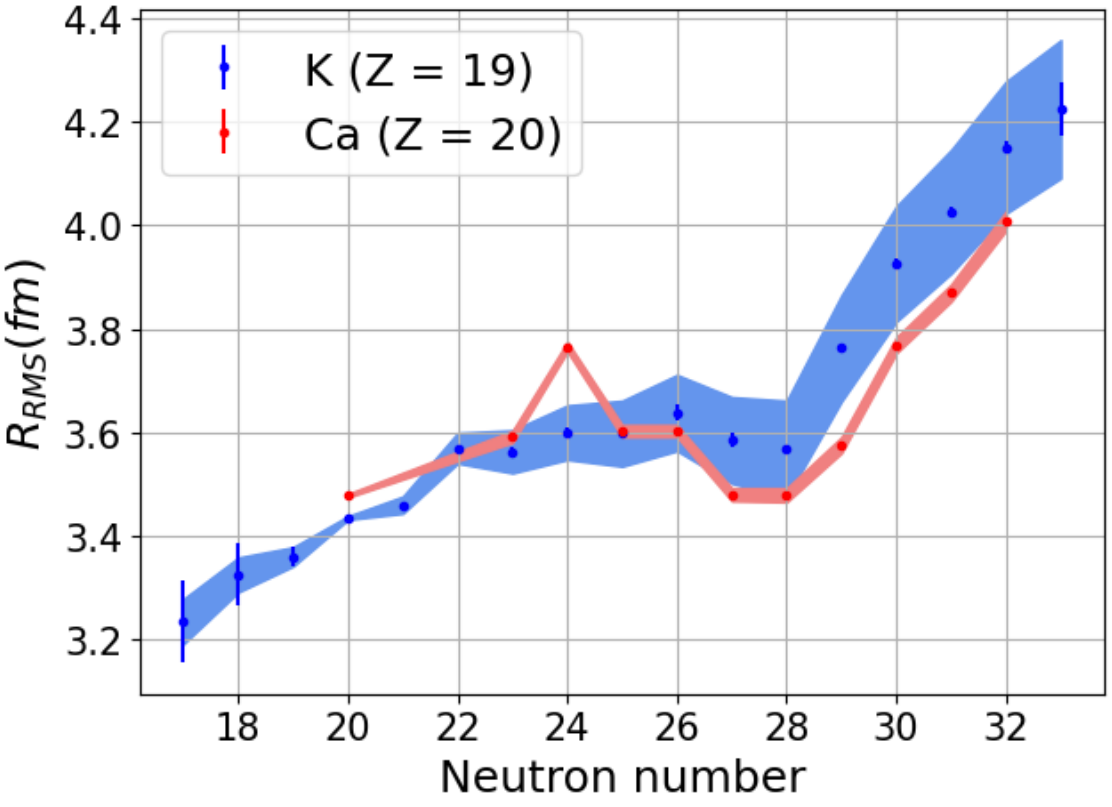

ReferenceRadii

muX with lighter nuclei

g pl

$$\delta < r^2 >^{A,A'} = \frac{1}{F_i}\left(\delta\nu^{A,A'} - \frac{A - A'}{A\,A'} M_i\right)$$

M_i Mass shift

F_i Field shift

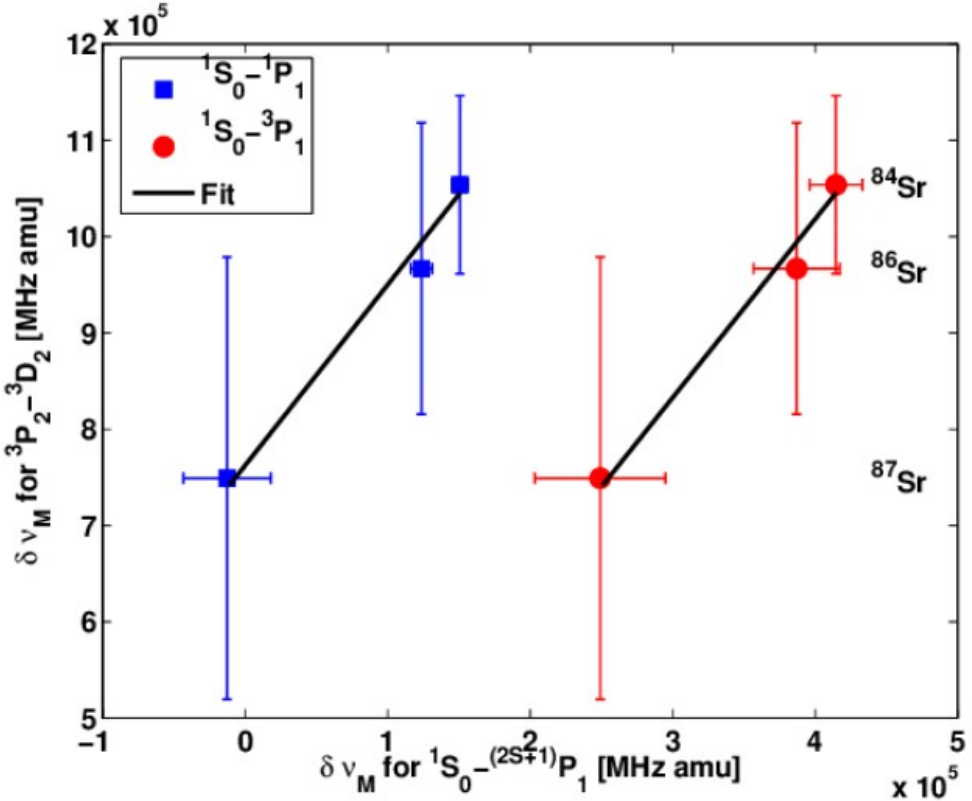

different for each element and transition

ReferenceRadii

Modified King plot

$$\frac{A - A'}{A\,A'}\delta\nu_i^{A,A'} = M_i + F_i \frac{A - A'}{A\,A'}\delta < r^2 >^{A,A'}$$

- Mass shift: intercept
- Field shift: slope

- Absolute charge radii
  - One → Absolute values
  - Two → $\frac{M_i}{F_i}$
  - Three → M_i and F_i

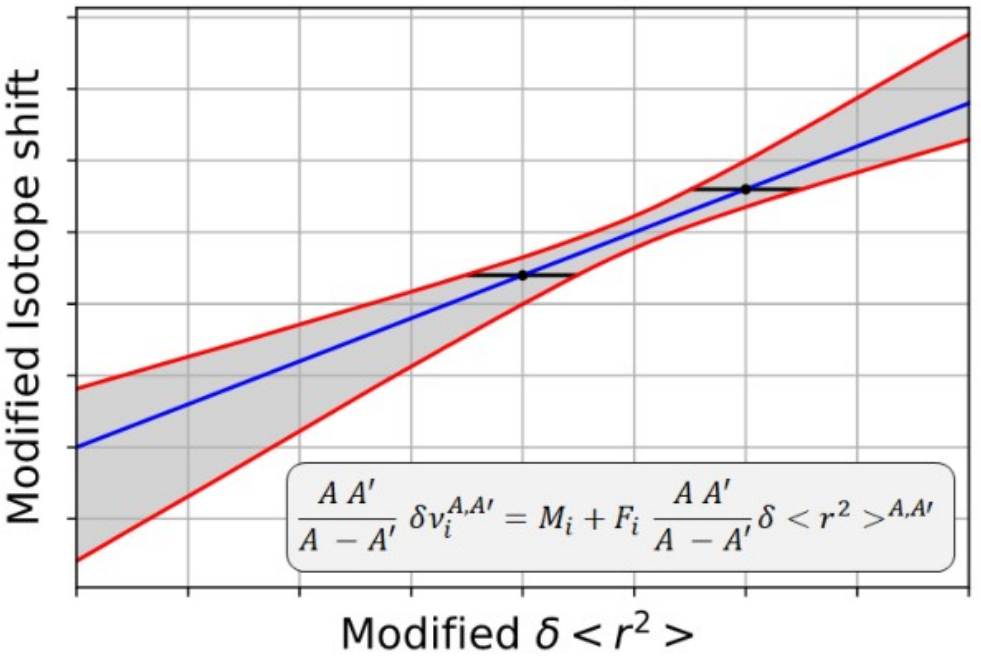

muonic ^{16}O, ^{17}O, ^{18}O